Finite Strain Elastoplasticity:
Consistent Eulerian and Lagrangian Approaches

by

Mohammad Amin Eshraghi

A thesis
presented to the University of Waterloo
in fulfillment of the
thesis requirement for the degree of
Doctor of Philosophy
in
Mechanical Engineering

Waterloo, Ontario, Canada, 2009

Author's Declaration

I hereby declare that I am the sole author of this thesis. This is a true copy of the thesis, including any required final revisions, as accepted by my examiners.

I understand that my thesis may be made electronically available to the public.

Mohammad Amin Eshraghi

Abstract

Infinitesimal strain approximation and its additive decomposition into elastic and plastic parts used in phenomenological plasticity models are incapable of predicting the hardening behavior of materials for large strain loading paths. Experimentally observed second-order effect in finite torsional loading of cylindrical bars, known as the Swift effect, as well as deformations involving significant amount of rotations are examples for which infinitesimal models fail to predict the material response accurately. Several different Eulerian and Lagrangian formulations for finite strain elastoplasticity have been proposed based on different decompositions of deformation and their corresponding flow rules. However, issues such as spurious shear oscillation in finite simple shear and elastic dissipation in closed-path loadings as well as elastic ratchetting under cyclic loading have been identified with the classical formulations for finite strain analysis.

A unified framework of Eulerian rate-type constitutive models for large strain elastoplasticity is developed here which assigns no preference to the choice of objective corotational rates. A general additive decomposition of arbitrary corotational rate of the Eulerian strain tensor is proposed. Integrability of the model for the elastic part of the deformation is investigated and it is shown that the proposed unified model is consistent with the notion of hyperelasticity for its elastic part. Based on this, the stress power is physically separable into its reversible and irreversible parts using the proposed constitutive model irrespective of the objective rate used in the model. As a result, all of the issues of finite strain elastoplasticity are resolved using the proposed Eulerian rate model for arbitrary corotational rate of stress.

A modified multiplicative decomposition of the right stretch tensor is proposed and used to set up a new Lagrangian framework for finite strain elastoplasticity. Decomposition of the deformation is solely defined by the

multiplicative decomposition of the total right stretch tensor into its elastic and plastic parts. The flow rule and evolution of the plastic internal variables are based on the Hencky measure of the plastic right stretch tensor instead of the strain rate tensor. As a result, the issue of mismatch between the elastic and plastic parts of the deformation which mostly exists in the classical multiplicative models does not exist in the proposed Lagrangian model. The problem of back stress oscillation observed in the classical Lagrangian models is also resolved using the proposed Lagrangian model and results are identical to those of the proposed unified Eulerian rate model for finite strain elastoplasticity.

In the context of nonlinear elasticity, no preference for either Lagrangian or Eulerian formulations exists since the two formulations can be related through proper transformations and are equivalent form of each other in different backgrounds. However, classical Eulerian and Lagrangian models of elastoplasticity do not provide such an equivalency under the same loading path. This is due to different definitions used for the elastic and plastic parts of the deformation and different flow rules used in the classical Eulerian and Lagrangian models. In this research it is shown that both the proposed Lagrangian and unified Eulerian rate models are equivalent and results obtained from both models are identical for the same finite strain loading path. Such an equivalency verifies that the proposed Eulerian and Lagrangian models are unified and transformable to each other.

The unified Eulerian and Lagrangian models are extended to mixed nonlinear hardening material behavior. Predicted results for the second-order effect (the well-known Swift effect) are in good agreement with experimental data for fixed-end finite torsional loading of SUS 304 stainless steel tubes. The proposed models are therefore good candidates to be implemented in the displacement-based formulation of the finite element method for the Lagrangian and Eulerian frameworks of finite strain elastoplasticity.

Acknowledgments

I would like to express my sincere gratitude to my supervisors, Professor Hamid Jahed and Professor Steve Lambert for their guidance, technical support, and helpful discussions during the course of this research.

Financial support from the Natural Sciences and Engineering Research Council of Canada (NSERC) is gratefully acknowledged.

I would also like to express my gratitude to Professor Behrooz Farshi for his guidance and encouragement during my MASc program at Iran University of Science and Technology.

The knowledge and efforts of my colleagues in our group was a valuable source of inspiration and success. In particular, Mohammad Noban, Morvarid Karimi Ghovanlou, Arash Tajik, and Jafar Al Bin Mousa, are thanked for the great discussions we had.

Many thanks to my friends Amir Poursaee, Amir Noroozi, Semyon Mikheevskiy, Ramtin Movassaghi, Hamidreza Alemohammad and other wonderful friends. Their friendship has made the past four years full of joy and pleasure.

Finally, I would like to express my profound gratitude to my parents for their support and encouragement throughout my education and professional career.

Table of Contents

List of Figures

List of Tables

Nomenclature

A	Stretching parameter
A_f	Armstrong-Frederick parameter
b	Saturation parameter
b^{-1}	Finger deformation tensor
B_f	Armstrong-Frederick parameter
C	Metric (Green deformation) tensor
d	Strain rate tensor
$d^{p,eq}$	Equivalent plastic strain rate
ds	Deformed line element
dS	Undeformed line element
D	Rotated rate of deformation
E	Lagrangian or Rotated Eulerian strain tensor
E_i	Principal logarithmic strain
$\dot{E}^{p,eq}$	Rate of the equivalent plastic strain
E_η	Closure of the elastic region
f	Yield surface
F	Deformation gradient
h	Anti-symmetric spin function
H	Hardening modulus

I	Second order identity tensor
I_i	Stretch tensor invariants
J	Jacobian of deformation
K	Hardening modulus
l	Velocity gradient
M	Fourth-order elasticity tensor
n	Unit normal vector to yield surface
n_i	Direction vectors of deformed surface
N_i	Direction vectors of undeformed surface
P	First Piola-Kirchhoff stress
$\vec{q}$	Heat flux vector
Q	Orthogonal transformation
Q^p	Modified plastic rotation
r	Internal heat generation
R	Rigid rotation
R_*	Rotation of an Ω_*-spinning frame
$\dot{s}$	Rate of specific enthropy per unit mass
S	Second Piola-Kirchhoff stress
t	time
T	Temperature
U	Right stretch tensor

$\bar{\bar{U}}_L^e$	Rotated Lagrangian right stretch
v	Particle velocity
v_k	Vector of internal variables
V	Left stretch tensor
w	Material spin
$\dot{W}$	Stress power
x	Current coordinate vector
X	Initial coordinate vector
z	Metric tensor of the current configuration
Z	Metric tensor of the initial configuration
α	Integration parameter
β	Back stress tensor
γ	Shearing parameter
δ	Kronocker delta
δe	Increment of the Eulerian strain tensor
δt	Increment of the Eulerian stress tensor
ε	Eulerian logarithmic strain
ζ	Scalar function of stress
η	Shift stress tensor
κ	Bulk modulus

$\dot{\lambda}$	Plastic (Lagrange) multiplier
λ_i	Principal stretches
μ	Shear modulus
ν	Poisson's ratio
ξ	Almansi-Euler strain tensor
ρ	Current density
ρ_0	Initial density
ϱ	Green-Saint-Venant strain tensor
σ	Cauchy stress
σ_0	Yield limit
σ_{Y0}	Initial yield limit
σ_{Ys}	Saturation yield limit
τ	Kirchhoff stress
$\bar{\tau}$	Rotated Kirchhoff stress
$\bar{\bar{\tau}}_L$	Rotated Lagrangian Kirchhoff stress
φ_M	Mechanical dissipation
φ_T	Thermal dissipation
ϕ	Dissipation (plastic) potential
ϕ^*	Dual scalar dissipation potential
χ^p	Modified plastic deformation tensor
ψ	Free energy potential

Γ	Scalar hypoelastic potential
Λ	Diagonalized stretch tensor
Ξ	Mandel stress tensor
Π	Scalar hypoelastic potential
Σ	Rotated Stress tensor
Υ	Scalar yield surface size function
Ω	Spin tensor
Ω^p	Modified plastic spin
$\mathscr{b}_k$	conjugate internal variables vector
e	General Eulerian strain tensor
$\mathcal{E}$	General Lagrangian strain tensor
$\mathscr{f}$	Strain scale function
$\mathcal{G}$	Stress functional
$\mathscr{h}$	Scalar scaling function
$\mathcal{H}$	Cauchy stress function
$\mathscr{k}$	Kinematic hardening function
$\mathcal{L}$	Lagrangian function
$\mathcal{M}$	Fourth order hypoelasticity tensor
$\mathcal{P}$	Particle
$\mathscr{q}$	Vector of hardening plastic variables

$\mathcal{Q}$	Dual vector of hardening variables
$\mathcal{r}$	Position vector in the current configuration
$\mathcal{R}$	Position vector in the initial configuration
$\mathcal{s}$	General plastic flow direction
$\mathcal{t}$	Arbitrary Eulerian stress tensor
$\mathcal{T}$	Arbitrary Lagrangian stress tensor
$\mathcal{Z}$	Complementary hyperelastic function
$\dot{e}$	Rate of the specific internal energy
$\mathfrak{t}$	Traction on the current surface
$\mathbb{I}$	Fourth order identity tensor
$\mathbb{L}$	Fourth-order transformation tensor
$\mathbb{P}$	Fourth-order projection tensor

Operators

dev	Deviatoric of a tensor
L_v	Lie derivative operator
MAX	Maximization
Skew	Skew-symmetric part of a tensor
Sup	Supremum
Superposed dot $\dot{}$	Time rate
Superposed $\overset{*}{\cdot}$	Objective rate in Ω_*-spinning frame

Superposed $\overset{J}{\cdot}$	Objective J rate
Superposed $\overset{c}{\cdot}$	Upper Oldroyd rate
Superposed $\overset{C}{\cdot}$	Lower Oldroyd rate
Superposed $\overset{E}{\cdot}$	Objective E rate
Superposed $\overset{Z}{\cdot}$	Objective Z (GMN) rate
Superposed $\overset{*-Z}{\cdot}$	Objective rate relative to Z frame
Sym	Symmetric part of a tensor
tr	Trace of a tensor
ϕ^*	Pull-back operator
ϕ_*	Push-forward operator
∇	Gradient
:	Dot product of tensors
$\|\quad\|$	Norm of a tensor
$\otimes$	Dyadic product
$\widehat{\ }$	Volumetric/deviatoric decoupling

Superscripts

e	Elastic part
(e)	Eulerian representation of a tensor
p	Plastic part

T	Transpose
$-T$	Inverse transpose
$*$	Trial state

Subscripts

d	Deviatoric part
$D\ (log)$	Related to the $D\ (log)$-frame
E	Eulerian representation
GMN	Related to the Z-frame
J	Related to the J-frame
L	Lagrangian representation
n	State variable on configuration n
$n+1$	State variable on configuration $n+1$
$n+\alpha$	Configuration $n+\alpha$
r	Rotated counterpart

Chapter 1
Introduction

Finite plasticity has a wide range of applications, including deformation due to impact and metalworking, which involve significant amounts of plastic deformation. Applications to rubber-like or bio-related materials, as well as shape memory alloys (SMA), involve large recoverable elastic deformations known as hyperelasticity and pseudoelasticity, respectively. In addition, applications involving cyclic loading with finite deformations cannot be accurately predicted with available infinitesimal cyclic plasticity models. Experiments with cyclic loading of hollow cylinders under free-end finite torsion have shown that the axially induced strain affects the cyclic hysteresis response of the material remarkably [1]. For example, prediction of cyclic behavior of superelastic SMA under cyclic loading is important for vibration damping devices in seismic applications where large recoverable elastic strains exist during service [2].

To accurately predict the material response in such applications, constitutive models should be formulated in a large deformation framework. Due to significant amounts of deformation, alternate configurations can be used as the reference configuration resulting in either Lagrangian or Eulerian formulations for finite deformation. Various material models based on the corresponding kinematics of finite deformation have been introduced in the literature; however, issues have been identified with these constitutive models when the deformation involves significant material rotations.

Finite torsional loading is one example in which shearing of the material causes significant rotations. Spurious shear oscillation have been observed and reported as issues for constitutive models undergoing large deformation [3]. Elastic dissipation and elastic ratchetting in cyclic closed path loading is another issue which has been reported for Eulerian rate formulations of finite strain analysis [4,5]. Another issue with the kinematics of finite deformation is the choice of a physically acceptable decomposition of the deformation into its elastic and inelastic parts. There has been a large degree of disagreement on the choice for such decomposition in the finite strain analysis literature and as a result a unified definition does not exist [5]. Different definitions for the plastic part of the deformation result in different flow rules and as a result different stress responses under finite deformation loading path.

Constitutive models for finite deformation plasticity must be consistent with the thermodynamics of irreversible phenomena. Issues such as elastic dissipation and shear oscillation are not physically acceptable for the elastic part of the deformation,

due to a violation of thermodynamic principles. Furthermore, additional requirements should be met in setting up constitutive models for finite deformations as compared to models for infinitesimal elastoplasticity. Several attempts have been made to resolve the issues of finite deformation analysis, leading to a number of different constitutive models in the literature of finite strain elastoplasticity formulated using both Lagrangian and Eulerian descriptions [5]. Figure 1-1 shows the general trend in the development of Lagrangian and Eulerian formulations of elastoplasticity for finite deformation, and their corresponding issues and limitations.

As shown in Figure 1-1, issues of finite deformation plasticity has limited the use of Eulerian rate models to a specific objective rate of stress known as the D or logarithmic rate [5]. On the other hand, currently available Lagrangian models are unable to accurately predict material response under finite torsional loading, as observed in free- and fixed-end experiments done on cylindrical bars [1]. In addition, some of the available Lagrangian models exhibit a spurious shear oscillation for back stress components under simple shear motion, which is not physically sound.

In the context of nonlinear elasticity, no preference for either Lagrangian or Eulerian formulations exists since the two formulations can be related through proper transformations. Such correspondence motivates the development of a unified Eulerian-Lagrangian formulation of plasticity for large strain analysis. This is the focus of the present work.

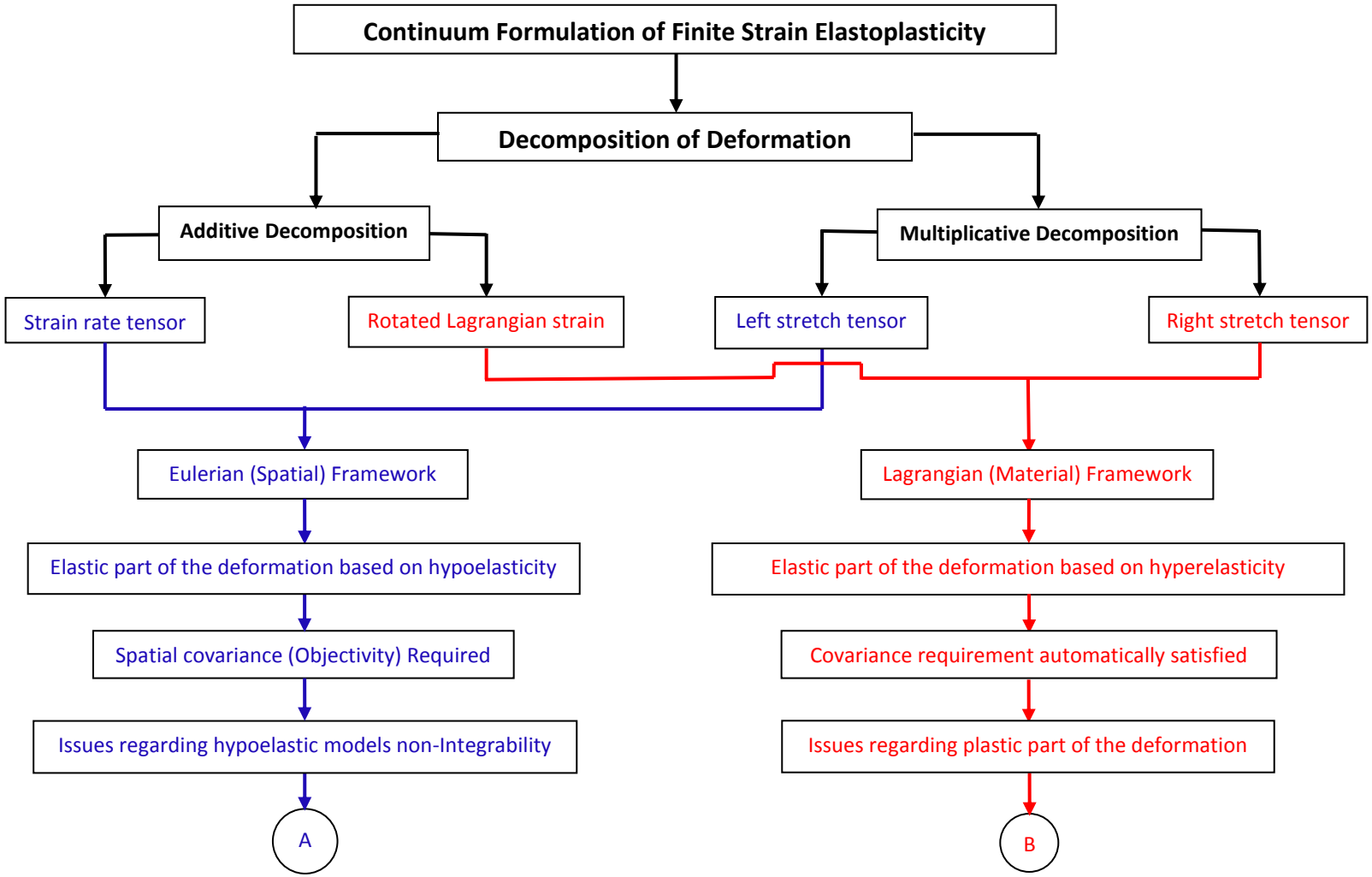

Figure 1-1- Eulerian and Lagrangian formulations of elastoplasticity for finite strain analysis

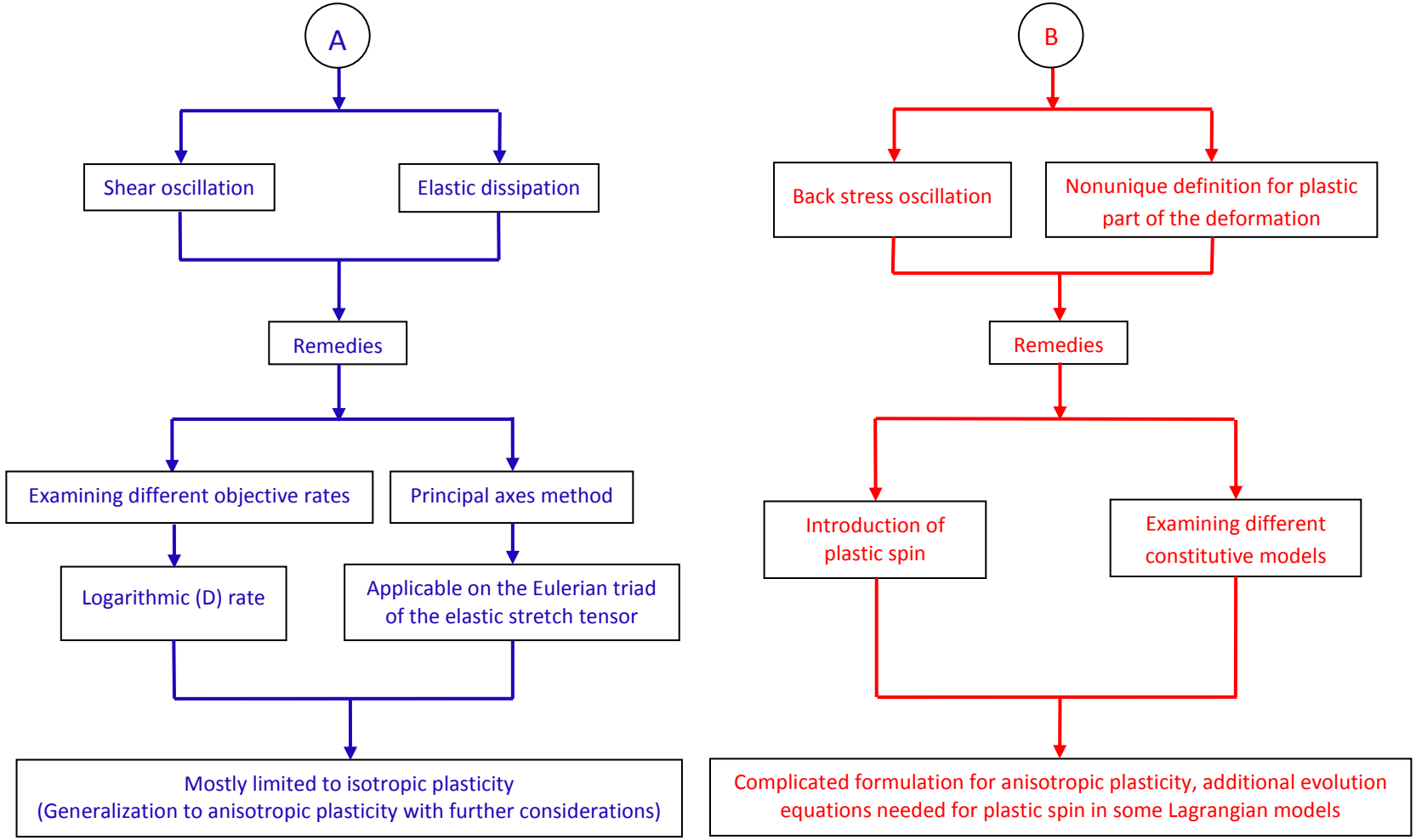

Figure 1-1- Eulerian and Lagrangian formulations of elastoplasticity for finite strain analysis (continued)

The main goal of the current research is to develop a unified Eulerian rate model for finite strain elastoplasticity, which is correct for all of objective corotational rates of stress, including the Jaumann, Green- McInnis-Naghdi, and D or logarithmic rates. All of the issues of finite strain analysis discussed above should be resolved with the proposed unified model. Thermodynamic consistency of the proposed model will be satisfied using the unified work conjugacy theorem. The model would be exactly integrable for its elastic part and consistent with the notion of hyperelasticity. The equivalent Lagrangian framework of the proposed Eulerian model is further developed based on the logarithmic measure of the Lagrangian strain. A new right stretch decomposition is proposed and the evolution of the plastic internal variables derived based on the logarithmic measure of the right plastic stretch tensor. A new back stress evolution equation is proposed and used in the Lagrangian model. The Lagrangian model is integrated on the principal axis of the plastic stretch tensor without any reference to objective rates of stress.

1.1 Background

Phenomenological plasticity models have been widely used to predict inelastic deformation of metals and polycrystalline solids under multiaxial loading. Various plasticity models, depending on the type of application, have been proposed for rate independent and rate dependent plastic behavior of hardening materials under monotonic and cyclic loading. Several different constitutive models for large strain

elastoplasticity have been proposed in the literature [5]; however, issues for finite strain analysis exist when significant material rotation happens during deformation.

One of the issues of finite strain analysis is spurious shear oscillation in finite shear, which has been attributed to inconsistent choices for the objective rates of the kinematic and kinetic variables used in the Eulerian rate-type constitutive models [5,6]. Different frames of reference (observations) for the rate of quantities impose different rotations on the material response, which cause shear oscillation. Although objective tensor variables are used and the objectivity requirement of the constitutive model for finite deformation is met, involvement of different observations for the corresponding objective rates causes a non-physical shear oscillation response.

The issue of elastic dissipation for closed path loading also questions the physical plausibility of available constitutive models for finite deformation. This happens as a result of inconsistent observations in rate-type constitutive models. An elastic material should not dissipate energy for closed path loading. Therefore, elastic dissipation observed using rate-type constitutive models for finite deformation implies their non-integrability in the sense of Green elasticity (hyperelasticity) [5,6].

From a thermodynamic point of view, these issues are inconsistent with the thermodynamics of elastic systems, for which the elastic energy must be recoverable and non-dissipative. In general, a physical requirement for consistent constitutive models for finite deformation is this thermodynamic consistency. The balance of energy defines the associated (conjugate) variables or driving forces of internal

variables used in a constitutive model [7]. Furthermore, any dissipative phenomenon should be in accordance with the second law of thermodynamics. This means that any irreversible phenomenon must dissipate energy during inelastic deformation while internal variables corresponding to the elastic part of the deformation must be non-dissipative. These important requirements, though trivial, must be satisfied in setting up any constitutive model for finite deformation analysis.

1.2 Finite deformation plasticity models

Several multiaxial plastic constitutive models for finite deformation have been published in the literature of finite deformation elastoplasticity. Two different classes of kinematics decomposition have been used in setting up such models: additive decomposition of the strain rate tensor used mostly in Eulerian rate-type models and multiplicative decomposition of the deformation gradient used in both Lagrangian and Eulerian formulations [5].

The first class of constitutive models uses an additive decomposition of the strain rate tensor (rate of deformation) into elastic and inelastic parts. Constitutive models based on this class of decomposition use spatial (Eulerian) internal variables and are rate-type models. One requirement for spatial rate-type models is that they should account for the effect of material rotations. A rigid rotation of the body cannot impose any stress inside the material and as a result constitutive models for finite deformation should be independent of applied rigid rotations. This requirement

restricts the use of the time rate of Eulerian quantities to the special class of objective time rates in rate-type models. This requirement was first introduced by Zaremba and Jaumann [5,6,8] who used a spinning frame of reference based on the skew-symmetric part of the velocity gradient for objective rates of tensor variables. Noll [9] introduced a general framework for rate-type constitutive models based on the Jaumann rate of stress and related it to the symmetric part of the velocity gradient through a fourth-order stress dependent hypoelasticity tensor. A similar constitutive model based on the Jaumann rate was introduced by Truesdell [10] and Cotter-Rivlin [11]. Truesdell and Noll [6] discussed the general framework of constitutive models with the use of various objective rates and showed that hypoelastic models written in one frame of reference can be transformed into another frame of reference with different spins.

Truesdell and Noll [6] further applied the Jaumann version of the hypoelastic model for an isotropic elastic response of the material under simple shear loading. An oscillatory stress response was obtained at high strains. Application of the same hypoelastic model for linear kinematic hardening of the material under simple shear loading by Nagtegaal and de Jong [3] showed the same oscillatory response for the back stress tensor. Use of different frames of reference in hypoelastic models showed different oscillatory and/or non-oscillatory stress responses for the problem of simple shear [12,13]. This led to the conclusion that the stress response of a hypoelastic model can be remarkably affected by the selected objective rate of stress. Green and Naghdi [12] substituted the body spin from the polar decomposition of the

deformation gradient with the Jaumann rate and removed the oscillatory response of the model under simple shear. Dafalias [14] modified the hypo-based plasticity model with the linear kinematic hardening behavior by substituting the Green-McInnis-Naghdi rate for back stress and stress evolutions and obtained a non-oscillatory response. Lee at al. [15] used a modified version of the Jaumann rate in their kinematic hardening model and obtained a non-oscillatory stress response under simple shear.

Truesdell and Noll [6], Bernstein [16,17] and Ericksen [18] investigated the integrability of hypoelastic models. The conclusion was that in general all elastic models were hypoelastic; however, the reverse statement did not apply in general. Bernstein [16,17] showed that a hypoelastic model is exactly integrable in the sense of Cauchy and Green elasticity if a hydrostatic state of stress exists. For a stress-dependent fourth-order hypoelasticity tensor, integrability conditions and the existence of a hypoelastic potential were obtained by Bernstein [16,17] and Ericksen [18]. The issue of elastic dissipation in closed path loading observed by Koji and Bathe [4] was consistent with the hypoelastic model non-integrability in the sense of Green elasticity (hyperelasticity) reported earlier by Bernstein [16,17].

None of the original or modified hypoelastic models were consistent with the isotropic finite deformation behavior of elastic materials. Furthermore, hypo-based plasticity models could not accurately predict the experimentally observed second order effects under shear loading of cylindrical bars (the so-called Swift effect [19]).

A more realistic prediction of the Swift effect was obtained by Atluri and Reed [20]. The Jaumann rate of back stress and the back stress tensor itself were employed in their back stress evolution.

A different approach was used by Reinhardt and Dubey [21] and Xiao et al. [22] to derive a consistent rate of stress for which the hypoelastic model is unconditionally integrable and consistent with the notion of elasticity. The concept of Green elasticity entails existence of an elastic potential from which a direct relation between conjugate stress and strain is derivable. Experimental results by Anand [23,24] have shown that the logarithmic measure of strain (Hencky's strain) provides a good approximation to the elastic part of the deformation for metals subject to large deformation. Based on this observation it is desirable to have a hypoelastic material model which in its integrated form returns a Hookean response for the material based on the Hencky strain. Following the work of Lehmann et al. [25], Reinhardt and Dubey [21] and Xiao et al. [22] introduced a new objective rate of stress called the D or logarithmic rate. This new rate of stress resolved the issues of finite deformation. Later, it was shown by Xiao et al. [26] that this specific rate makes the grade-zero hypoelastic model unconditionally integrable as a Cauchy and Green elastic material. The logarithmic (D) rate of stress made the hypoelastic model integrable as an elastic material, which related the Kirchhoff stress to the logarithmic strain in its integrated form. Based on this, Bruhns et al. [27] developed a self-consistent Eulerian rate form of elastoplasticity using the D or logarithmic rate of stress and applied it to the solution of the simple shear problem. The so-called Swift effect was accurately

predicted when the logarithmic (D) rate of stress was used [28]. As a result, it has been suggested by Xiao et al. [26] that the logarithmic rate is the only rate of stress that can produce consistent results. It will be shown in this work that other well-known rates such as the Jaumann and Green-McInnis-Naghdi rates can equally produce consistent results for elastic and elastoplastic behavior of hardening materials.

The second class of constitutive models uses a multiplicative decomposition of the deformation gradient and is based on the assumption of an intermediate stress-free configuration. This decomposition and its corresponding intermediate configuration are physically well grounded based on the observations of crystal plasticity [29]. This class of constitutive models mostly uses a hyperelastic strain energy function for the elastic part of deformation and as a result issues regarding model non-integrability as found in hypo-based models do not appear in this class of models. Decomposition of the deformation into elastic and plastic parts results in a modified additive decomposition of the strain rate tensor. Unlike Eulerian rate models, constitutive models of this class are involved with two different configurations. The intermediate configuration is usually used to update the plastic internal variables and is stress-free while the elastic part is updated on the current deformed configuration. Mathematically, using such constitutive models requires successive pulling-back and pushing-forward of kinematic and kinetic state variables during the stress update procedure [30,31]. The problem of back stress oscillation might still be present in some hyper-based model of elastoplasticity due to

inconsistent use of tensors and their corresponding transformations [32]. Furthermore, for cases other than isotropic plasticity, for which principal axes of elastic stretch and Kirchhoff stress do not coincide, a complicated measure of stress is the work conjugate to the logarithmic strain which complicates the formulation [32,33].

Numerical implementation of the above mentioned classes of constitutive models is another key factor in developing constitutive models for finite deformations. From one point of view, Eulerian rate models provide simple algorithmic implementations due to the fact that only one configuration is involved during the integration process. However, the requirement of objectivity and more generally spatial covariance entails use of objective integration schemes [30]. Furthermore, an exact (closed form) algorithmic linearization of the Eulerian rate-type models might not exist if different objective rates of stress are used [30]. On the other hand, the class of models based on multiplicative decomposition of the right stretch tensor bypasses the requirement of an objective time integration scheme [30,32,34]. However, due to the involvement of two different configurations for elastic and plastic parts of the deformation, successive pull-back and push-forward of state variables are required during time integration, which complicates the algorithmic implementation of such models. One major drawback in numerical implementation of this class of models is that pull-back and push-forward of tensors are not orthogonal transformations. As a result, constitutive models formulated in the deviatoric space, such as evolution equations for back stress, do not preserve the deviatoric property during transformation from one configuration to the other [35,36].

A volumetric/deviatoric decoupling of the kinematics and kinetics variables is therefore needed during time integration.

For both classes of constitutive models, the well-known return mapping algorithm [37,38] can be used for the plastic update. However, material rotations for finite deformation affect the applicability of the corrective step in the direction of the trial normal vector. For some constitutive models, return in the trial direction is exact, while for others return mapping can be used in an approximate sense [30].

1.3 Objectives and outline of the thesis

The primary aim of the present work is to develop a consistent Eulerian rate form of elasticity and to apply it to set up a self-consistent plasticity model for arbitrary rates of stress. The derived model can be used for any objective rate of stress, resulting in identical stress responses. Furthermore, a new multiplicative decomposition of the right stretch tensor is proposed and used for a Lagrangian formulation of finite deformation plasticity. This formulation is based on the logarithmic measure of the plastic stretch tensor and a new back stress evolution equation is used in the model based on this measure of plastic strain. The proposed Lagrangian model is a unified hyper-based model which is equivalent to the self-consistent Eulerian rate-type model for finite strain elastoplasticity. Both the proposed Eulerian and Lagrangian models resolve all of the issues reported in finite strain elastoplasticity and produce results that are in excellent agreement with

experimental results. The models are capable of correctly modeling large deformation induced phenomena such as the well-known Swift effect. It is worth mentioning that the developed models do not break at larger deformation and are valid over a large range of finite strains. The organization of the thesis is as follows.

In Chapter 2, the basic kinematics of finite deformation is discussed in detail. Objective rates of stress corresponding to different spinning frames of reference are presented. Different measures of stress on different configurations are reviewed. Work conjugacy in its original and unified forms is discussed in detail and as a result the physically accepted Lagrangian and Eulerian conjugate pairs of stress and strain are introduced. The hypoelastic models based on the conjugate pair of stress and strain for different objective rates of stress is presented next. Integrability conditions for the hypoelastic model are used to show the soundness of the recently discovered logarithmic (D) rate of stress for a self-consistent Eulerian rate model of elastoplasticity for finite deformations.

In Chapter 3, classical infinitesimal plasticity models are reviewed and their thermodynamic consistency is discussed. Additional requirements for the extension of classical infinitesimal plasticity models to hypo-based plasticity models for finite strain analysis are discussed. The physical applicability of the additive decomposition of the strain rate tensor, widely used in hypo-based plasticity models, is further discussed. Finally, numerical integration of classical hypo-based plasticity models is

presented and implemented in a general finite element code. The finite element implementation is used to solve finite strain problems for different loading paths.

In Chapter 4, a generalized Eulerian rate form of elasticity is proposed. Integrability conditions of this model for a general stress-dependent elasticity tensor is examined and it is shown that the grade-zero model is unconditionally integrable for arbitrary corotational rates. Closed form solutions for different problems including simple shear and four-step closed path elastic loading are presented and compared to available results. Numerical implementation of the proposed model is also developed and discussed in detail. The model is further implemented for setting up an Eulerian rate form of plasticity which does not assign any preference to the choice of objective rates. The proposed unified model is integrated for two cases of deformation where the principal axes of the Kirchhoff stress and stretch are either coinciding or non-coinciding. Finally, the model is extended to combined nonlinear kinematic/isotropic hardening behavior. Response of the model is compared with experimental results for finite torsional loading of SUS 304 stainless steel tubes. The predicted Swift effect from the model is compared with the experiments on SUS 304 cylindrical bars under finite fixed-end torsion available in the literature.

In Chapter 5, a novel kinematic decomposition of the right stretch tensor is proposed. Based on this decomposition a hyper-based Lagrangian form of elastoplasticity is proposed which utilizes Hencky's plastic strain for plastic internal variables. The Lagrangian axis of the plastic right stretch tensor is used for the

integration of the proposed model. Response of the model for the linear kinematic hardening behavior of the material under simple shear is compared with those of the self-consistent Eulerian rate form of elastoplasticity developed earlier. The proposed Lagrangian model updates all of the elastic and plastic variables with no reference to objective rates. Finally, the model is applied to predict the mixed nonlinear hardening behavior of SUS 304 stainless steel. The so-called Swift effect predicted by the proposed model is compared with available experimental observations.

Finally, in Chapter 6 the concluding remarks are presented and recommendations for future work are suggested.

Chapter 2

Review of Elastic constitutive models for finite deformations

Constitutive models used to describe the deformation of a continuum body must satisfy a set of general principles. These rules are mainly associated with rational continuum mechanics and are described in detail by Truesdell and Noll [6] and Malvern [8]. Constitutive models should be consistent with thermodynamic considerations such as balance of mass and energy as well as being invariant under change of units. The following is a brief review of principles in constitutive modeling.

2.1 General principles

The principle of local action states that the state variables used in any constitutive model at each point are affected by the history of a small neighborhood around this point. Any motion outside this small neighborhood may be disregarded in determining the evolution of state variables.

The principle of determinism states that the current state of the body depends only on the history of its motion and states of the points belonging to the body. In other words, history of the motion of a continuum body determines the stress in that body.

The principle of material frame-indifference (Objectivity) enforces constitutive models for finite deformation to be invariant under rigid motion and a change in the frame of reference. This principle in fact requires use of objective quantities in constitutive models and states that different observations should not affect the response of a constitutive model.

The principle of work conjugacy requires use of consistent measures of stress and strain in a constitutive model. Such consistency is defined by the thermodynamics of the system and is based on the balance of energy.

Additional principles apply for simple rate-type constitutive models and will be discussed at the end of this chapter.

2.2 Kinematics for finite deformation

In the description of the motion of a deforming body, two different reference configurations can be used. The spatial (Eulerian) configuration, which is fixed in space, is usually used for spatial measures of tensor variables, while a Lagrangian or convected (material) one is used for convected variables and deforms along with the body.

The coordinate vector $\mathcal{R}$ of a particle $\mathcal{P}$ in its initial configuration at time $t = 0$ is given by

$$\mathcal{R} = X_i N_i = X_i n_i \tag{2-1}$$

The vectors N_i and n_i represent the material and spatial direction vectors, respectively. At time $t = \tau$ the particle has the same coordinate representation in the Lagrangian system, whereas the coordinate vector in the Eulerian system changes to

$$\mathcal{r} = x_i n_i \tag{2-2}$$

The deformation gradient of this motion is described by

$$F = \left[\frac{\partial x_i}{\partial X_j}\right] \tag{2-3}$$

Such a measure of deformation given by (2-3) contains both the rigid rotation and stretch of the material. A polar decomposition of the deformation gradient can be used to decompose it into a pure stretch of the body and its orthogonal rigid rotation

$$F = RU = VR \tag{2-4}$$

in which R is the rigid rotation and U and V are the right and left stretch tensors, respectively. The decomposition (2-4) offers two different representations of the deformation of the body. The left stretch tensor is representation in the fixed or Eulerian background, while the right stretch tensor is observed in a rotated frame, referred to as the Lagrangian (but not convected) frame. The components of the two-point tensor F are however expressed on a mixed Lagrangian/Eulerian basis.

Due to the symmetry of the stretch tensor, an orthogonal transformation can be applied to transform the right and left stretch tensors onto their principal axes as follows:

$$\Lambda = R_E^T V R_E = R_L^T U R_L = diag(\lambda_i) \tag{2-5}$$

in which λ_i's are eigenvalues of the stretch tensor and R_L and R_E are the rotations of the Lagrangian and Eulerian triads, respectively. Use of equations (2-4) and (2-5) gives the following relationship between the Lagrangian and Eulerian rotations:

$$R_E = R R_L \tag{2-6}$$

The deformation gradient and the stretch of the body is one way of measuring deformation; however, it is more convenient to describe the deformation of a body through strain-displacement relationships. Assuming an infinitesimal line element on the undeformed and deformed surfaces of the continuum body, the square of the corresponding arc length can be given by

$$dS^2 = d\mathcal{R}.d\mathcal{R} = dX_i dX_i$$
$$ds^2 = \frac{\partial r}{\partial X_i}.\frac{\partial r}{\partial X_j} dX_i dX_j = C_{ij} dX_i dX_j \quad (2\text{-}7)$$

where C_{ij} is the matrix of the metric tensor and is called Cauchy-Green deformation tensor. A measure of strain can be defined by the difference between the square of the current and initial arc lengths as follows:

$$ds^2 - dS^2 = \left(C_{ij} - \delta_{ij}\right) dX_i dX_j = 2\varrho_{ij} dX_i dX_j \quad (2\text{-}8)$$

where ϱ_{ij} represents the components of the Green-Saint-Venant strain tensor and δ_{ij} is the Kronocker delta.

Push-forward of the Green strain tensor onto the current (spatial) configuration leads to the Eulerian measure of the strain tensor given by

$$\xi_{ij} = F_{ki}^{-1} \varrho_{kl} F_{lj}^{-1} = \frac{1}{2}\left(\delta_{ij} - F_{ki}^{-1} F_{kj}^{-1}\right) \quad (2\text{-}9)$$

in which ξ_{ij} represents the components of the Almansi-Euler strain tensor.

A general definition of the strain measure was given by Hill [8] based on the right stretch tensor:

$$\mathcal{E}^{\left(\frac{n}{2}\right)} = \frac{1}{n}(U^n - I) \quad (2\text{-}10)$$

in which I is the identity tensor and n is an integer number. Setting $n = 2$ gives the definition of the Green strain tensor, i.e. $\mathcal{E}^{(1)} = \varrho$. The Lagrangian Hencky (logarithmic) strain tensor can be found by setting $n = 0$

$$\mathcal{E}^{(0)} = ln\, U = I + \frac{1}{1!}\mathcal{E}^{(0)} + \frac{1}{2!}\left[\mathcal{E}^{(0)}\right]^2 + \cdots \tag{2-11}$$

$\mathcal{E}^{(0)}$ represents the Lagrangian form of Hencky's strain measure. The Lagrangian Hencky strain can be rotated onto the current configuration to define its Eulerian counterpart through

$$e^{(0)} = ln\, V = ln(RUR^T) = R\, ln\, U\ R^T \tag{2-12}$$

2.3 Tensor transformation, objectivity, and objective rates

For a body experiencing an orthogonal transformation Q, quantities with reference to the Eulerian triad change while quantities measured with reference to the material frame do not. Eulerian tensors of any order should follow the general transformation rule under any orthogonal transformation (rotation) Q as follows:

$$t^*_{ij\,\ldots mn} = Q_{ip}\, Q_{jr}\, \ldots Q_{ms}\, Q_{nt}\, t_{pr\,\ldots st} \tag{2-13}$$

where t^* represents the components of the Eulerian tensor t in the rotated background. Similarly, two-point second order tensors such as the deformation gradient should transform by

$$F_{ij}^{*} = Q_{ik} F_{kj} \tag{2-14}$$

Let's assume that a body subjected to a constant stress during the deformation history experiences a rigid rotation. Since the stress is held constant on the body its time rate should be zero, i.e. $\dot{\sigma} = 0$. In spatial coordinates under rigid rotation one finds

$$\sigma^{*} = Q\sigma Q^{T} \rightarrow \dot{\sigma}^{*} = \frac{d}{dt}(Q\sigma Q^{T}) = \dot{Q}\sigma Q^{T} + Q\sigma\dot{Q}^{T} \neq 0 \tag{2-15}$$

which shows that the rate of change of stress is not zero. If such a rate of stress is used in a rate-type constitutive model, the response of the body will be incorrectly predicted. According to the principle of frame-indifference, constitutive models should not be affected by any rigid rotation. This leads to the conclusion that material time rates of Eulerian quantities cannot be used in Eulerian rate-type constitutive models. In order to use the time derivative of Eulerian tensors, a rotation independent measure of rate of change is required. Objective rates of Eulerian tensors have been widely used in the literature of continuum mechanics as rotation-independent rates and are briefly reviewed in the next section.

2.3.1 Objective corotational rates

Assuming a spinning frame of reference with spin Ω_{*}, it is possible to relate an orthogonal rotation tensor to this spin by

$$\Omega_* = \dot{Q}_* {Q_*}^T \tag{2-16}$$

The rotated components of any Eulerian tensor such as t on this spinning frame are $t_r = Q_* t {Q_*}^T$. An objective corotational rate of this Eulerian tensor can be defined by

$$\dot{t} = {Q_*}^T (\dot{t}_r + t_r \Omega_* - \Omega_* t_r) Q_* \tag{2-17}$$

Defining $\overset{*}{\dot{t}}_r = \dot{t}_r + t_r \Omega_* - \Omega_* t_r$ as the objective rate of the rotated Eulerian tensor t_r, equation (2-17) follows the general rule of tensor transformation for $\dot{t}$. In other words, if $\dot{t} = 0$ during deformation, the objective rate of its rotated counterpart is also zero. This property satisfies the objectivity requirement for the time rate of Eulerian tensors and therefore equation (2-17) is rotation-independent.

Mathematically, an infinite number of objective rates can be defined [8]. Among these rates are some well-known rates used widely in the literature.

The velocity gradient l can be additively decomposed into a symmetric part d, and a skew-symmetric part w:

$$l = d + w \tag{2-18}$$

in which $l = \left[\frac{\partial v_i}{\partial x_j}\right]$ and v is the particle velocity. The symmetric part d, which is the rate of deformation, is also called the "stretching" or "strain rate" tensor and w is called the material or Jaumann spin and is dual to the vorticity tensor. Other measures of spins are the spin of the Eulerian triad Ω_E and rigid spin Ω_R defined by

$$\Omega_E = \dot{R}_E R_E^T$$
$$\Omega_R = \dot{R} R^T \tag{2-19}$$

Another spin introduced by Hill [39] is the spin of the Lagrangian axis defined by

$$\Omega_L = \dot{R}_L R_L^T \tag{2-20}$$

where the relation $\Omega_R + R_E \Omega_L R_E^T = \Omega_E$ exists between the rigid spin and the Eulerian and Lagrangian spins. It should be noted that the spin of the Lagrangian triad should not be used for the objective rate of Eulerian tensors since under rigid rotation the Lagrangian spin is zero [40]. Relationships between different spin tensors can be obtained on the principal axis of the stretch tensor. Knowing that $\dot{V} = lV - V\Omega_R$, the following relationships can be obtained for different objective rates of the left stretch tensor:

$$\overset{Z}{\dot{V}} = dV + (w - \Omega_R)V$$
$$\overset{J}{\dot{V}} = dV + V(w - \Omega_R) \tag{2-21}$$
$$\overset{E}{\dot{V}} = dV + (w - \Omega_E)V - V(\Omega_R - \Omega_E)$$

in which $\overset{Z}{\dot{V}}$, $\overset{J}{\dot{V}}$, and $\overset{E}{\dot{V}}$ are the objective Z-rate, J-rate, and E-rate of the left stretch tensor, respectively. Transferring equation (2-21) on the principal axis of the left stretch tensor and knowing that $\dot{\Lambda} = R_E^T \overset{E}{\dot{V}} R_E$ in which $\Lambda = \mathrm{diag}(\lambda_i)$ is the diagonalized matrix of the principal stretch tensor, gives:

$$\frac{d\Lambda}{dt} = d^{(e)}\Lambda + \left(w^{(e)} - \Omega_E^{(e)}\right)\Lambda - \Lambda\left(\Omega_R{}^{(e)} - \Omega_E^{(e)}\right) \tag{2-22}$$

in which superscript $^{(e)}$ indicates tensor components taken on the principal axis of the left stretch tensor. Taking the symmetric and skew-symmetric parts of equation (2-22) gives the following relationships [41]

$$w_{ij}^{(e)} - \Omega_{R,ij}^{(e)} = -\frac{\lambda_j - \lambda_i}{\lambda_j + \lambda_i} d_{ij}^{(e)} \; ; (no\ sum, i \neq j)$$

$$\Omega_{R,ij}^{(e)} - \Omega_{E,ij}^{(e)} = -\frac{2\lambda_j \lambda_i}{\lambda_j^2 - \lambda_i^2} d_{ij}^{(e)} \; ; (no\ sum, i \neq j) \tag{2-23}$$

$$\frac{\dot{\lambda}_i}{\lambda_i} = d_{ii}^{(e)} \; ; (no\ sum, i \neq j)$$

Therefore, the following relationships can be obtained for the off-diagonal components of objective rates of the logarithmic strain, ε, [21,40]:

$$\overset{Z}{\dot{\varepsilon}}_{ij}^{(e)} = \frac{2\lambda_j \lambda_i}{\lambda_j^2 - \lambda_i^2} ln \frac{\lambda_j}{\lambda_i} d_{ij}^{(e)} = \frac{E_i - E_j}{sin\, h(E_i - E_j)} d_{ij}^{(e)} \; ; (no\ sum, i \neq j)$$

$$\overset{J}{\dot{\varepsilon}}_{ij}^{(e)} = \frac{\lambda_j^2 + \lambda_i^2}{\lambda_j^2 - \lambda_i^2}\, ln \frac{\lambda_j}{\lambda_i} d_{ij}^{(e)} = \frac{E_i - E_j}{tan\, h(E_i - E_j)} d_{ij}^{(e)} \; ; (no\ sum, i \neq j) \tag{2-24}$$

$$\overset{E}{\dot{\varepsilon}}_{ij}^{(e)} = 0 \; ; (no\ sum, i \neq j)$$

in which $E_i = \ln \lambda_i$ are the principal logarithmic strains. The diagonal components are given by

$$\overset{Z}{\dot{\varepsilon}}_{ii}^{(e)} = \overset{J}{\dot{\varepsilon}}_{ii}^{(e)} = \overset{E}{\dot{\varepsilon}}_{ii}^{(e)} = d_{ii}^{(e)} = \dot{E}_i = \frac{\dot{\lambda}_i}{\lambda_i} \;\; (no\ sum) \tag{2-25}$$

Equations (2-24) and (2-25) show that on the principal axis of stretch the off-diagonal components of the Eulerian rate of the logarithmic strain vanish. This specific property of the E-rate of the logarithmic strain has been extensively used in setting up Eulerian rate-type constitutive models for finite deformation [42,43].

2.3.2 Convected rates

Another class of objective rates can be defined in the material (convected) background. Since the material frame is covariant, a covariant convected rate of Eulerian tensors can be defined. As a result, the general requirement of spatial covariance in constitutive modeling of finite deformation can be met using such convected rates [30]. One example is the covariant rate of the Kirchhoff stress given by

$$\tau = FSF^T \rightarrow \dot{\tau} - l\tau - \tau l^T = F\dot{S}F^T \tag{2-26}$$

where τ is the Kirchhoff stress and S is the second Piola-Kirchhoff stress tensor. Equation (2-26) leads to $\dot{S} = F^{-1}(\dot{\tau} - l\tau - \tau l^T)F^{-T} = F^{-1}\overset{c}{\dot{\tau}}F^{-T}$ where $\overset{c}{\dot{\tau}}$ is the convected covariant rate of the Kirchhoff stress also known as the upper Oldroyd rate of stress.

A general definition of the class of Lie derivatives of spatial tensors can be given by

$$L_v t = \phi_* \frac{d}{dt} \phi^*(t) \tag{2-27}$$

where L_v is the Lie operator, ϕ_* is the push-forward operator, and ϕ^* is the pull-back operator [34,44]. Operators ϕ_* and ϕ^* act differently on the kinematic and kinetic tensor variables in order to be consistent with the invariance of the stress power in different backgrounds. Table 2-1 briefly shows the effect of these operators on tensor variables.

Table 2-1 Pull-back and push-forward operators [34]

Type of tensor	Push-forward ϕ_*	Pull-back ϕ^*
Kinematic (covariant-covariant tensors)	$\phi_*(\blacksquare) = F^{-T}(\blacksquare)F^{-1}$	$\phi^*(\blacksquare) = F^T(\blacksquare)F$
Kinetic (contravariant-contravariant tensors)	$\phi_*(\bullet) = F(\bullet)F^T$	$\phi^*(\bullet) = F^{-1}(\bullet)F^{-T}$

$L_v \tau$ has a much stronger condition of objectivity which is called "spatial covariance" and as a result this derivative can be used in setting up Eulerian rate models for finite deformation [44]. The principle of material frame-indifference requires invariance under rigid motion and therefore the metric tensor remains unchanged during transformation. However, in the spatial covariance requirement rigid motions (spatial isometries) are replaced by diffeomorphisms where the metric tensor changes tensorially based on the push-forward of the kinematics variables [35,44]. It can be easily shown that the Lie derivative of the Kirchhoff stress tensor is the push-forward of the material time rate of the second Piola-Kirchhoff stress on the current configuration, and is covariant.

Another possibility is to set up an objective rate based on the dual contravariant convected frame. Such a convected derivative can be given by

$$\overset{c}{\dot{t}} = \dot{t} + l^T \tau + \tau l \tag{2-28}$$

Equation (2-28) is defined in the dual space of equation (2-26). This rate of the Kirchhoff stress is also known as the lower Oldroyd rate of the Kirchhoff stress.

The above mentioned Oldroyd rates can be expressed in the mixed covariant-contravariant space as well; however, the two mixed rates obtained do not preserve the symmetry of the tensor on which they are applied.

The requirement of spatial covariance of the constitutive models for finite deformation can be met with the use of the class of convected Lie derivatives; however, some drawbacks may appear with the application of the convected rates. First, orthogonality of the corotational frames no longer exists for the convected frames. One drawback of this is that the deviatoric property of a deviatoric tensor is not preserved for its convected rate. As a result, constitutive equations which are formulated in deviatoric space, such as back stress evolution equations, need further consideration during integration. A detail description of constitutive models based on convected rates and their algorithmic treatment is given in Chapter 5.

2.4 Stress measures

In large deformation analysis a proper measure of stress must be used. Constitutive models formulated on the Eulerian configuration should use a measure of stress which is expressed using the current configuration of the body. One such spatial measure is the Cauchy (true) stress σ, which is a tensor defined by the effect of the actual traction $\mathfrak{t}$ on the current surface (configuration) of the body, with the unit outward normal vector n as observed by a spatially fixed observer

$$\mathfrak{t} = \sigma : n \tag{2-29}$$

Based on the balance of energy, the weighted Cauchy stress (Kirchhoff stress), τ, generates power on the current configuration and is defined by

$$\tau = J\sigma = \frac{\rho_0}{\rho}\sigma \tag{2-30}$$

in which J is the Jacobian of deformation and defines the ratio of the current density of the body to its initial density prior to deformation. Therefore, for a deformation to be physically acceptable, the Jacobian of deformation should be positive.

Another measure of stress can be obtained using Nanson's formula and finding the effect of the applied force on the undeformed configuration. A surface element on the undeformed configuration $N\mathrm{d}S$ is related to its spatial counterpart on the deformed configuration $n\mathrm{d}s$ by

$$JN_j\,dS = F_{ij}\,n_i\,ds \tag{2-31}$$

The boundary force f applied on the current configuration relates the Cauchy stress to its transformed counterpart by

$$f = \sigma : n\,ds = J\sigma F^{-T} : N\,dS \tag{2-32}$$

which results in the following definition for the stress on the undeformed configuration

$$P = \tau F^{-T} \tag{2-33}$$

where P is the non-symmetric first Piola-Kirchhoff stress. The non-symmetry property of this tensor is due to the involvement of two different configurations; the boundary force is measured on the deformed configuration while the effect of it is considered on the original undeformed configuration. The first Piola-Kirchhoff stress tensor is a two-point (mixed) tensor similar to the deformation gradient. If the state of the boundary force is also measured on the undeformed configuration, the second Piola-Kirchhoff stress, *S*, is obtained

$$S = F^{-1}\tau F^{-T} \tag{2-34}$$

Unlike the first Piola-Kirchhoff stress, the second Piola-Kirchhoff stress is a symmetric tensor.

2.5 Work conjugacy

2.5.1 Hill's original work conjugacy

For constitutive models for finite deformations, different measures of strain and stress can be used. A criterion is therefore required for the proper choice of stress and strain measures in constitutive models. The stress power has been shown to be a physically acceptable criterion for the choice of a conjugate stress-strain pair. Based on Hill's original work [39], and Truesdell and Noll [6], any pair of Lagrangian or Eulerian measures of stress and strain can be used in a constitutive model provided they produce equivalent stress power. According to the first law of thermodynamics, conservation of energy should be satisfied for any deforming continuum body. From the balance of energy the stress power is given by

$$\dot{W} = \tau : l = \tau : (d + w) = \tau : d \tag{2-35}$$

in which $\dot{W}$ is the stress power. Equation (2-35) shows that the material spin has no effect on the stress power.

Hill [45,46] states that Lagrangian measures of strain and stress can be used in constitutive models for finite deformation if they furnish the same stress power given in equation (2-35). This implies that a pair of Lagrangian strain $\mathcal{E}$ and stress $\mathcal{T}$ is work conjugate if

$$\dot{W} = \mathcal{T} : \dot{\mathcal{E}} = \tau : d \tag{2-36}$$

Such a criterion for Lagrangian measures of strain and stress has been found to be successful in setting up constitutive models for finite deformation [39,45,46].

The original definition of Hill's work conjugacy fails to define a similar criterion when Eulerian measures of strain and stress are used, as stated by Hoger [33] and Ogden [47]. Furthermore, the rotated Kirchhoff stress, $\bar{\tau} = R^T \tau R$, which is a Lagrangian measure of Kirchhoff stress and has a wide application in Lagrangian constitutive models (cf. Green and Naghdi [12], and Simo and Marsden [48]) cannot be assigned any conjugate strain through the original Hill's work conjugacy [33,47]. As a result, a unified definition of work conjugacy for both the Lagrangian and Eulerian measures of stress and strain is required.

2.5.2 Unified work conjugacy

For the Eulerian strain and stress measures, Hill's original work conjugacy cannot be used because of the non-objectivity of the material time rate of the Eulerian strain. Hoger [33] derived expressions for the conjugate stress to the Lagrangian logarithmic strain on the principal axis of the right stretch tensor. It was further shown that for the case of isotropic elasticity, for which the principal axes of stress and stretch tensor coincide, the rotated Kirchhoff stress is conjugate to the Lagrangian logarithmic strain. Basis-free expressions for the conjugate stress to the Jaumann rate of the Eulerian logarithmic strain were derived by Lehmann and Liang [49]. Xiao [50] derived basis-free expressions for the conjugate stress to arbitrary Lagrangian measures of the Hill's strain tensor. Nicholson [51,52] derived relations for conjugate

measures of stress to the Jaumann rate of different measures of deformation, using the method of the Kronecker product [53]. More recently, Asghari et al. [54] derived basis-free expressions for the Jaumann rate of arbitrary Eulerian measures of strain based on Hill's original work conjugacy. In general, the derived conjugate stress tensors to the Eulerian strain tensors are based on objective rates of the Eulerian strains. A unified definition of Hill's original work conjugacy can be obtained using objective rates of the Eulerian strain.

With the help of three orthogonal eigenvectors of the right and left stretch tensors, denoted by the Lagrangian triad $\{N\}$ and the Eulerian triad $\{n\}$, and the eigenvectors of the stretch tensor λ_i, a general definition of Hill's strain tensor can be given by

$$e = \sum_{i=1}^{3} \mathfrak{f}(\lambda_i) n_i \otimes n_i = \mathfrak{f}(V)$$
$$\mathcal{E} = \sum_{i=1}^{3} \mathfrak{f}(\lambda_i) N_i \otimes N_i = \mathfrak{f}(U) \tag{2-37}$$

in which $\mathfrak{f}(\lambda_i)$ is a smooth and monotonically increasing scale function with the property $\mathfrak{f}(1) = \mathfrak{f}'(1) - 1 = 0$. According to Hill [39], Ogden [47] and Doyle and Ericksen [55], a general form for such a scale function can be defined by

$$\mathfrak{f}(\lambda) = \frac{1}{m}(\lambda^m - 1) \tag{2-38}$$

where m is an integer number. As a result, Hill's generalized strain definition can be given by

$$e = \frac{1}{m}(V^m - I)$$
$$\mathcal{E} = \frac{1}{m}(U^m - I) \tag{2-39}$$

in which the relation $\mathcal{E} = R^T e R$ exists. Let's assume that a Lagrangian stress measure $\mathcal{T}$ and its Eulerian counterpart $\boldsymbol{t} = R\mathcal{T}R^T$ are given. Furthermore, in an Ω_*-spinning frame with rotation R_* the rotated counterparts of stress and strain are given by $\boldsymbol{t}_r = R_*^T \boldsymbol{t} R_*$ and $e_r = R_*^T e R_*$, respectively. An observer in the spinning background sets up the following scalar product:

$$\boldsymbol{t}_r : \dot{e}_r = (R_*^T \boldsymbol{t} R_*) : \overline{(R_*^T e R_*)}^{\cdot} \tag{2-40}$$

The scalar product given by equation (2-40) is the same as a scalar product set up by a fixed observer for a Lagrangian stress and strain pair. Following a similar definition for Hill's original work conjugacy, a modified form of work conjugacy can be found in an arbitrary spinning background as follows:

$$\dot{W} = \boldsymbol{t}_r : \dot{e}_r = (R_*^T \boldsymbol{t} R_*) : \overline{(R_*^T e R_*)}^{\cdot} = \boldsymbol{t} : \overset{*}{\dot{e}} \tag{2-41}$$

Equation (2-41) defines a unified work conjugacy in an Ω_*-spinning frame for any pair of Eulerian strain and stress measures $(\boldsymbol{t}, e)$ [56]. Since both $\dot{W}$ and $\boldsymbol{t}$ are objective, use of equation (2-41) requires that the corresponding rate of the Eulerian strain be also an objective rate. In other words, the spinning background in which the rates are measured should be an objective corotational frame. Xiao et al. [56] further discussed the applicability of the unified work conjugacy given by (2-41) for all of

the objective rates. According to Xiao et al. [56] a linear transformation tensor relates the stretching tensor to the objective rate of the Eulerian strain tensor by

$$\overset{*}{\dot{e}} = \mathbb{L}_*[d] \tag{2-42}$$

where $\mathbb{L}_* = \widetilde{\mathbb{L}}_*(b)$ is a fourth-order transformation tensor function of the left Cauchy-Green tensor b possessing the major and minor symmetries. Use of equations (2-41) and (2-42) results in

$$\tau = \mathbb{L}_*[t] \tag{2-43}$$

Equation (2-43) implies that the fourth-order transformation tensor $\mathbb{L}_*$ should be a nonsingular transformation between symmetric second-order tensors. This means that a one to one correspondence between the stretching tensor d and $\overset{*}{\dot{e}}$ should exist [56]. As a result, the unified work conjugacy is applicable for all of the objective corotational rates provided that $\mathbb{L}_*$ is a nonsingular transformation.

The unified work conjugacy can also be used for the Lagrangian measures of stress and strain [56]. Knowing that $\mathcal{E} = R^T e R$ and $\mathcal{T} = R^T t R$, pre and post multiplying the work conjugacy (2-41) by the rigid rotation gives:

$$\dot{W} = R^T \left(t : \overset{*}{\dot{e}} \right) R = (R^T t R) : \left(R^T \overset{*}{\dot{e}} R \right) = \mathcal{T} : \overset{*-Z}{\dot{\mathcal{E}}} \tag{2-44}$$

which is similar to Hill's original work conjugacy for Lagrangian measures of stress and strain. In equation (2-44) $\overset{*-Z}{\dot{\mathcal{E}}} = \dot{\mathcal{E}} - \Omega_{*-Z}\mathcal{E} + \mathcal{E}\Omega_{*-Z}$ is the relative objective rate of the Lagrangian strain and $\Omega_{*-Z} = R^T(\Omega_* - \Omega_R)R$. Equation (2-44) defines a

conjugate pair of the Lagrangian measure of the stress and strain in an Ω_{*-Z}-spinning frame. It is clear that, for the case of Z-frame with rigid spin $\Omega_* = \Omega_R$, the relative spin Ω_{*-Z} vanishes and Hill's original work conjugacy is obtained.

2.6 Finite Elasticity and Hypoelastic material models

For an isotropic linear elastic material the generalized Hook's law is given by

$$\tau = \kappa\, tr(\varepsilon) I + 2\mu\varepsilon \tag{2-45}$$

in which "tr" indicates the trace function and κ and μ are Lame's constants. For the case of infinitesimal elasticity, any measure of strain and stress can be used in (2-45) because the deformations are so small that deviation from infinitesimal engineering strain is negligible. However, for finite deformation analysis a proper choice for strain and stress measures should be used in (2-45). From work conjugacy, any conjugate pair of Lagrangian or Eulerian measure of stress and strain can be used in the Hookean model given by (2-45). One possible choice is the Eulerian Hencky (logarithmic) strain and the Kirchhoff stress. Another choice is the Green-Lagrange strain and the symmetric second Piola-Kirchhoff stress. Another possibility is the use of the Kirchhoff stress and the Eulerian counterpart of Green's strain. From one point of view, use of Green's strain is more convenient because the reference configuration is the initial undeformed configuration of the body, while the Eulerian logarithmic strain refers to the current deformed configuration. However, unlike to the

logarithmic strain, Green's strain cannot be simply decoupled into an additive deviatoric/volumetric form. Therefore, use of the logarithmic strain is more convenient in this case. Furthermore, response of the model using the Kirchhoff stress and the logarithmic strain shows better agreement with experimental observations for moderate elastic deformations of metals [21,24]. Therefore, use of the Kirchhoff stress and the Eulerian logarithmic strain in the Hookean model given by (2-45) gives good prediction of finite elastic Hookean response of metals.

For the case of small strain elasticity, a quadratic strain energy function exists from which the Hookean model is derivable [8]. As a result, the infinitesimal Hookean elastic model given in (2-45) is consistent with the notion of hyperelasticity. In finite deformation analysis, a rate-type form of the linear elasticity is required because of the differential-type constitutive models for the inelastic part of the deformation. One important consideration is whether the integrated form of a rate-type model yields the Hookean response for finite deformation or not. In other words, integrability of the rate-type models in the sense of Cauchy and Green elasticity (hyperelasticity) should be considered when rate-type models are used for finite deformation analysis. Such integrability conditions are discussed in more detail in the following sections.

2.6.1 Simple materials and Cauchy elasticity

Assuming an observer O reports the motion of a body $\mathcal{B}$ using

$$x = x(X,t)\ ; X \in \mathcal{B} \tag{2-46}$$

If $\sigma(x,t)$ represents the Cauchy stress at time t corresponding to the material point X with current coordinates $x = x(X,t)$, then according to the principle of determinism the Cauchy stress depends on the history of the motion of the body [47]

$$\sigma(x,t) = \mathcal{G}(\chi^t; X, t) \tag{2-47}$$

where $\mathcal{G}$ is the stress functional with respect to its first argument and a function of its second and third arguments, and $\chi^t(X,s) = \chi(X, t-s)$ is the history of the motion of the body for $s \geq 0$. A new observer O_* under the frame transformation $x_* = Q(t)x + c(t)$ and $t_* = t - a$ reports the Cauchy stress using $\sigma_r(x_*, t_*) = Q(t)\sigma(x,t)Q(t)^T$. Material objectivity then requires that

$$\sigma_r(x_*, t_*) = \mathcal{G}({\chi_*}^{t_*}; X, t_*) \tag{2-48}$$

Assumption of the spatial locality of material response simplifies the constitutive law given by (2-47). If two motions χ and $\bar{\chi}$ are present such that for all the particles X' belonging to a small neighborhood $\mathcal{N}(X)$ of the body, the relation $\bar{\chi}(X', s) = \chi(X', s)$ exists and if $\mathcal{G}(\bar{\chi}^t; X, t) = \mathcal{G}(\chi^t; X, t)$, then the history of any motion outside the neighborhood $\mathcal{N}(X)$ has no effect on the material response. This condition is a mathematical representation of the principle of local action used in classical constitutive models.

A material is said to be a "simple material" at coordinate X if for every deformation at X its response is uniquely defined by its response to deformations

homogeneous in a neighborhood of X [47]. As a result, relative to any chosen reference configuration χ_0 the Cauchy stress is related to deformation by

$$\sigma(x,t) = \mathcal{G}_0(Grad\ \chi_X^t; X, t) \tag{2-49}$$

where $\text{Grad}\ \chi_X^t$ is the history of the deformation gradient at X relative to a chosen reference configuration and $\chi_X^t(X', s) = \chi^t(X', s) - \chi^t(X, s)$. If in equation (2-49) the Cauchy stress is assumed to be a function of the deformation gradient only (excluding history dependency), then the simple material is an elastic Cauchy material. For Cauchy elastic materials, the stress response is independent of the rate at which the deformation occurs and the path of loading. However, the work done by the stress is not necessarily path independent and the stress is not derivable from a scalar potential function, and therefore has a non-conservative structure [47]. For a Cauchy elastic material the functional given by equation (2-49) reduces to a function as follows:

$$\sigma\{\chi(X,t), t\} = \mathcal{G}_0(F; X) \tag{2-50}$$

where $F(X,t) = \text{Grad}\ \chi(X,t)$. With the assumption of homogeneity of the elastic properties, the constitutive model for a Cauchy elastic material can be further simplified to:

$$\sigma = \mathcal{G}(F) \tag{2-51}$$

where $\mathcal{G}$ is the response function of the Cauchy elastic material. The requirement of objectivity restricts the response function to satisfy the following transformation [8,30,47]

$$\mathcal{G}(QF) = Q\mathcal{G}(F)Q^T \tag{2-52}$$

for all orthogonal transformations Q and arbitrary deformation gradients F. Such a restriction suggests the use of a Lagrangian measure of deformation, such as the right Green-Cauchy deformation tensor, the Green-Lagrange strain tensor (or Green's Strain) and/or objective Eulerian measures of deformation in (2-51), instead of the deformation gradient [30,47]. One possible choice for the orthogonal transformation in (2-52) is the rigid rotation of the material, i.e. $Q = R$. Use of relation $F = RU$ and $Q = R$ in equation (2-52), gives the following Cauchy elastic model based on the right stretch tensor:

$$\sigma = \mathcal{G}(F) = R\mathcal{G}(U)R^T \tag{2-53}$$

The stress function given in equation (2-51) can also be expressed in terms of the first Piola-Kirchhoff stress by

$$P = JF^{-1}\sigma = JF^{-1}\mathcal{G}(F) = \mathcal{H}(F) \tag{2-54}$$

Equation (2-54) is another form of the response function for a Cauchy elastic material in terms of the nominal stress and deformation gradient. Due to the symmetry of the Cauchy stress, the restriction $F\mathcal{H}(F) = \mathcal{H}(F)^T F^T$ applies on the stress function

given by (2-54). Also material objectivity requires that $\mathcal{H}(QF) = \mathcal{H}(F)Q^T$ and as a result:

$$P = \mathcal{H}(U)R^T \tag{2-55}$$

where $\mathcal{H}(U) = JU^{-1}\mathcal{G}(U)$.

2.6.2 Green elasticity

The stress power per unit volume can be expressed in terms of $\dot{W} = P:\dot{F} = \mathrm{tr}\left\{\mathcal{H}(F)\dot{F}\right\}$. In general $\mathrm{tr}\{\mathcal{H}(F)\mathrm{d}F\}$ is not an exact differential for Cauchy elastic materials. However, if a scalar function exists such that $\dot{W} = \mathrm{tr}\left\{\mathcal{H}(F)\dot{F}\right\} = \mathrm{tr}\left\{\frac{\partial W}{\partial F}\dot{F}\right\}$, then the stress function $\mathcal{H}(F)$ is derivable from the elastic potential energy function (strain energy function) by

$$P = \mathcal{H}(F) = \frac{\partial W}{\partial F} \tag{2-56}$$

A Cauchy elastic material for which such a strain energy function exists is called a Green elastic or hyperelastic material and W is its corresponding hyperelastic function (strain energy function). Green elasticity is a more special form of the class of Cauchy elastic materials and therefore all characteristics and restrictions applied to Cauchy elastic materials should also be applied to Green elastic materials [47].

The same requirement of objectivity leads to the conclusion that $W(F) = W(U) = W(V)$. For the case of isotropic elasticity the strain energy function can be expressed in terms of principal stretches as follows:

$$W(U) = W(V) = W(\lambda_1, \lambda_2, \lambda_3) \tag{2-57}$$

Or more generally it might be expressed as a function of the stretch tensor invariants by

$$W(U) = W(V) = W(I_1, I_2, I_3) \tag{2-58}$$

in which $I_1 = \lambda_1^2 + \lambda_2^2 + \lambda_3^2$, $I_2 = \lambda_1^2\lambda_2^2 + \lambda_1^2\lambda_3^2 + \lambda_2^2\lambda_3^2$, and $I_3 = \lambda_1^2\lambda_2^2\lambda_3^2$. The strain energy function given by (2-58) can be a linear or nonlinear function of the stretch invariants for the class of hyperelastic materials. A simple quadratic strain energy function results into the well-known linear Hookean model. Use of higher order polynomials for the strain energy function results in nonlinear hyperelasticity [6,8,47]. For the Hookean constitutive model given in equation (2-45) the following quadratic complementary hyperelastic function exists [30]

$$\mathcal{Z}(\tau) = \frac{1+\nu}{2E} tr\,\tau^2 - \frac{\nu}{2E}(tr\,\tau)^2 \tag{2-59}$$

where ν and E are the material Poisson's ratio and elastic modulus. As a result, the Eulerian logarithmic strain is derivable from the complementary potential $\mathcal{Z}$ as follows:

$$\varepsilon = \frac{\partial \mathcal{Z}}{\partial \tau} = M^{-1} : \tau \tag{2-60}$$

where $M^{-1} = \frac{\partial^2 \mathcal{Z}}{\partial \tau \partial \tau} = \frac{1+\nu}{E}\mathbb{I} - \frac{\nu}{E} I \otimes I$ is the fourth-order isotropic compliance tensor, I is the second order identity tensor, and $\mathbb{I}$ is the fourth order identity tensor. Equation (2-60) clearly shows that the extended finite deformation Hookean model given by equation (2-45) is consistent with the notion of hyperelasticity.

2.6.3 Hypoelasticity

Eulerian rate-type models for finite elastoplasticity use a spatial rate model for the elastic part of the deformation. The additive decomposition of the strain rate tensor into its elastic and inelastic parts has been widely used in the literature of finite deformation [57]. Hypoelastic models introduced by Rivlin [58] and Truesdell [59] are simple rate-type material models expressed as a linear function of the strain rate tensor and relate an objective rate of the Kirchhoff stress to the elastic part of the strain rate tensor by

$$\overset{*}{\dot{\tau}} = \mathcal{M}(\tau) : d \tag{2-61}$$

where $\mathcal{M}(\tau)$ is the fourth-order stress-dependent hypoelasticity tensor. For a grade-zero hypoelastic model, the fourth-order hypoelastic tensor is stress-independent and the hypoelastic model given in (2-61) reduces to

$$\overset{*}{\dot{\tau}}_d = 2\mu d_d \tag{2-62}$$

where a subscript "*d*" denotes the deviatoric part of a tensor. The hydrostatic part of the stress is related to the trace of the strain rate tensor by $\dot{p} = \frac{1}{3}\mathrm{tr}(\dot{\tau}) = \frac{3\kappa+2\mu}{3}\mathrm{tr}(d)$.

In general, no restrictions on the choice of objective rate of the Kirchhoff stress were given in the classical model of hypoelasticity and any objective rate of stress (corotational or convected) could be used with this model. However, recent development in finite deformation analysis restricts the use of hypoelastic models to a specific rate of stress [21,22,26].

2.6.4 Issues with hypoelasticity

Hypoelastic models have been widely used in setting up the Eulerian rate formulation of elastoplasticity and viscoplasticity. The hypoelastic part of such Eulerian models is used for the elastic deformation and stress update. It is expected that a hypoelastic model returns the Hookean response in its integrated form; as a result, one important concern about hypoelastic materials is whether they are elastic materials and consistent with the notion of Cauchy or Green elasticity.

While all Elastic materials are hypoelastic (cf. Truesdell and Noll [6]) the reverse statement is not true in general. This means that, a given hypoelastic model does not necessarily provide an elastic response in its integrated form. This fact can be shown using two different approaches. The first approach is through direct integration of a hypoelastic model for certain simple elastic loading paths to obtain the stress response of the model. The second approach is more general and is through

examining hypoelastic model integrability mathematically. Both approaches are discussed here.

2.6.4.1 Hypoelastic response for certain elastic loading paths

We assume here two cases of deformation. The first case is shear deformation of a cube fixed at one end and sheared at the other end as shown in Figure 2-1. The deformation is homogeneous and the hypoelastic model is integrated using the Jaumann (J) and Green-McInnis-Naghdi (GMN) rates.

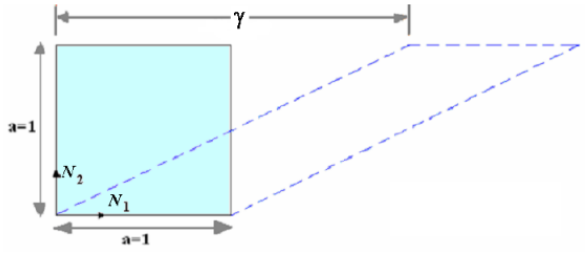

Figure 2-1- Problem of simple shear

The deformation gradient of this motion is given by:

$$F = N_1 \otimes N_1 + N_2 \otimes N_2 + \gamma N_1 \otimes N_2 \tag{2-63}$$

in which γ is the applied shear. The polar decomposition of the deformation gradient yields the following for the rigid rotation and the left and right stretch tensors:

$$\begin{aligned} V &= \frac{1}{\sqrt{4+\gamma^2}}[(2+\gamma^2)N_1 \otimes N_1 + 2N_2 \otimes N_2 + \gamma(N_1 \otimes N_2 + N_2 \otimes N_1)] \\ U &= \frac{1}{\sqrt{4+\gamma^2}}[2N_1 \otimes N_1 + (2+\gamma^2)N_2 \otimes N_2 + \gamma(N_1 \otimes N_2 + N_2 \otimes N_1)] \\ R &= \frac{1}{\sqrt{4+\gamma^2}}[2N_1 \otimes N_1 + 2N_2 \otimes N_2 + \gamma(N_1 \otimes N_2 - N_2 \otimes N_1)] \end{aligned} \tag{2-64}$$

The rigid spin of the material Ω_R is given by

$$\Omega_R = \dot{R}R^T = \frac{2\dot{\gamma}}{4+\gamma^2}(N_1 \otimes N_2 - N_2 \otimes N_1) \tag{2-65}$$

The velocity gradient and its symmetric and skew-symmetric parts are given by

$$l = \dot{\gamma} N_1 \otimes N_2$$

$$d = \frac{\dot{\gamma}}{2}(N_1 \otimes N_2 + N_2 \otimes N_1) \tag{2-66}$$

$$w = \frac{\dot{\gamma}}{2}(N_1 \otimes N_2 - N_2 \otimes N_1)$$

The Kirchhoff stress tensor is a traceless (deviatoric) tensor for this motion. As a result, the hypoelastic model given in equation (2-62) yields the following coupled differentials for the Jaumann and Green-McInnis-Naghdi rates under simple shear motion:

$$J\,rate \begin{cases} \frac{d\tau_{11}}{d\gamma} - \tau_{12} = 0 \\ \frac{d\tau_{12}}{d\gamma} + \tau_{11} = \mu \end{cases} \tag{2-67}$$

$$GMN\,rate \begin{cases} \frac{d\tau_{11}}{d\gamma} - \frac{4}{4+\gamma^2}\tau_{12} = 0 \\ \frac{d\tau_{12}}{d\gamma} + \frac{4}{4+\gamma^2}\tau_{11} = \mu \end{cases} \tag{2-68}$$

Solution of the above coupled linear differential equations yields the following stress response for the J and GMN stress rates

$$\tau_{12} = \mu \sin\gamma \text{ ; (J rate)} \tag{2-69}$$

$$\tau_{12} = 2\mu\left\{\frac{4\gamma\, ln\frac{4+\gamma^2}{4} + (4-\gamma^2)\left(2\, atan\frac{\gamma}{2} - \frac{\gamma}{2}\right)}{4+\gamma^2}\right\};\ (GMN\ rate)$$

To compare the above hypoelastic results with the finite Hookean model, the stress response of the Hookean model given by (2-45) is given as follows. The components of the logarithmic strain for the simple shear problem can be found as

$$\varepsilon = \gamma\eta(N_1 \otimes N_1 - N_2 \otimes N_2) + 2\eta(N_1 \otimes N_2 + N_2 \otimes N_1) \tag{2-70}$$

where $\eta = \frac{\mathrm{asinh}\frac{\gamma}{2}}{\sqrt{4+\gamma^2}}$. Using the Hookean model given by (2-45), the stress components are given by

$$\tau = 2\mu\gamma\eta(N_1 \otimes N_1 - N_2 \otimes N_2) + 4\mu\eta(N_1 \otimes N_2 + N_2 \otimes N_1) \tag{2-71}$$

It should be noted that for the problem of simple shear the Cauchy stress and Kirchhoff stress are the same because $J = 1$. Figure 2-2 shows the stress response for the problem of simple shear using the hypoelastic model with the J and GMN rates of stress as well as the response from the hyperelastic Hookean model.

As shown in Figure 2-2 the stress response from the J rate shows an oscillatory response. The GMN rate shows a monotonically increasing stress response. However, it is not clear whether either solution is physically acceptable. If we are expecting a Hookean response from the hypoelastic model, neither the J rate nor the GMN rate returns the correct response. This example shows that grade-zero hypoelastic models cannot be integrated to return a Hookean elastic response for

arbitrary rates of stress. As a result, the question of a consistent rate of stress is raised here, which will be discussed in details in section 2.6.4.2.

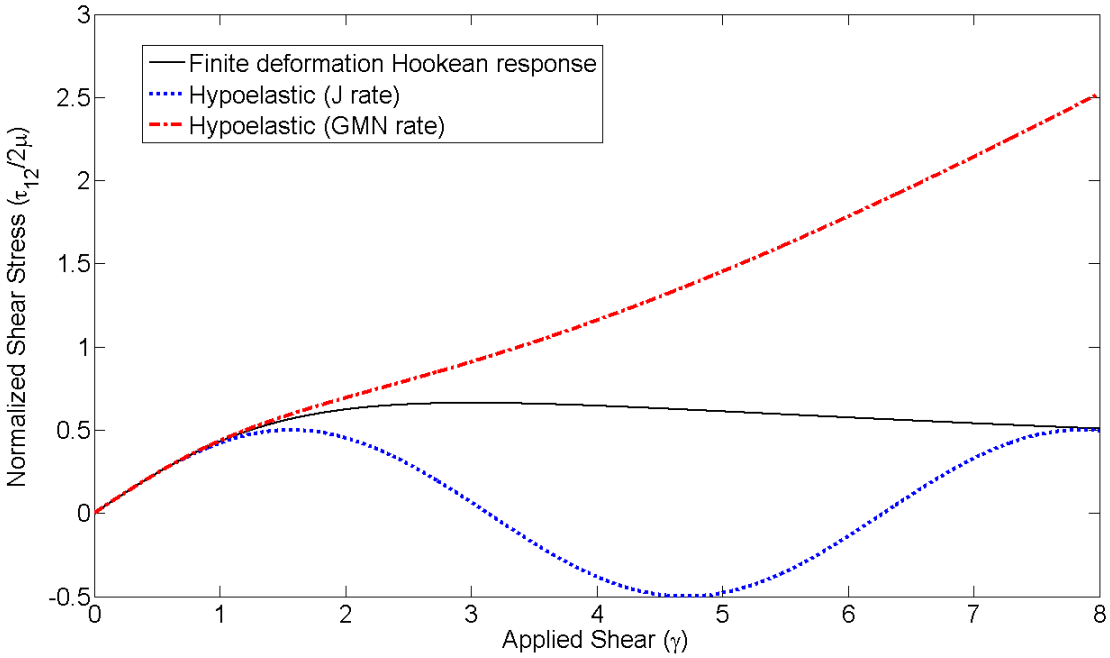

Figure 2-2- Shear stress responses for the problem of simple shear using the hypoelastic and Hookean model

The second example is four-step closed path elastic deformation of a cube. This problem is used to show if hypoelastic models are consistent with the notion of hyperelasticity. As shown in Figure 2-3 a cube of unit length is fixed at one end and the other end is subjected to closed path loading with the following deformation steps:

Step 1- Tension

Step 2- Shearing while previous tension is maintained

Step 3- Removing tension while the previous shear is maintained

Step 4- Removing shear to return to the original configuration

This problem was originally solved by Koji and Bathe [4] for the case of the J rate of stress. In what follows we consider the solution for both the J and GMN rates as well as the Hookean response of the model. The details of the closed form solutions for the J and GMN rates can be found in Lin et al. [60] and only the final stress solutions at the end of each deformation step are reported herein.

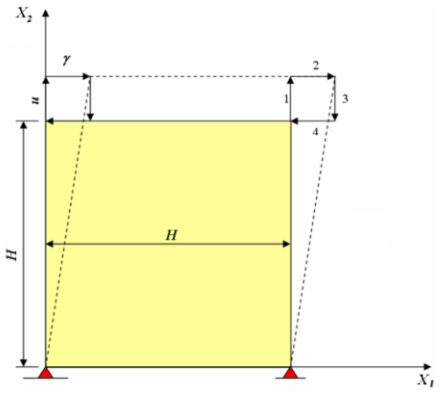

Figure 2-3- Four-step loading

Step 1- Stretching $0 \leq t \leq 1$

The deformation for this step can be expressed by $x_1 = X_1$; $x_2 = AX_2$; $x_3 = X_3$, in which $A = 1 + \frac{u}{H}$ and u linearly increases from zero at $t = 0$ to the maximum of u at $t = 1$. Parameters related to the kinematics of this deformation step are expressed as follows:

$$F = N_1 \otimes N_1 + AN_2 \otimes N_2 + N_3 \otimes N_3$$

$$l = \dot{F}F^{-1} = \frac{\dot{A}}{A} N_2 \otimes N_2 \tag{2-72}$$

$$d = l \; ; \; \Omega_J = w = \underset{\sim}{0} \; ; \; \Omega_R = \dot{R}R^T = \underset{\sim}{0}$$

Since both the material spin tensor Ω_J and the rigid spin Ω_R are zero, both the J and GMN rates of stress are equivalent to their corresponding material time derivatives. Hence, the stress solution for this deformation step for both objective rates is given by

$$\tau_{11} = \kappa \, ln \, A \; ; \; \tau_{22} = (\kappa + 2\mu) \, ln \, A \; ; \; \tau_{12} = 0 \tag{2-73}$$

where κ and μ are Lame's constants.

Step 2- Shearing at constant stretch $1 \leq t \leq 2$

The motion of this step can be expressed by $x_1 = X_1 + \gamma \, X_2 \; ; \; x_2 = A_m X_2 \; ; \; x_3 = X_3$ where γ is the applied shear and linearly increases over time from zero to a maximum of γ_m. The kinematical parameters of this deformation step are given by

$$F = N_1 \otimes N_1 + A_m N_2 \otimes N_2 + N_3 \otimes N_3 + \gamma N_1 \otimes N_2$$

$$l = \dot{F} F^{-1} = \frac{\dot{\gamma}}{A_m} N_1 \otimes N_2$$

$$d = \frac{\dot{\gamma}}{2A_m} (N_1 \otimes N_2 + N_2 \otimes N_1) \tag{2-74}$$

$$\Omega_J = w = \frac{\dot{\gamma}}{2A_m} (N_1 \otimes N_2 - N_2 \otimes N_1)$$

$$\Omega_R = \dot{\theta} (N_1 \otimes N_2 - N_2 \otimes N_1) \; ; \; \dot{\theta} = \frac{\dot{\gamma}(1 + A_m)}{(1 + A_m)^2 + \gamma^2}$$

At the end of this step the stress solution for the J rate with the classical hypoelastic model is:

$$\tau_{11} = \kappa \, ln \, A_m + \mu (1 + ln \, A_m) \left(1 - cos \frac{\gamma}{A_m} \right) \tag{2-75}$$

$$\tau_{22} = (\kappa + 2\mu)\, ln\, A_m - \mu(1 + ln\, A_m)\left(1 - cos\frac{\gamma}{A_m}\right)$$

$$\tau_{12} = \mu(1 + ln\, A_m)\, sin\frac{\gamma}{A_m}$$

And for the GMN rate the solution is:

$$\tau_{11} = 2\mu\left(1 + \frac{1}{A_m}\right)\{cos\, 2\beta\, ln(cos\, 2\beta) + \beta\, sin\, 2\beta - sin^2\, \beta\}$$
$$- \mu\, ln\, A_m\, cos\, 2\beta + (\kappa + \mu)\, ln\, A_m$$

$$\tau_{22} = -2\mu\left(1 + \frac{1}{A_m}\right)\{cos\, 2\beta\, ln(cos\, 2\beta) + \beta\, sin\, 2\beta - sin^2\, \beta\} \qquad (2\text{-}76)$$
$$+ \mu\, ln\, A_m\, cos\, 2\beta + (\kappa + \mu)\, ln\, A_m$$

$$\tau_{12} = \mu\left(1 + \frac{1}{A_m}\right) cos\, 2\beta \left\{2\beta - 2\, tan\, 2\beta\, ln(cos\, 2\beta) - \frac{\gamma}{1 + A_m}\right\}$$
$$+ \mu\, ln\, A_m\, sin\, 2\beta$$

in which $tan\, \beta = \frac{\gamma}{1+A_m}$.

Step 3- Removing the extension at constant shear $2 \leq t \leq 3$

The motion of this step can be expressed by $x_1 = X_1 + \gamma_m\, X_2$; $x_2 = AX_2$; $x_3 = X_3$ in which $A = 1 + \frac{u_m - u}{H}$ and u linearly increases from zero at $t = 2$ to the maximum of u_m at $t = 3$. The kinematical parameters of this deformation step are:

$$F = N_1 \otimes N_1 + A N_2 \otimes N_2 + N_3 \otimes N_3 + \gamma_m N_1 \otimes N_2$$

$$l = \dot{F} F^{-1} = \frac{\dot{A}}{A} N_2 \otimes N_2$$

$$d = \frac{\dot{A}}{A} N_2 \otimes N_2 \tag{2-77}$$

$$\Omega_J = w = \underset{\sim}{0}$$

$$\Omega_{GMN} = \dot{\theta}(N_1 \otimes N_2 - N_2 \otimes N_1)\ ;\ \dot{\theta} = -\frac{\gamma_m \dot{A}}{(1+A)^2 + \gamma_m^2}$$

In step 3 the stress solution for the J rate with the classical hypoelastic model is

$$\tau_{11} = \kappa\, ln\, A + \mu(1 + ln\, A_m)\left\{1 - cos\frac{\gamma_m}{A_m}\right\}$$

$$\tau_{22} = (\kappa + 2\mu)\, ln\, A - \mu(1 + ln\, A_m)\left\{1 - cos\frac{\gamma_m}{A_m}\right\} \tag{2-78}$$

$$\tau_{12} = \mu(1 + ln\, A_m)\, sin\frac{\gamma_m}{A_m}$$

And for the GMN rate is given by

$$\tau_{11} = B_1(\beta) + [C_2 + B_2(\beta)]\, cos\, 2\beta + [C_3 + B_3(\beta)]\, sin\, 2\beta$$

$$\tau_{22} = B_1(\beta) - [C_2 + B_2(\beta)]\, cos\, 2\beta - [C_3 + B_3(\beta)]\, sin\, 2\beta \tag{2-79}$$

$$\tau_{12} = -[C_3 + B_3(\beta)]\, cos\, 2\beta + [C_2 + B_2(\beta)]\, sin\, 2\beta$$

in which:

$$B_1(\beta) = (\kappa + \mu)\, ln\, A$$

$$B_2(\beta) = \frac{\mu}{1+\gamma_m^2}\{2\gamma_m[\beta - \gamma_m\, ln(cos\,\beta)] + (1-\gamma_m^2)\, ln\, A\}$$

$$B_3(\beta) = -\frac{2\gamma_m \mu}{1+\gamma_m^2}\{\beta\gamma_m + ln(cos\,\beta) + ln\, A\}$$

$$C_2 = [\tau_{11}|_{t=2} - B_1(\beta_m)]\, cos\, 2\beta_m + \tau_{12}|_{t=2}\, sin\, 2\beta_m - B_2(\beta_m)$$

$$C_3 = [\tau_{11}|_{t=2} - B_1(\beta_m)]\, sin\, 2\beta_m - \tau_{12}|_{t=2}\, cos\, 2\beta_m - B_3(\beta_m)$$

$$\beta_m = atan\frac{1+A_m}{\gamma_m}$$

Step 4- Removing shear and unloading $3 \leq t \leq 4$

The deformation at this step is given by $x_1 = X_1 + \gamma X_2$; $x_2 = X_2$; $x_3 = X_3$ where γ linearly decreases from γ_m at $t = 3$ to zero at $t = 4$. The solution of this step is identical to the solution given in the first example for the simple shear problem. The only difference is the nonzero initial conditions for the stresses. The stress solution for the J rate with the classical hypoelastic model is

$$\tau_{11} = -\tau_{22} = \mu + \mu\, ln\, A_m\, cos(\gamma_m - \gamma) - \mu(1 + ln\, A_m)\, cos\left(\gamma - \gamma_m \frac{A_m - 1}{A_m}\right)$$

$$\tau_{12} = \mu\, ln\, A_m\, sin(\gamma_m - \gamma) + \mu(1 + ln\, A_m)\, sin\left(\gamma - \gamma_m \frac{A_m - 1}{A_m}\right) \quad (2\text{-}80)$$

And for the GMN rate the stress solution is given by

$$\tau_{11} = -\tau_{22} = [C_1 + 4\mu\, ln(cos\,\beta)]\, cos\, 2\beta + [C_2 + \mu(4\beta - \gamma)]\, sin\, 2\beta$$

$$\tau_{12} = [C_2 + \mu(4\beta - \gamma)]\, cos\, 2\beta - [C_1 + 4\mu\, ln(cos\,\beta)]\, sin\, 2\beta \quad (2\text{-}81)$$

in which:

$$C_1 = -4\mu\, ln(cos\,\beta_m) + \tau_{11}|_{t=3}\, cos\, 2\beta_m - \tau_{12}|_{t=3}\, sin\, 2\beta_m$$

$$C_2 = -\mu(4\beta_m - \gamma_m) + \tau_{11}|_{t=3}\, sin\, 2\beta_m + \tau_{12}|_{t=3}\, cos\, 2\beta_m$$

$$\beta_m = atan\frac{\gamma_m}{2}$$

The solution from the finite elastic Hookean response for each deformation step is as follows:

Step 1- Stretching $0 \leq t \leq 1$

$$\tau_{11} = \kappa\, ln\, A\ ;\ \tau_{22} = (\kappa + 2\mu)\, ln\, A\ ;\ \tau_{12} = 0 \tag{2-82}$$

Step 2- Shearing at constant stretch $1 \leq t \leq 2$

$$\tau_{11} = (\kappa + 2\mu)\left[\frac{1}{2} ln\, A_m + \frac{1}{2}\left(\frac{\Im - A_m}{\sqrt{\Im^2 - 1}}\right) cosh^{-1}\Im\right] + \kappa\left[\frac{1}{2} ln\, A_m - \frac{1}{2}\left(\frac{\Im - A_m}{\sqrt{\Im^2 - 1}}\right) cosh^{-1}\Im\right]$$

$$\tau_{22} = \kappa\left[\frac{1}{2} ln\, A_m + \frac{1}{2}\left(\frac{\Im - A_m}{\sqrt{\Im^2 - 1}}\right) cosh^{-1}\Im\right] + (\kappa + 2\mu)\left[\frac{1}{2} ln\, A_m - \frac{1}{2}\left(\frac{\Im - A_m}{\sqrt{\Im^2 - 1}}\right) cosh^{-1}\Im\right] \tag{2-83}$$

$$\tau_{12} = \mu\frac{\gamma}{\sqrt{\Im^2 - 1}} cosh^{-1}\Im$$

where $\Im = \frac{1+\gamma^2+A_m^2}{2A_m}$.

Step 3- Removing the stretch at constant shear $2 \leq t \leq 3$

$$\tau_{11} = \frac{\kappa + 2\mu}{2}\left[ln\, A + \left(\frac{\Im - A}{\sqrt{\Im^2 - 1}}\right) cosh^{-1}\Im\right] + \frac{\kappa}{2}\left[ln\, A - \left(\frac{\Im - A}{\sqrt{\Im^2 - 1}}\right) cosh^{-1}\Im\right]$$

$$\tau_{22} = \frac{\kappa}{2}\left[ln\, A + \left(\frac{\Im - A}{\sqrt{\Im^2 - 1}}\right) cosh^{-1}\Im\right] + \frac{\kappa + 2\mu}{2}\left[ln\, A - \left(\frac{\Im - A}{\sqrt{\Im^2 - 1}}\right) cosh^{-1}\Im\right] \quad (2\text{-}84)$$

$$\tau_{12} = \mu\frac{\gamma_m}{\sqrt{\Im^2 - 1}} cosh^{-1}\Im$$

where $\Im = \frac{1+\gamma_m^2 + A}{2A}$.

Step 4- Removing the shear and back to the initial configuration $3 \leq t \leq 4$

$$\tau_{11} = 2\mu\gamma\eta$$

$$\tau_{12} = 4\mu\eta \quad (2\text{-}85)$$

where $\eta = \frac{\text{asinh}\frac{\gamma}{2}}{\sqrt{4+\gamma^2}}$.

To plot the different stress responses for the J and GMN rates with the response of the finite Hookean model, a Young's modulus of $E = 30000$ and a Poisson's ratio of $\upsilon = 0.3$ is used. Furthermore, it is assumed that $H = 1$, $u_m = 0.8$, and $\gamma_m = 1$. Figure 2-4 shows the Cauchy stress responses for the J and GMN rates using the classical hypoelastic model and the finite elastic Hookean stress response vs. the deformation steps. It should be noted that in this problem Cauchy stress and Kirchhoff stress are not identical because $J \neq 1$.

Since the deformation is a closed elastic path it is expected that the material retains its initial stress-free configuration after the cycle is completed. However, from

Figure 2-4 it is obvious that the classical hypoelastic model fails to predict such a physical response. The finite elastic Hookean model does not show any residual elastic stress while the classical hypoelastic model shows residual stresses at the end of the cycle for both the J and GMN rates. The conclusion here is that the hypoelastic model is not consistent with the notion of Cauchy and Green elasticity and in general a hyperelastic potential from which a hypoelastic model is derivable does not exist. This results have been reported by many authors (cf. Koji and Bathe [4], Truesdell and Noll [6], and Lin et el. [60]).

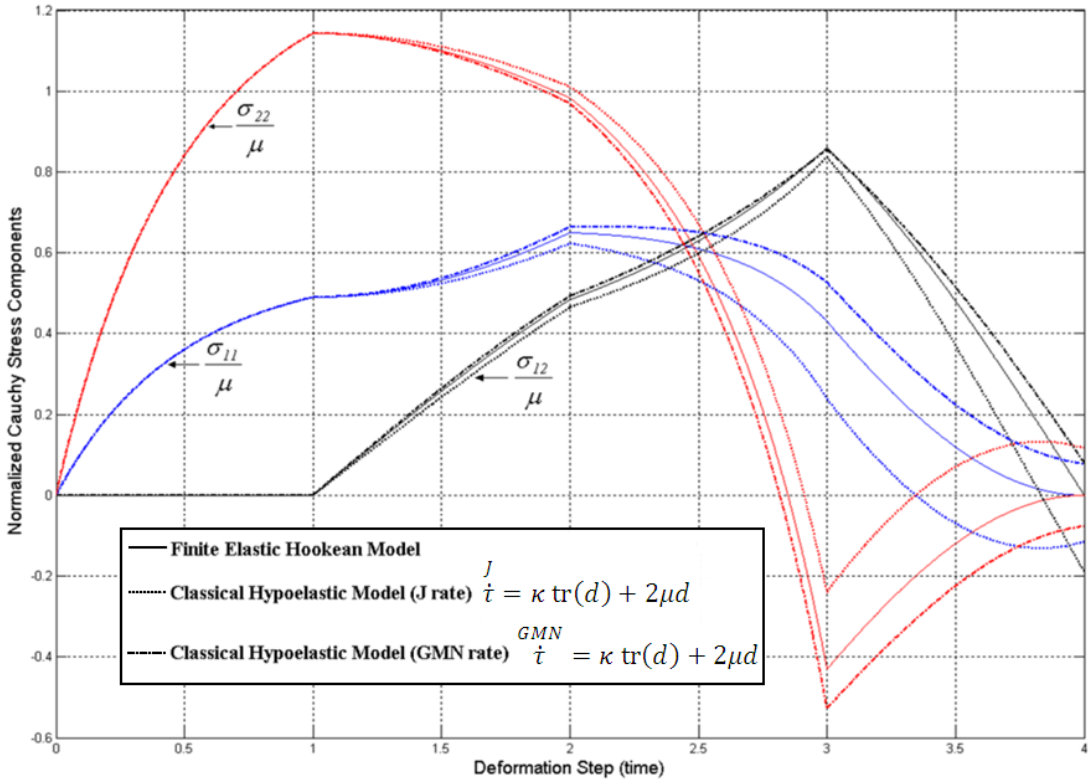

Figure 2-4- Cauchy stress components using the classical hypoelastic model and Finite elastic Hookean model

The question which remains to be answered is: under which conditions hypoelastic models are integrable and consistent with the notion of elasticity? This is discussed mathematically in the next section.

2.6.4.2 Integrability conditions for hypoelastic models

A general conclusion by Bernstein [16,17] and Truesdell and Noll [6] states that hypoelastic models are not elastic materials. Mathematically, this means that hypoelastic models, as simple rate-type constitutive models, are not exact differentials and therefore are not unconditionally integrable. Investigating the integrability conditions of hypoelastic materials is helpful to examine the conditions under which the model might provide an elastic response.

Bernstein [16,17] examined the conditions under which the classical hypoelastic model based on the J rate is elastic. Bernstein derived the following conditions for hypoelastic model to be integrable in the sense of Cauchy elasticity:

$$\frac{\partial B_{ijkl}}{\partial \tau_{rs}} B_{rspq} - \frac{\partial B_{ijpq}}{\partial \tau_{rs}} B_{rskl} - B_{ijkq}\,\delta_{pl} + B_{ijpl}\,\delta_{kq} = 0 \tag{2-86}$$

in which $B_{ijkl} = \frac{1}{2}\left(\tau_{il}\delta_{jk} + \tau_{jl}\delta_{ik} - \tau_{ik}\delta_{jl} - \tau_{jk}\delta_{il}\right) + [\mathcal{M}(\tau)]_{ijkl}$. Bernstein further showed that the hypoelastic model based on the J rate is integrable in the sense of Green elasticity if in addition to conditions (2-86) the following conditions are satisfied:

$$[\mathcal{M}(\tau)]_{ijkl} + \tau_{ij}\,\delta_{kl} = [\mathcal{M}(\tau)]_{klij} + \tau_{kl}\,\delta_{ij} \tag{2-87}$$

Integrability conditions (2-86) and (2-87) show that the grade-zero hypoelastic model based on the J rate, where $\mathcal{M}$ is constant, is not integrable in general. The only case where the model returns an elastic response is under the application of a hydrostatic state of stress.

Since hypoelastic models are affected by the choice of objective rates of stress, the final question regarding their integrability is whether any specific objective rate of stress exists which makes the model exactly integrable as an elastic material. This question is discussed in more detail in the following section.

2.6.5 Logarithmic (D) rate of stress and integrability conditions

Unconditional integrability of the hypoelastic model requires that the hypoelastic model be an exact differential for at least one specific rate of stress, i.e.:

$$\overset{*}{\dot{\tau}} = \mathcal{M}:d \Leftrightarrow \frac{d}{dt}(R_*^T \tau R_*) = \mathcal{M}:\frac{d}{dt}(R_*^T \varepsilon R_*) \tag{2-88}$$

This condition is equivalent to the existence of an objective rate for which $d = \overset{*}{\dot{\varepsilon}}$. In other words, we are looking for at least one objective frame of reference for which the rate of the Eulerian logarithmic strain in this background is identical to the rate of deformation tensor.

Reinhardt and Dubey [21] derived the following relationship between the objective rate of the Eulerian logarithmic strain and the strain rate tensor on the principal axis of stretch:

$$\overset{*}{\dot{\varepsilon}}_{ij}^{(e)} = \overset{*}{\mathcal{Q}}_{ij}\left(E_i - E_j\right)d_{ij}^{(e)} = \overset{*}{\mathcal{P}}_{ij}\, d_{ij}^{(e)}\ ; i \neq j\ \textit{(no sum)}$$

$$\overset{*}{\dot{\varepsilon}}_{ii}^{(e)} = d_{ii}^{(e)}\ \textit{(no sum)} \tag{2-89}$$

where the E_i's are the principal logarithmic strains and $\overset{*}{\mathcal{P}}_{ij}$ is a scalar scale function, which has the following forms for the Jaumann, Green-McInnis-Naghdi and Eulerian frames, respectively:

$$\overset{J}{\mathcal{P}}_{ij} = \frac{E_i - E_j}{tanh\left(E_i - E_j\right)}$$

$$\overset{GMN}{\mathcal{P}}_{ij} = \frac{E_i - E_j}{sinh\left(E_i - E_j\right)} \tag{2-90}$$

$$\overset{E}{\mathcal{P}}_{ij} = 0$$

Therefore, to find a corotational frame for which $d = \overset{*}{\dot{\varepsilon}}$, the requirement $\overset{*}{\mathcal{P}}_{ij} = 1$ should be met. For such a frame the corresponding $\overset{*}{\mathcal{Q}}$ should be

$$\overset{*}{\mathcal{Q}}_{ij} = \frac{1}{E_i - E_j} \tag{2-91}$$

Based on equation (2-91) and using the principal axis method, Reinhardt and Dubey [21] further derived the following relationship for the spin of the D frame on the principal axis of stretch:

$$\Omega_{D,ij}^{(e)} = \left[\frac{1}{E_i - E_j} - \frac{\lambda_j^2 + \lambda_i^2}{\lambda_j^2 - \lambda_i^2}\right] d_{ij}^{(e)} + w_{ij}^{(e)} \tag{2-92}$$

This relationship is valid when the stretch tensor has distinct eigenvalues. Reinhardt [40] further derived basis-free expressions for the D spin for the cases of distinct and coincident eigenvalues of the stretch tensor.

A similar approach was used by Xiao et al. [22] to derive relations between the logarithmic strain and strain rate tensor. Xiao et al. [61] proved that any material spin Ω_M can be obtained by the following general relationship:

$$\Omega_M = w + \sum_{i \neq j}^{m} h\left(\frac{\lambda_i^2}{I_1}, \frac{\lambda_j^2}{I_1}\right) P_i dP_j = w + N_M \tag{2-93}$$

in which λ_i^2's and P_i's are the eigenvalues and eigenprojections of the left Cauchy-Green tensor, $b = FF^T$, $I_1 = \mathrm{tr}\, b$, and h is the corresponding skew-symmetric spin function. For the case of the logarithmic rate and defining $\lambda_{ij} = \frac{\lambda_i}{\lambda_j}$, the spin function N_{log} is given by

$$N_{log} = \sum_{i \neq j}^{m} \left[\frac{1 + \lambda_{ij}^2}{1 - \lambda_{ij}^2} + \frac{1}{ln\, \lambda_{ij}}\right] P_i dP_j \tag{2-94}$$

A basis-free expression for the logarithmic spin was further derived by Xiao et al. [61] as follows:

$$N_{log} = \begin{cases} 0 & ; \lambda_1 = \lambda_2 = \lambda_3 \\ \hbar[bd] & ; \lambda_1 \neq \lambda_2 = \lambda_3 \\ \hbar_1[bd] + \hbar_2[b^2 d] + \hbar_3[b^2 db] & ; \lambda_1 \neq \lambda_2 \neq \lambda_3 \end{cases}$$

$$\hbar = \frac{1}{\lambda_1^2 - \lambda_2^2}\left[\frac{1+\lambda_{12}^2}{1-\lambda_{12}^2} + \frac{1}{ln\,\lambda_{12}}\right]$$

$$\hbar_k = -\frac{1}{\Delta}\sum_{i=1}^{3}\left(-\lambda_i^2\right)^{3-k}\left[\frac{1+e_i^2}{1-e_i^2} + \frac{1}{ln\,e_i}\right]; k = 1,2,3 \tag{2-95}$$

$$[bd] = bd - db$$

$$[b^r d] = b^r d - db^r$$

$$[b^r db^s] = b^r db^s - b^s db^r$$

where $e_1 = \frac{\lambda_2}{\lambda_3}$, $e_2 = \frac{\lambda_3}{\lambda_1}$, $e_3 = \frac{\lambda_1}{\lambda_2}$, and $\Delta = (\lambda_1^2 - \lambda_2^2)(\lambda_2^2 - \lambda_3^2)(\lambda_3^2 - \lambda_1^2)$.

Xiao et al. [26,62] further examined the integrability of the hypoelastic model based on the logarithmic (D) spin. For a general hypoelastic model $\overset{\log}{\dot{\tau}} = \mathcal{M}(\tau) : d$ and following the work of Bernstein [16,17], the following integrability conditions were expressed for the hypoelastic model based on the logarithmic spin in the sense of Cauchy elasticity

$$\frac{\partial \mathcal{M}_{klmn}^{-1}}{\partial \tau_{pq}} = \frac{\partial \mathcal{M}_{klpq}^{-1}}{\partial \tau_{mn}}$$

$$\frac{\partial \mathcal{M}_{klmn}}{\partial \tau_{rs}}\mathcal{M}_{rspq} = \frac{\partial \mathcal{M}_{klpq}}{\partial \tau_{rs}}\mathcal{M}_{rsmn} \tag{2-96}$$

where $\mathcal{M}^{-1}_{ijpq}\,\mathcal{M}_{pqkl} = \mathbb{I}_{ijkl} = \frac{1}{2}\left(\delta_{jk}\,\delta_{il} + \delta_{ik}\,\delta_{jl}\right)$. Integrability conditions (2-96-1) and (2-96-2) are two equivalent conditions applied to the hypoelasticity tensor and its inverse form. Xiao et al. [26,62] further showed that in order to satisfy the above mentioned integrability conditions, it suffices that a symmetric second order tensor-valued function of the Kirchhoff stress $\Psi(\tau)$ exist such that

$$\mathcal{M}^{-1} = \nabla\Psi(\tau) \tag{2-97}$$

where the operator ∇ denotes gradient with respect to τ.

Xiao et al. [62] further showed that a hypoelastic model based on the logarithmic spin, which is also integrable as an isotropic Cauchy elastic material, will be consistent with the notion of Green elasticity (hyperelasticity) if the fourth-order hypoelasticity tensor possesses main diagonal symmetry

$$\mathcal{M}_{ij\,kl} = \mathcal{M}_{klij} \tag{2-98}$$

Ericksen [18] investigated the existence of a hypoelastic potential for the case of the Jaumann spin for which a scalar invariant hypoelastic potential Π exist such that with another scalar invariant potential Γ, the stress power can be expressed by

$$\tau : d = \Gamma\dot{\Pi} \tag{2-99}$$

For such existence, Ericksen [18] showed that the following conditions should be met:

$$\left(\frac{\partial \Theta_{ij}}{\partial \tau_{km}} - \frac{\partial \Theta_{km}}{\partial \tau_{ij}}\right)\Theta_{rs} + \left(\frac{\partial \Theta_{km}}{\partial \tau_{rs}} - \frac{\partial \Theta_{rs}}{\partial \tau_{km}}\right)\Theta_{ij} + \left(\frac{\partial \Theta_{rs}}{\partial \tau_{ij}} - \frac{\partial \Theta_{ij}}{\partial \tau_{rs}}\right)\Theta_{km} = 0 \tag{2-100}$$

in which $\Theta_{ij} = \Gamma \frac{\partial \Pi}{\partial \tau_{ij}}$. A similar approach was used by Xiao et al. [62] for the case of the logarithmic spin. They extended the Ericksen's conditions for arbitrary rates of stress as follows:

$$\tau : d = \Gamma \dot{\Pi} = \Theta : \dot{\tau} = \Theta : \overset{*}{\tau} = \Theta : \mathcal{M}(\tau) : d \tag{2-101}$$

Therefore, the same condition (2-100) is required for the existence of a hypoelastic potential for the case of the logarithmic rate.

2.6.6 Unconditional integrability of the grade-zero hypoelastic model based on the logarithmic (D) spin

According to the Bernstein's integrability conditions for a grade-zero hypoelastic model, the hypoelastic model based on the Jaumann rate is not integrable for a general state of stress. However, for the grade-zero logarithmic-based hypoelastic model the Xiao et al. integrability conditions are automatically satisfied since $\frac{\partial \mathcal{M}}{\partial \tau} = \underset{\sim}{0}$. Therefore, the grade-zero hypoelastic model based on the logarithmic spin is unconditionally integrable as a Cauchy and Green elastic model. This means that the hypoelastic model based on the logarithmic rate is an exact differential and is equivalent to the extended finite isotropic elastic (Hookean) model given in equation (2-45)

$$\overset{log}{\dot{\tau}} = \mathcal{M}: d \leftrightarrow \tau = \kappa\, tr(\varepsilon) I + 2\mu\varepsilon \tag{2-102}$$

Equation (2-102) is unconditionally satisfied and as a result all of the issues of hypoelasticity can be resolved when the logarithmic (D) spin is used.

2.7 Summary

Issues of hypoelasticity have been attributed to model non-integrability as elastic materials. Such issues have questioned the applicability of hypoelastic models for constitutive modeling for finite deformation. Integrability conditions of hypoelastic models showed that in general the model in not integrable as an elastic material. Solution of the inverse problem, which searched for a spinning background in which the rate of the logarithmic strain is equivalent to the strain rate tensor, resulted into a new spinning frame called the D or logarithmic frame. This frame resolved the issues of hypoelasticity and is a good candidate for application in finite deformation analysis of elastoplastic hardening materials.

As a general conclusion, an extra principle for rate-type constitutive models for finite deformation should be introduced. According to this principle, objective rates of Eulerian quantities used in a rate-type constitutive model should be observed in the same background. This principle is called here the principle of rate homogeneity and should be satisfied in Eulerian rate-type constitutive models.

Chapter 3

Review of Eulerian rate plasticity models and their algorithmic implementation

Infinitesimal plasticity models are based on additive decomposition of strain into elastic and plastic parts. Flow rules are obtained through the choice of a specific plastic potential and relate the plastic internal variables to their corresponding driving forces. Plasticity, as a dissipative phenomenon, should be consistent with the thermodynamics of irreversible systems. Therefore, flow rules should be in accordance with the second law of thermodynamics.

Extension of infinitesimal plasticity to finite deformation can be done by considering further modifications of the flow rule. The strain rate tensor and its decomposition into elastic and plastic parts are primarily used in the Eulerian rate form of elastoplasticity for finite deformations. Numerical implementation of finite strain elastoplastic models should maintain the objectivity of the model during time integration.

In this chapter formulation of classical infinitesimal plasticity models based on the thermodynamics of irreversible phenomena is reviewed. Next, extension of infinitesimal plasticity models for finite deformation based on hypoelastic material models and an additive decomposition of the strain rate tensor is reviewed. Finally, numerical implementation of the classical rate plasticity models is discussed. The integration of classical models is implemented in the ABAQUS finite element software through a user subroutine UMAT for different objective rates of stress.

3.1 Thermodynamics of irreversible deformations

State variables defining the state of a system can be either observable variables which are measurable experimentally or internal variables representing the irreversible phenomena of system dissipation [7]. Mathematically, it can be assumed that a scalar thermodynamics potential function of state variables exists which defines the state laws and relates the state variables to their corresponding driving forces.

For the case of elasticity, viscoelasticity, plasticity, viscoplasticity, damage and fracture of hardening materials, two observable variables, i.e. the temperature T and the total strain ε, can be introduced. Furthermore, for different dissipative phenomena additional internal variables (scalar or tensorial) can be introduced and used in macro or micro scale modeling. Examples of internal variables are the plastic strain and back stress tensors associated with the relaxed configuration in plasticity and the scalar or tensorial damage parameter in ductile damage of materials. Internal variables are representative of physical phenomena (for example density of dislocations, microstresses, microcracks and cavities) happening during irreversible deformation which are not directly measurable by experiment [7].

Mathematically, the free specific energy potential ψ can be defined in terms of observable and internal variables by

$$\psi = \psi(\varepsilon, T, \varepsilon^e, \varepsilon^p, v_k) \tag{3-1}$$

where ε^e and ε^p are the elastic and plastic parts of the strain, and v_k represents the vector of additional internal variables related to system dissipation. Considering the case of infinitesimal plasticity where an additive decomposition of strain is valid, i.e. $\varepsilon = \varepsilon^e + \varepsilon^p$, the thermodynamics potential can be modified as follows:

$$\psi = \psi(\varepsilon^e, T, v_k) \tag{3-2}$$

Balance of energy for such a system relates the elements of internal work to the elements of external work. The differential form of the first law of thermodynamics (conservation of energy) is given by

$$\rho\dot{\mathfrak{e}} = \tau : d + r - \vec{\nabla}.\vec{q} \tag{3-3}$$

where ρ is the density of the material, $\mathfrak{e}$ is the specific internal energy, r is the volumetric density of internal heat generation, $\vec{q}$ is the heat flux vector, and τ and d are the Kirchhoff stress and the rate of deformation tensors.

According to the second law of thermodynamics, for any dissipative system the rate of the specific entropy per unit mass of the system $\dot{s}$ should be greater than or equal to the rate of heating divided by temperature

$$\rho(T\dot{s} - \dot{\mathfrak{e}}) + \tau : d - \vec{q}.\frac{\vec{\nabla}T}{T} \geq 0 \tag{3-4}$$

Assuming that the free energy potential is given by $\psi = \mathfrak{e} - Ts$, with the help of equation (3-4) the Clausius-Duhem inequality can be obtained as follows [63]:

$$\tau : d - \rho\left(\dot{\psi} + s\dot{T}\right) - \vec{q}.\frac{\vec{\nabla}T}{T} \geq 0 \tag{3-5}$$

For the case of infinitesimal deformation it can be assumed that $d = \dot{\varepsilon}$. Use of equations (3-2) and (3-5) gives

$$\left(\tau - \rho\frac{\partial\psi}{\partial\varepsilon^e}\right) : \dot{\varepsilon}^e + \tau : \dot{\varepsilon}^p - \rho\left(s + \frac{\partial\psi}{\partial T}\right)\dot{T} - \rho\frac{\partial\psi}{\partial v_k} : \dot{v}_k - \vec{q}.\frac{\vec{\nabla}T}{T} \geq 0 \tag{3-6}$$

Let's assume that the elastic deformation happens at constant and uniform temperature, i.e. $\dot{T} = 0$ and $\vec{\nabla}T = 0$ and does not affect the plastic internal variables. From (3-6) it necessarily follows that

$$\tau = \rho \frac{\partial \psi}{\partial \varepsilon^e} = -\rho \frac{\partial \psi}{\partial \varepsilon^p} = \rho \frac{\partial \psi}{\partial \varepsilon} \tag{3-7}$$

Next, assume that a thermal deformation happens at uniform temperature, which has no effect on internal plastic variables, and equality (3-7) holds. Equation (3-6) yields [7]

$$s = -\frac{\partial \psi}{\partial T} \tag{3-8}$$

Equations (3-7) and (3-8) define the thermoelastic laws of any deforming continuous system. Equation (3-7) shows that the stress tensor τ is the conjugate variable (driving force) associated with the total, elastic, and plastic strains. Similarly, setting $\mathscr{b}_k = \rho \frac{\partial \psi}{\partial v_k}$ in (3-6) defines the conjugate variables (driving forces) to the internal variables v_k. The associated (conjugate) variables define the dual space to the space of the observable and internal state variables [7]. Use of equations (3-6) to (3-8) leads to the simplified form of the Clausius-Duhem inequality as follows:

$$\varphi = \tau : \dot{\varepsilon}^p - \mathscr{b}_k : \dot{v}_k - \vec{q}.\frac{\vec{\nabla}T}{T} \geq 0 \tag{3-9}$$

which enforces that the dissipation of the system be positive. The dissipation potential φ can further be decoupled into an intrinsic (mechanical) dissipation $\varphi_M = \tau : \dot{\varepsilon}^p - \mathscr{b}_k : \dot{v}_k$ and a thermal dissipation $\varphi_T = -\vec{q}.\frac{\vec{\nabla} T}{T}$.

Complementary laws for the dissipative state variables are obtained through the definition of a continuous and convex scalar valued dissipation potential. Such a potential is a function of the flux variables, i.e. $\phi\left(\dot{\varepsilon}^p, \dot{v}_k, \frac{\vec{q}}{T}\right)$, which has a zero value at the origin of the space and relates the internal dissipative variables to their corresponding associative (dual) variables by [7]

$$\tau = \frac{\partial \phi}{\partial \dot{\varepsilon}^p} \; ; \; \mathscr{b}_k = -\frac{\partial \phi}{\partial \dot{v}_k} \; ; \; \vec{\nabla} T = -\frac{\partial \phi}{\partial \left(\frac{\vec{q}}{T}\right)} \tag{3-10}$$

Equivalent expressions can be obtained in the dual space of conjugate variables using the Legendre-Fenchel transformation [7]

$$\dot{\varepsilon}^p = \frac{\partial \phi^*}{\partial \tau} \; ; \; -\dot{v}_k = \frac{\partial \phi^*}{\partial \mathscr{b}_k} \; ; \; -\frac{\vec{q}}{T} = \frac{\partial \phi^*}{\partial \left(\vec{\nabla} T\right)} \tag{3-11}$$

where ϕ^* is dual to ϕ and is given by

$$\phi^*\left(\tau, \mathscr{b}_k, \vec{\nabla} T\right) = \underset{\dot{\varepsilon}^p, \dot{v}_k, \frac{\vec{q}}{T}}{Sup}\left[\tau : \dot{\varepsilon}^p - \mathscr{b}_k : \dot{v}_k - \vec{q}.\frac{\vec{\nabla} T}{T} - \phi\left(\dot{\varepsilon}^p, \dot{v}_k, \frac{\vec{q}}{T}\right)\right] \tag{3-12}$$

Two further simplifications can be applied to (3-10) and (3-11). Firstly, as stated above it can be assumed that thermal and mechanical dissipations are

decoupled. Secondly, it can be assumed that the dual potential φ^* has a positive-definite quadratic form in terms of the dual variables and therefore a linear relationship exists between the flux variables and their dual driving forces, which is known as Onsager's symmetry property [7].

3.2 Classical infinitesimal plasticity

3.2.1 A general quadratic form

For the class of rate independent plasticity models, internal variables are chosen to represent the current size Υ and center coordinates β of the yield surface in stress space. A general quadratic flow potential for rate independent plasticity can be given as follows [30]:

$$\phi(\eta) = \sqrt{\eta : \mathbb{P} : \eta} \tag{3-13}$$

where $\eta = \mathrm{dev}\,\tau - \beta$, $\mathbb{P}$ is a symmetric positive-definite fourth order projection tensor, and "dev" denotes the deviatoric part of a symmetric tensor. Such a flow potential is homogenous of degree one, i.e. $\frac{\partial \phi(\eta)}{\partial \eta} : \eta = \phi(\eta)$ [30].

The yield criterion for the rate independent plasticity can take the following form:

$$f(\tau, \beta, \Upsilon) = \sqrt{\eta : \mathbb{P} : \eta} - \Upsilon \leq 0 \tag{3-14}$$

Let's assume that $q = \{\beta, Y\}$ defines the vector of hardening plastic variables in stress space. The evolution equations for the internal variables can be given by

$$\dot{\tau} = M : (\dot{\varepsilon} - \dot{\varepsilon}^p)$$

$$\dot{\varepsilon}^p = \dot{\lambda} s(\tau, q) \tag{3-15}$$

$$\dot{q} = \dot{\lambda} h(\tau, q)$$

where M is the fourth order elasticity tensor, $s(\tau, q)$ and $h(\tau, q)$ define the direction of the plastic flow and the hardening functions, respectively, and $\dot{\lambda}$ is the plastic multiplier used to satisfy the consistency condition. The hardening function can be a constant (linear), piecewise linear, or nonlinear function of plastic internal variables.

3.2.2 Principle of maximum plastic dissipation

Assuming that the vector of hardening internal variables are given by $q = \{\beta, Y\}$ in the stress space and its corresponding dual vector is given by $Q = \{v_1, v_2\}$ in the strain space, using equation (3-9) the plastic dissipation is given by

$$\varphi^p(\tau, q; \dot{\varepsilon}^p, \dot{Q}) = \tau : \dot{\varepsilon}^p + q : \dot{Q} \tag{3-16}$$

where the internal hardening variables are related to their conjugate variables through general evolution equations. If the closure of the elastic region is denoted by E_η, any state of stress (τ, q) on the boundary of the elastic region ∂E_η should satisfy

$$\partial E_\eta = \{(\tau, q) | f(\tau, q) = 0\} \tag{3-17}$$

And any stress state for which $f(\tau, q) > 0$ is a non-admissible one. The principle of maximum plastic dissipation defines the actual state of stress point (τ^*, q^*) among all admissible states (τ, q) for which the plastic dissipation is maximum [30]. Its corresponding mathematical representation is given by a constrained maximization problem as follows:

$$\varphi^p(\tau^*, q^*; \dot{\varepsilon}^p, \dot{Q}) = \underset{(\tau,q)\in E_\eta}{MAX} \{\tau : \dot{\varepsilon}^p + q : \dot{Q}\} \qquad (3\text{-}18)$$

$$\textit{Subject to: } f(\tau, q) = 0$$

Using the method of Lagrange multipliers, a solution for the optimization problem given in (3-18) can be found. The Lagrangian of this problem is given by

$$\mathcal{L}(\tau, q, \dot{\lambda}; \dot{\varepsilon}^p, \dot{Q}) = -\tau : \dot{\varepsilon}^p - q : \dot{Q} + \dot{\lambda} f(\tau, q) \qquad (3\text{-}19)$$

which results in the following relations between internal variables and their corresponding dual variables

$$\frac{\partial \mathcal{L}}{\partial \tau} = 0 \rightarrow \dot{\varepsilon}^p = \dot{\lambda} \frac{\partial f(\tau, q)}{\partial \tau}$$
$$\frac{\partial \mathcal{L}}{\partial q} = 0 \rightarrow \dot{Q} = \dot{\lambda} \frac{\partial f(\tau, q)}{\partial q} \qquad (3\text{-}20)$$

Equations (3-20) define the well-known classical associative plasticity rules for the evolution of the state variables. The Kuhn-Tucker loading/unloading (optimality) conditions are therefore given by

$$\dot{\lambda} \geq 0 \, , f(\tau, q) \leq 0 \, , \dot{\lambda} f(\tau, q) = 0 \qquad (3\text{-}21)$$

Another consequence of the principle of maximum plastic dissipation is the convexity requirement of the elastic region E_η, proof of which is given in [30].

3.3 Algorithmic implementation of infinitesimal plasticity

Integration of plasticity models discussed in section 3.2 is based on the iterative solution of the discretized momentum equations. In general three steps are used for numerical integration of nonlinear boundary value problems as follows [30,34,64]:

Step1- The incremental displacement vector (or vector of incremental strain) is obtained based on the previously converged load increment and linearized form of the momentum equations.

Step 2- State variables are updated for the given incremental strain by integrating the corresponding constitutive models.

Step 3- The balance of the momentum equations is examined based on the updated state variables. If the solution is not converged the iterative solution continues by returning to step 1.

In what follows the numerical treatment of step 2 is discussed in detail and the numerical treatment of steps 1 and 3 is excluded; the reader is referred to references [30,34,64]. The focus is on the integration of the constitutive models in step 2 and its corresponding linearized form.

3.3.1 Closest point projection method

Let's assume that a set of differentials for classical plasticity is given by the following evolution equations:

$$\begin{aligned} \dot{\tau} &= M:(\dot{\varepsilon} - \dot{\varepsilon}^p) \\ \dot{\varepsilon}^p &= \dot{\lambda}\mathcal{s}(\tau, q) \\ \dot{q} &= \dot{\lambda}\mathcal{h}(\tau, q) \\ f(\tau, q) &\leq 0 \end{aligned} \tag{3-22}$$

where the elasticity tensor M is assumed to be constant. An associative plasticity version of (3-22) can be obtained by choosing $\mathcal{s}(\tau, q) = \frac{\partial f(\tau,q)}{\partial \tau}$ and $\mathcal{h}(\tau, q) = -\nabla H(Q):\frac{\partial f(\tau,q)}{\partial q}$ where ∇ denotes the gradient operator of a scalar or tensor with respect to its argument. The objective is to integrate the evolution equations (3-22) with the known initial conditions

$$\{\varepsilon, \varepsilon^p, \tau, q\}_{t=t_n} = \{\varepsilon_n, \varepsilon_n^p, \tau_n, q_n\} \tag{3-23}$$

for a given incremental strain (displacement) of $\Delta\varepsilon$ (Δu) such that the updated state variables $\varepsilon_{n+1}, \varepsilon_{n+1}^p, \tau_{n+1}, q_{n+1}$ at time $t_{n+1} = t_n + \Delta t$ satisfy the consistency condition $f(\tau_{n+1}, q_{n+1}) = f_{n+1} = 0$.

Applying an implicit backward-Euler integration scheme to the set of equations given in (3-22) yields

$$\tau_{n+1} = \tau_n + M : (\Delta\varepsilon - \Delta\varepsilon^p)$$

$$\varepsilon^p_{n+1} = \varepsilon^p_n + \Delta\lambda_{n+1}\mathcal{s}(\tau_{n+1}, q_{n+1}) \tag{3-24}$$

$$q_{n+1} = q_n + \Delta\lambda_{n+1}\mathcal{k}(\tau_{n+1}, q_{n+1})$$

which yields the following form for the case of associative plasticity:

$$\tau_{n+1} = \tau_n + M : (\Delta\varepsilon - \Delta\varepsilon^p)$$

$$\varepsilon^p_{n+1} = \varepsilon^p_n + \Delta\lambda_{n+1}\partial_\tau f(\tau_{n+1}, q_{n+1}) \tag{3-25}$$

$$q_{n+1} = q_n - \Delta\lambda_{n+1}\nabla_{n+1}H(Q_{n+1}) : \partial_q f(\tau_{n+1}, q_{n+1})$$

The Kuhn-Tucker optimality conditions however require that at time t_{n+1} the following be satisfied:

$$f_{n+1} \leq 0\ , \Delta\lambda_{n+1} \geq 0\ , \Delta\lambda_{n+1} f_{n+1} = 0 \tag{3-26}$$

Let's define an elastic predictor (trial) step by freezing the plastic internal variables as follows:

$$f^*_{n+1} = f(\tau^*_{n+1}, q^*_{n+1})$$

$$\tau^*_{n+1} = \tau_n + M : \Delta\varepsilon \tag{3-27}$$

$$q^*_{n+1} = q_n$$

where a superscript * indicates the trial state of the state variables. The Kuhn-Tucker optimality condition is solely defined by the state of the trial yield function [30]

$$f_{n+1}^{*} < 0 \Leftrightarrow \Delta\lambda_{n+1} = 0$$
$$f_{n+1}^{*} > 0 \Leftrightarrow \Delta\lambda_{n+1} > 0 \tag{3-28}$$

Proof of (3-28) can be found by first proving that $f_{n+1}^{*} \geq f_{n+1}$. The convexity of elastic region requires that the following be satisfied [30]

$$f_{n+1}^{*} - f_{n+1} \geq (\tau_{n+1}^{*} - \tau_{n+1}) : \partial_{\tau} f_{n+1} + (q_{n+1}^{*} - q_{n+1}) : \partial_{q} f_{n+1} \tag{3-29}$$

with the help of (3-25) and (3-27), equation (3-29) yields

$$f_{n+1}^{*} - f_{n+1} \geq \Delta\lambda_{n+1}\left[\partial_{\tau} f_{n+1} : M : \partial_{\tau} f_{n+1} + \partial_{q} f_{n+1} : \nabla_{n+1} H(\mathcal{Q}_{n+1}) : \partial_{q} f_{n+1}\right] \tag{3-30}$$

Assuming that both M and $\nabla_{n+1} H(\mathcal{Q}_{n+1})$ are positive definite fourth-order tensors, equation (3-30) is either zero or positive and as a result $f_{n+1}^{*} \geq f_{n+1}$. Now let's assume that $f_{n+1}^{*} < 0$, which immediately indicates that $f_{n+1} < 0$ and the discrete Kuhn-Tucker optimality condition leads to $\Delta\lambda_{n+1} = 0$. As a result, the incremental step is elastic and the updated variables are the same as their trial states. On the other hand, if $f_{n+1}^{*} > 0$ then the discrete Kuhn-Tucker optimality condition implies that $\Delta\lambda_{n+1} > 0$ and as a result $f_{n+1} = 0$ for plastic consistency. Therefore, the step is plastic and the trial state should be corrected in order to satisfy plastic consistency.

Geometrically, it can be shown that the plastic corrector step is the closest point projection of the trial state τ_{n+1}^{*} onto the current yield surface as shown in Figure 3-1[30].

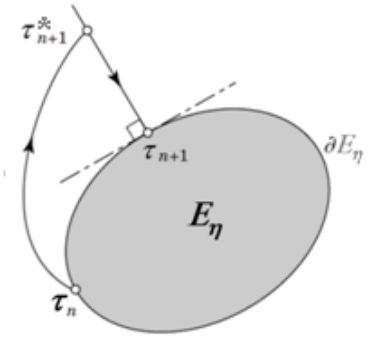

Figure 3-1- Geometric representation of the closest point projection concept [30]

3.3.2 Plastic corrector step using the return mapping algorithm

In what follows the radial return mapping algorithm originally proposed by Wilkins [65] is used for numerical integration of the special case of the J_2 associative flow theory and nonlinear mixed isotropic/kinematic hardening.

Assuming that the vector of internal variables is given by $q = \{\beta, \Upsilon\}$ where β is the back stress tensor and $E^{p,eq}$ represents the accumulated plastic strain, the Mises yield potential is given by

$$f(\tau,\beta,\Upsilon) = \sqrt{\eta:\eta} - \sqrt{\frac{2}{3}}[\sigma_0 + \Upsilon(E^{p,eq})]$$

$$\dot{\Upsilon}(E^{p,eq}) = \dot{K}(E^{p,eq})$$

$$\dot{\beta} = -\sqrt{\frac{2}{3}}\dot{H}(E^{p,eq})\partial_\beta f(\tau,\beta,\Upsilon) \tag{3-31}$$

$$\dot{E}^{p,eq} = \sqrt{\frac{2}{3}}\dot{\lambda}$$

where $\eta = \mathrm{dev}\,\tau - \beta$ is the shift stress tensor, and $K(E^{p,eq})$ and $H(E^{p,eq})$ are the nonlinear hardening moduli for the subsequent yield surface size and center, respectively. Defining $n = \partial_\eta f = \frac{\partial f}{\partial \eta} = \partial_\tau f = -\partial_\beta f$ as the unit normal vector to the yield surface in the deviatoric stress space and using the implicit backward-Euler method yield:

$$
\begin{aligned}
&\varepsilon_{n+1}^{p} = \varepsilon_n^{p} + \Delta\lambda_{n+1} n_{n+1} \\
&s_{n+1} = dev\,\tau_{n+1} = s_n + 2\mu(dev\,\Delta\varepsilon - \Delta\varepsilon^{p}) = s_n + 2\mu dev\Delta\varepsilon - 2\mu\Delta\lambda_{n+1} n_{n+1} \\
&Y_{n+1} = Y_n + \left[K\left(E_{n+1}^{p,eq}\right) - K\left(E_n^{p,eq}\right)\right] = Y_n + \Delta K \\
&\beta_{n+1} = \beta_n + \sqrt{\frac{2}{3}}\left[H\left(E_{n+1}^{p,eq}\right) - H\left(E_n^{p,eq}\right)\right] n_{n+1} = \beta_n + \sqrt{\frac{2}{3}}\Delta H n_{n+1} \\
&E_{n+1}^{p,eq} = E_n^{p,eq} + \sqrt{\frac{2}{3}}\Delta\lambda_{n+1}
\end{aligned}
\tag{3-32}
$$

where μ is the shear modulus of the material. The trial state is defined by freezing the plastic internal variables

$$
{\varepsilon_{n+1}^{p}}^{*} = \varepsilon_n^{p}\ ;\ Y_{n+1}^{*} = Y_n\ ;\ \beta_{n+1}^{*} = \beta_n \tag{3-33}
$$

Knowing that $s_{n+1} = s_n + 2\mu\mathrm{dev}\Delta\varepsilon - 2\mu\Delta\lambda_{n+1} n_{n+1} = s_{n+1}^{*} - 2\mu\Delta\lambda_{n+1} n_{n+1}$ the trial shift stress tensor is $\eta_{n+1}^{*} = s_{n+1}^{*} - \beta_{n+1}^{*} = s_{n+1}^{*} - \beta_n$. Therefore, the trial yield function takes the following form:

$$f_{n+1}^{*} = \|\eta_{n+1}^{*}\| - \sqrt{\frac{2}{3}}(\sigma_0 + Y_n) \tag{3-34}$$

where $\|\eta_{n+1}^{*}\| = \sqrt{\eta_{n+1}^{*} : \eta_{n+1}^{*}}$ is the norm of the trial shift stress tensor. The actual state of the yield surface is given by $f_{n+1} = \|\eta_{n+1}\| - \sqrt{\frac{2}{3}}(\sigma_0 + Y_{n+1})$. Knowing that $\eta_{n+1} = s_{n+1} - \beta_{n+1} = s_{n+1}^{*} - \beta_n - 2\mu\Delta\lambda_{n+1}n_{n+1} - \sqrt{\frac{2}{3}}\Delta H n_{n+1}$ yields:

$$\eta_{n+1} = \eta_{n+1}^{*} - \left(2\mu\Delta\lambda_{n+1} + \sqrt{\frac{2}{3}}\Delta H\right)n_{n+1} \tag{3-35}$$

From equation (3-35) the coaxiality of the trial and actual unit normal vectors can be concluded. Knowing that $\eta_{n+1} = \|\eta_{n+1}\|n_{n+1}$ and $\eta_{n+1}^{*} = \|\eta_{n+1}^{*}\|n_{n+1}^{*}$, equation (3-35) yields

$$\|\eta_{n+1}\|n_{n+1} = \|\eta_{n+1}^{*}\|n_{n+1}^{*} - \left(2\mu\Delta\lambda_{n+1} + \sqrt{\frac{2}{3}}\Delta H\right)n_{n+1} \tag{3-36}$$

Equation (3-36) implies that the trial unit normal vector $n_{n+1}^{*} = \frac{\eta_{n+1}^{*}}{\|\eta_{n+1}^{*}\|}$, which is known from the trial state, is in the direction of the actual unit normal vector $n_{n+1} = \frac{\eta_{n+1}}{\|\eta_{n+1}\|}$, which is not known and should be found. This property shows that the plastic corrector step is in the radial direction to the yield surface and the trial unit vector remains unchanged during the plastic update. As a result, the trial unit normal vector

solely defines the direction of the return to the actual yield surface. Knowing that trial and actual directions are coincident, equation (3-36) yields

$$\|\eta_{n+1}\| = \|\eta^*_{n+1}\| - \left(2\mu\Delta\lambda_{n+1} + \sqrt{\frac{2}{3}}\Delta H\right) \tag{3-37}$$

Using equation (3-37), the actual state of the yield surface is given by

$$f_{n+1} = \|\eta_{n+1}\| - \sqrt{\frac{2}{3}}(\sigma_0 + \Upsilon_{n+1}) = f^*_{n+1} - 2\mu\Delta\lambda_{n+1} - \sqrt{\frac{2}{3}}\Delta H - \sqrt{\frac{2}{3}}\Delta K = 0 \tag{3-38}$$

Equation (3-38) is a nonlinear function of the plastic multiplier $\Delta\lambda_{n+1}$, which can be iteratively solved using a local Newton-Raphson algorithm. Since this function is a convex function, its convergence is guaranteed. Details of the local Newton iterative solution is given in [30].

Once the plastic consistency $\Delta\lambda_{n+1}$ is calculated, the actual state of stress and back stress tensors can be found using equation (3-32). A geometric representation of the radial return mapping algorithm is given in Figure 3-2.

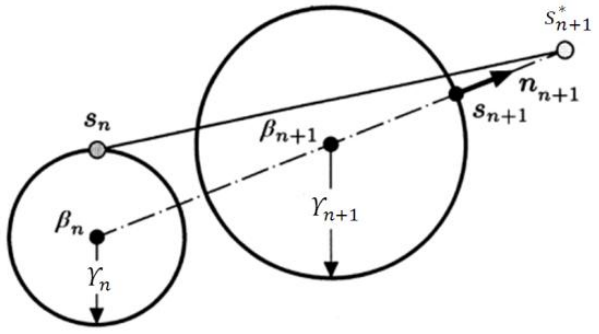

Figure 3-2- Geometric representation of the radial return mapping algorithm [30]

The plastic corrector step is completed by updating the plastic internal variables for the current increment of strain; however, linearization of the algorithm is necessary for the calculation of the vector of incremental displacement corresponding to the next load increment. A simple way is to use the continuum tangent modulus for the linearized modulus; however, quadratic convergence of the Newton method is not guaranteed because the linearized modulus is dependent on the method of integration. An algorithmic linearization based on the integration scheme has been suggested instead of a continuum tangent modulus by several researchers (cf. Simo and Hughes [30] and Bathe [64]), which guarantees the quadratic convergence norm of the Newton method and is called the "algorithmic or consistent tangent modulus". An exact linearization of the radial return mapping algorithm for the J_2 flow theory and mixed nonlinear hardening has been given in [30] which will be summarized below.

Knowing that $\tau_{n+1} = \kappa \,\mathrm{tr}\, \varepsilon_{n+1}\, I + 2\mu(\mathrm{dev}\varepsilon_{n+1} - \Delta\lambda_{n+1} n_{n+1})$ yields

$$d\tau_{n+1} = \left(M - 2\mu n_{n+1} \otimes \frac{\partial \Delta\lambda_{n+1}}{\partial \varepsilon_{n+1}} - 2\mu\Delta\lambda_{n+1} \frac{\partial n_{n+1}}{\partial \varepsilon_{n+1}}\right) : d\varepsilon_{n+1} \tag{3-39}$$

where $M = \kappa I \otimes I + 2\mu \left(\mathbb{I} - \frac{1}{3} I \otimes I\right)$ is the constant elasticity tensor. It can be shown that $\frac{\partial n}{\partial \eta} = \frac{1}{\|\eta\|}(\mathbb{I} - n \otimes n)$. The consistency condition leads to

$$\frac{\partial \Delta\lambda_{n+1}}{\partial \varepsilon_{n+1}} = \left[1 + \frac{K'_{n+1} + H'_{n+1}}{3\mu}\right]^{-1} n_{n+1} \tag{3-40}$$

And as a result the algorithmic tangent modulus is given by

$$M_{n+1}^{alg} = \kappa I \otimes I + 2\mu C_{n+1}\left(\mathbb{I} - \frac{1}{3} I \otimes I\right) - 2\mu D_{n+1} n_{n+1} \otimes n_{n+1}$$

$$C_{n+1} = 1 - \frac{2\mu\Delta\lambda_{n+1}}{\|\eta_{n+1}^{*}\|} \tag{3-41}$$

$$D_{n+1} = \frac{3\mu}{3\mu + K_{n+1}^{'} + H_{n+1}^{'}} + \frac{2\mu\Delta\lambda_{n+1}}{\|\eta_{n+1}^{*}\|}$$

A general return mapping algorithm for the plastic corrector step for the cases of a general yield function and arbitrary flow rule is given in [30] based on two different iterative methods, i.e. the closest point projection method and the cutting plane algorithm.

3.4 Extension of the infinitesimal plasticity models to finite deformation based on hypoelastic material models

An extension of the classical plasticity to finite deformation is possible using the Eulerian strain rate tensor. The Eulerian strain rate tensor is a preferred measure of deformation for flow-type constitutive models since it does not need a reference configuration and is a pure Eulerian tensor [5]. The class of Eulerian rate-type formulation of elastoplasticity provides a simple extension of the classical model for finite deformation and their corresponding numerical implementation.

The strain rate tensor can be decomposed into its elastic and plastic parts similar to the case of infinitesimal plasticity. However, such an additive

decomposition of the strain rate tensor should be used only under certain conditions. Furthermore, extension of the infinitesimal loading/unloading conditions to hypo-based plasticity models requires additional restrictions on the yield condition and the objective rates used in the model. These are discussed in the following sections.

3.4.1 Hypo-based finite plasticity models

A proper decomposition of deformation into its elastic and inelastic parts is the key step for the extension of classical models to finite deformations. An Eulerian rate formulation of plasticity requires an Eulerian measure of deformation. Since the flow rules are differential types the strain rate tensor can be used as an appropriate measure of deformation. The strain rate tensor can be additively decomposed into its elastic and plastic parts by

$$d = d^e + d^p \tag{3-42}$$

However, physical applicability of decomposition (3-42) remains to be investigated, and will be discussed later in this section. The elastic part of the strain rate tensor can be related to the Kirchhoff stress through a hypoelastic model by

$$\overset{*}{\dot{\tau}} = \mathcal{M} : d^e \tag{3-43}$$

And the Mises flow potential can be expressed in terms of the Kirchhoff stress and the Eulerian back stress tensor

$$f = f(\tau, \beta, \Upsilon) \tag{3-44}$$

where β and Υ are the two tensorial and scalar variables representing the kinematic and isotropic hardening of the material in the stress space, respectively.

A spatial fixed observer in space sets up the dissipation potential on the current configuration by

$$\varphi^p\left(\tau, q_\beta; d^p, \overset{o}{\dot{Q}}\right) = \tau : d^p + q_\beta : \overset{o}{\dot{Q}} \tag{3-45}$$

where q_β is the vector of plastic internal variables in the stress space and $\overset{o}{\dot{Q}}$ is its corresponding objective rate of the dual vector in the strain space. Using the principle of maximum plastic dissipation, the following expression for the Lagrangian function is obtained

$$\mathcal{L}\left(\tau, q_\beta, \dot{\lambda}; d^p, \overset{o}{\dot{Q}}\right) = -\tau : d^p - q_\beta : \overset{o}{\dot{Q}} + \dot{\lambda} f(\tau, q_\beta) \tag{3-46}$$

Minimization of the Lagrangian function given in (3-46) leads to the following expressions for the flow rule:

$$\begin{aligned} &\frac{\partial \mathcal{L}}{\partial \tau} = 0 \rightarrow d^p = \dot{\lambda}\frac{\partial f(\tau, q_\beta)}{\partial \tau} \\ &\frac{\partial \mathcal{L}}{\partial q_\beta} = 0 \rightarrow \overset{o}{\dot{Q}} = \dot{\lambda}\frac{\partial f(\tau, q_\beta)}{\partial q_\beta} \end{aligned} \tag{3-47}$$

Use of (3-42), (3-43) and (3-47-1) yields

$$d = M^{-1} : \overset{*}{\dot{\tau}} + \dot{\lambda}\frac{\partial f(\tau, q_\beta)}{\partial \tau} \tag{3-48}$$

An evolution equation for the internal tensorial variables (back stress tensor) should be objective under rigid rotation. As a result, a general evolution equation for the back stress tensor should take the following form:

$$\overset{o}{\dot{\beta}} = \hbar(\beta, d^p) \tag{3-49}$$

Here for simplicity we assume the case of a linear evolution equation for the back stress tensor as follows:

$$\overset{o}{\dot{\beta}} = Hd^p \tag{3-50}$$

where H is the constant hardening modulus. It is worth mentioning that evolution equations for scalar plastic variables are objective under rigid rotations and no modification is therefore required for such equations. Equations (3-42) to (3-50) define the extended form of infinitesimal plasticity models to an Eulerian hypo-based model for finite deformations. Such an Eulerian rate model of plasticity has been widely used by several researchers for metal plasticity based on the J_2 associative flow theory (cf. Nagtegaal and DeJong [3], Pinsky et al. [38], Needleman [66], and Rolph and Bathe [67]).

Two concerns regarding the extended hypo-based Eulerian model must be discussed in detail. The first concern is toward the physical applicability of the additive decomposition of the strain rate tensor given by equation (3-42). The second concern is related to the choice of objective rates of stress and back stress given in equations (3-43) and (3-50). These are discussed in the following sections.

3.4.2 Prager's yielding stationary condition and choice of objective rates

In its original form Prager's yielding stationary states that for a perfect plastic material the yield function should be stationary when the stress does not change. The same condition applies for work hardening materials where vanishing stress rates should result in a stationary state of hardening. Prager [68] examined the suitability of different stress rates in the Eulerian rate formulation of elastoplasticity. As a result, the well-known Jaumann rate was proposed by Prager as a preferred rate of stress for the rate-type evolution equations. However, as was shown in Chapter 2, use of the classical Jaumann rate has issues regarding hypoelastic model integrability. While Prager's suggestion for the choice of the Jaumann rate in the stress and back stress evolution equations is still valid, the issues regarding the hypoelastic model non-integrability questions the physical applicability of the Jaumann rate in the Eulerian rate model of elastoplasticity.

Using Prager's yielding stationary condition, Xiao et al. [69] proved that identical objective rates should be used in the stress and back stress evolution equations. Furthermore, they have shown that among all of the possible objective rates, only the corotational rates can be used for such a purpose. This proof is in accordance with the original suggestion of Prager on the use of the Jaumann rate for both the stress and back stress evolutions.

3.4.3 Self-consistent Eulerian rate model

The second consideration is related to the physical applicability of the decomposition of the strain rate tensor into its elastic and plastic parts. The stress power from the balance of energy is given by

$$\dot{W} = \tau : d \tag{3-51}$$

A physical requirement for the additive decomposition of the strain rate tensor given by (3-42) is the exact decomposition of stress power into an elastic recoverable part and a dissipative (irrecoverable) part as follows:

$$\dot{W} = \tau : d = \dot{W}^e + \dot{W}^p = \tau : (d^e + d^p) \tag{3-52}$$

This means that the additive decomposition of the strain rate tensor is physically acceptable if the hypoelastic model used for the elastic part of the deformation given by equation (3-43) is exactly integrable as a Green elastic material. In other words, rate-type constitutive models used for the elastic part of the deformation should be non-dissipative. Based on the discussion given in Chapter 2, the logarithmic (D) rate has been introduced as the unique rate which makes the grade-zero hypoelastic model unconditionally integrable as a Cauchy and Green elastic material. As a result, use of the additive decomposition of the strain rate tensor is physically acceptable if and only if the logarithmic (D) spin is used.

The self-consistency requirement of the hypoelastic model along with the Prager's yielding stationary criterion suggests the use of the logarithmic spin as the

only acceptable objective corotational rate in the Eulerian rate form of elastoplasticity. Based on this, Bruhns et al. [27] have introduced a self-consistent Eulerian rate model of elastoplasticity for finite plastic deformations.

3.5 Numerical implementation of the hypo-based plasticity models

Integration of the plasticity models for finite deformation can be done using a similar approach as discussed in section 3.3. However, the integration method should preserve the objectivity of the model under rigid rotations. In this section such objective integration schemes are presented and implemented for the solution of homogenous and non-homogenous deformation paths.

3.5.1 Objective integration schemes for hypoelastic models

Hypoelastic models can be integrated in a rotated configuration. Considering a grade-zero hypoelastic model given by $\overset{*}{\dot{\tau}} = \mathcal{M}:d$ in an Ω_*-spinning frame and defining the rotated counterparts of the Kirchhoff stress and rate of deformation tensors by $\Sigma = R_*^T \tau R_*$ and $D = R_*^T d R_*$, the hypoelastic model takes the following form on the rotated configuration

$$\dot{\Sigma} = \mathcal{M}:D \tag{3-53}$$

In equation (3-53) it is assumed that the fourth-order hypoelasticity tensor is isotropic. Integrating equation (3-53) in the time interval $[t_n, t_{n+1}]$ using the midpoint rule yields

$$\Sigma_{n+1} = \Sigma_n + \mathcal{M}:(\Delta t D_{n+\alpha}) \tag{3-54}$$

where α defines the method of integration; $\alpha = 1$ and $\alpha = 0$ yield the well-known methods of implicit backward-Euler and explicit forward-Euler integration schemes. Rotating back equation (3-54) onto the fixed background yields

$$\tau_{n+1} = R_n^{n+1}\tau_n {R_n^{n+1}}^T + \mathcal{M}:\left(R_{n+\alpha}^{n+1}\Delta t d_{n+\alpha} {R_{n+\alpha}^{n+1}}^T\right) \tag{3-55}$$

where $R_n^{n+1} = R_{*n+1}{R_{*n}}^T$ and $R_{n+\alpha}^{n+1} = R_{*n+1}{R_{*n+\alpha}}^T$ are the relative frame rotation tensors.

Furthermore, an objective integrated form of $\Delta t d_{n+\alpha}$ in (3-55) is required. A second-order accurate approximation ($\alpha = 0.5$) for integration of the rate of deformation is given in [30] and is used here as follows:

$$\Delta t d_{n+\alpha} = f_{n+\alpha}^{-T} e_{n+1} f_{n+\alpha}^{-1} \tag{3-56}$$

where $e_{n+1} = \frac{1}{2}(f_{n+1}^T f_{n+1} - I)$ is the strain at the end of the interval. The relative deformation gradients are defined by:

$$\begin{aligned} f_{n+\alpha} &= F_{n+\alpha}F_n^{-1} \\ F_{n+\alpha} &= \alpha F_{n+1} + (1-\alpha)F_n \end{aligned} \tag{3-57}$$

and F_{n+1} and F_n are the known deformation gradients at the start and end of the time interval. Equation (3-56) is a rotation-independent integrated form of the rate of deformation tensor. This can be examined by assuming a rigid motion of the form $x_{n+1} = Qx_n + c$ in the interval $[t_n, t_{n+1}]$. Such a rigid motion results in $f_{n+1} = Q$ and $e_{n+1} = \frac{1}{2}(Q^T Q - I) = 0$; as a result, equation (3-56) preserves the objectivity of the strain rate tensor under rigid motion.

The final step to be considered when using equation (3-55) is the update of the frame rotation based on the given spin tensor. An integration scheme was proposed by Hughes and Winget [70] based on the generalized midpoint rule. According to their method for an arbitrary orthogonal transformation, the evolution of the rotation tensor is given by

$$\dot{R}_* = \Omega_* R_* \tag{3-58}$$

Integrating (3-58) using the generalized midpoint rule yields

$$R_{*n+1} - R_{*n} = \left(\Delta t \Omega_{*n+\alpha}\right)\left\{\alpha R_{*n+1} + (1-\alpha) R_{*n}\right\} \tag{3-59}$$

which yields the following relation for the rotation tensor at the end of the time interval:

$$R_{*n+1} = \left(I - \alpha \Delta t \Omega_{*n+\alpha}\right)^{-1}\left[I + \Delta t(1-\alpha)\Omega_{*n+\alpha}\right] R_{*n} \tag{3-60}$$

Another integration scheme has been proposed by Simo and Hughes [30] based on the exponential mapping method and is given by

$$R_{*n+1} = exp\left(\Delta t \Omega_{*n+\alpha}\right) R_{*n} \tag{3-61}$$

Use of equation (3-61) requires the exponential of the spin tensor during time integration. Several different numerical methods for exponential mapping have been proposed in the literature (cf. Moler and Loan [71]).

3.5.2 Extension of the algorithm to hypo-based plasticity models

Similar to the case of infinitesimal plasticity, the radial return mapping algorithm can be used for the integration of the hypo-based J_2 flow theory for finite deformations. The trial predictor step of the integration is done on the mid-configuration $(\alpha = 0.5)$ and a radial return mapping for the corrector step can be used on the current configuration $(\alpha = 1)$. An algorithmic chart for the case of J_2 flow theory and linear hardening rules is given in [30].

However, algorithmic (consistent) linearization of the integration scheme is complex and is directly affected by different spinning-frames used in the model. Exact linearization algorithms for the case of the Jaumann and Green-McInnis-Naghdi rates are given by Fish and Shek [72] and Voyiadjis and Abed [73].

3.6 Numerical integration of simple loading paths

In this section the integration schemes discussed above are used for the hypo-based plasticity models with three different corotational rates of stress, i.e. the

Jaumann, Green-McInnis-Naghdi, and logarithmic (D) rates. The formulation is implemented in the ABAQUS [74] commercial software with the help of the user defined subroutine UMAT.

Three different loading schemes have been defined for the stress integration. The first two are of the homogenous deformation path defined by simple shearing and closed path elliptical loading, respectively. The third loading scheme is a non-uniform deformation path of the four-step loading discussed in Chapter 2.

3.6.1 Simple shear problem

The problem of simple shear shown in Figure 2-1 is considered here first. Analytical elastic solutions are plotted in Figure 3-3 for a maximum applied shear γ_{max}=8. To verify the developed UMAT results, the simple shear problem was solved and compared with the analytical solutions given in section 2.6.4.1. Material properties used for the numerical integration of this problem are given in Table 3-1.

Table 3-1 Material properties for the simple shear problem

Elastic Modulus (GPa)	195
Shear Modulus (GPa)	75
Poisson's Ratio	0.3
Yield Stress (MPa)	180
Hardening Modulus (GPa)	2.0
Shear Yield Stress τ_Y (MPa)	104

The elastic numerical solution of the problem is obtained first. Finite element (FE) UMAT results as well as ABAQUS built-in formulation results are plotted in

Figure 3-3. FE results are consistent with the analytical elastic solutions for each rate of stress.

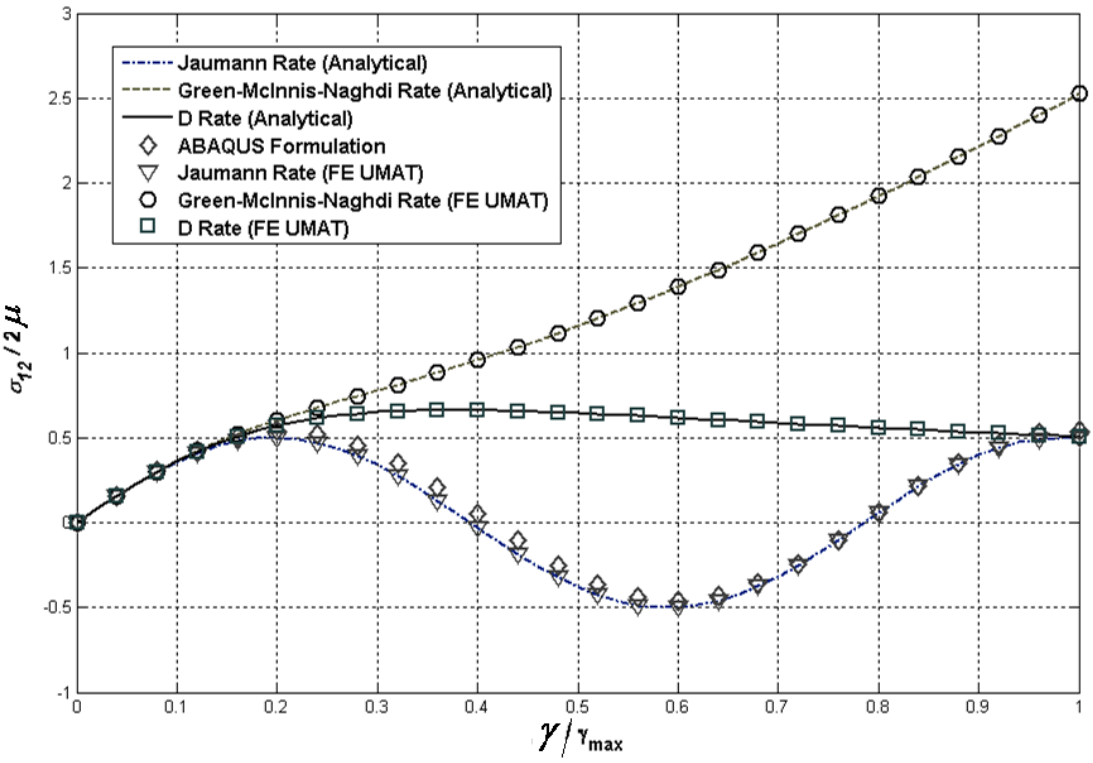

Figure 3-3- Simple shear problem, analytical [75] and FE results for normalized shear stress

The problem of simple shear was also solved for 50 elastic cycles of fully reversed shear, i.e. $[\gamma_{min} = -8\,, \gamma_{max} = 8]$, to examine the effect of different rates of stress. Figure 3-4 and Figure 3-5 show the components of the residual stress at the end of each cycle. As shown in Figure 3-4, no residual shear is observed for the D and the Jaumann rates as well as the ABAQUS built-in formulation. However, the Green-McInnis-Naghdi rate of stress shows residual shear stress accumulation. For the normal component of residual stress shown in Figure 3-5, the built-in ABAQUS formulation exhibits larger residual stress compared to the other formulations. The

normal residual stress component from the Green-McInnis-Naghdi formulation is also non-zero, but several orders of magnitude smaller than the ABAQUS built-in results.

The problem of simple shear is further solved using a bilinear material, following Ziegler's linear kinematic hardening rule. Figure 3-6 shows the material response for $\gamma_{max}=8$ using different rate formulations obtained from both FE analysis and the analytical solution given in [75].

Similar to the elastic response of material the problem of shear oscillation with the Jaumann rate of stress happens for the back stress tensor. No shear oscillation is observed for the Green-McInnis-Naghdi and D rates of stress.

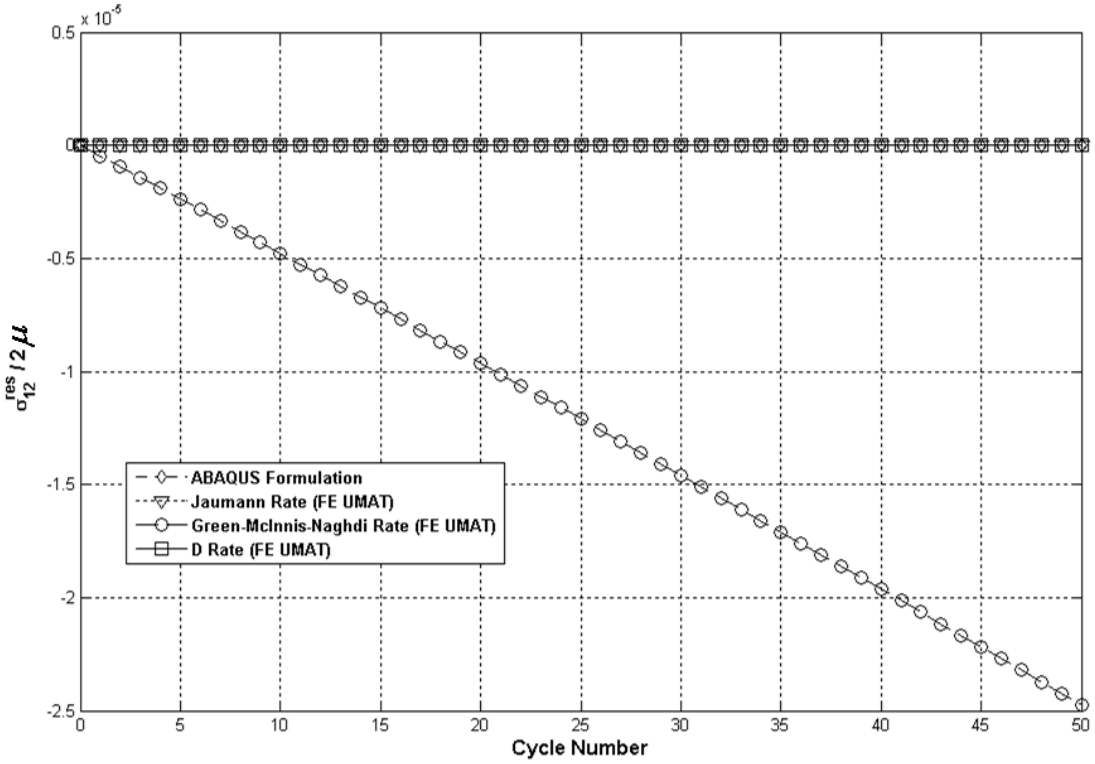

Figure 3-4- Cyclic simple shear, normalized elastic residual shear stress component results for different rate type formulations for 50 cycles

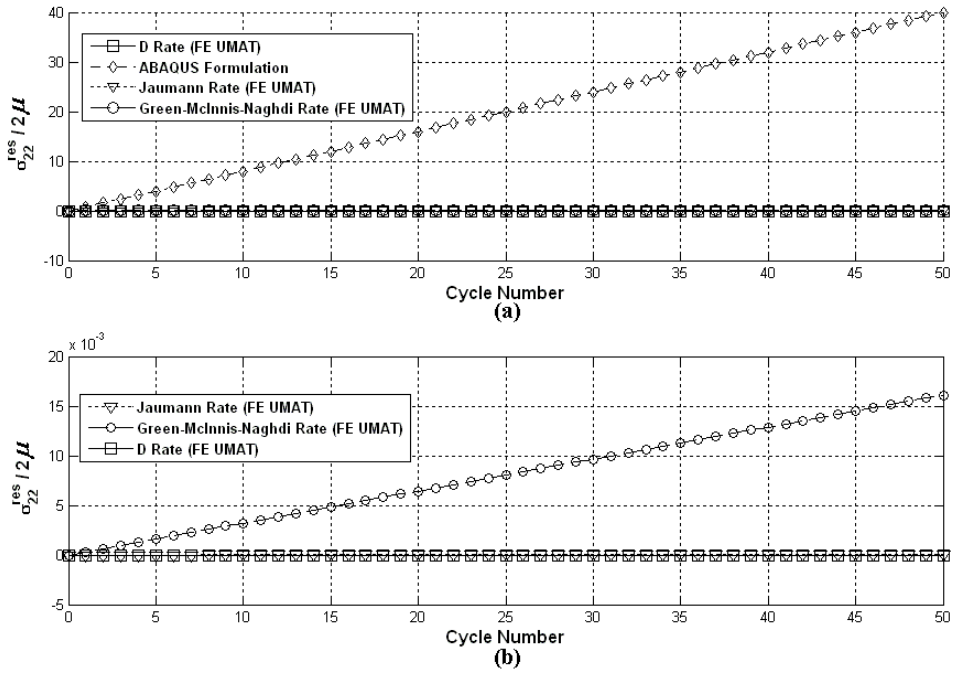

Figure 3-5- Cyclic simple shear results, normalized elastic residual normal stress component for 50 cycles, (a) UMAT and ABAQUS result, (b) UMAT results only

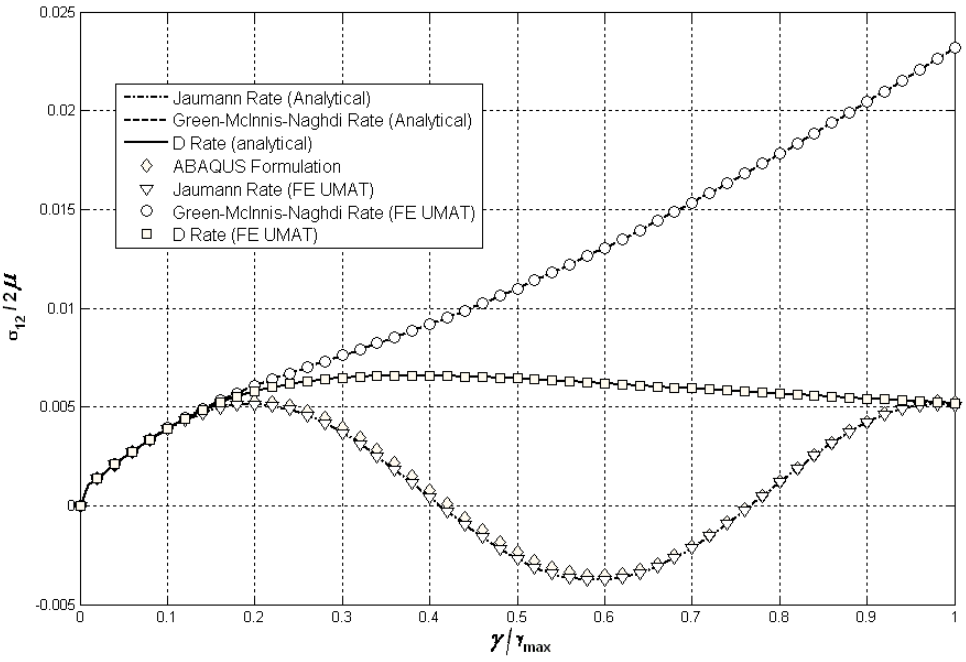

Figure 3-6- Elasto-plastic simple shear problem (linear kinematic hardening) response using different rate formulations from FE and analytical results

To investigate the elastoplastic behavior of the material under fully reversed cyclic shear loading, the same problem was solved for 50 cycles of fully reversed shear load for a maximum applied shear of γ_{max}=8. Figure 3-7 shows the normalized residual stress vs. cycle number for different rate formulations. Compared to the other formulations, the ABAQUS results show significantly higher residual shear stress beyond the first cycle. All formulations exhibit constant shear residual stresses and no strain ratchetting or cyclic stress hardening/softening were observed. The cyclic strain-stress curves are stabilized after the first cycle.

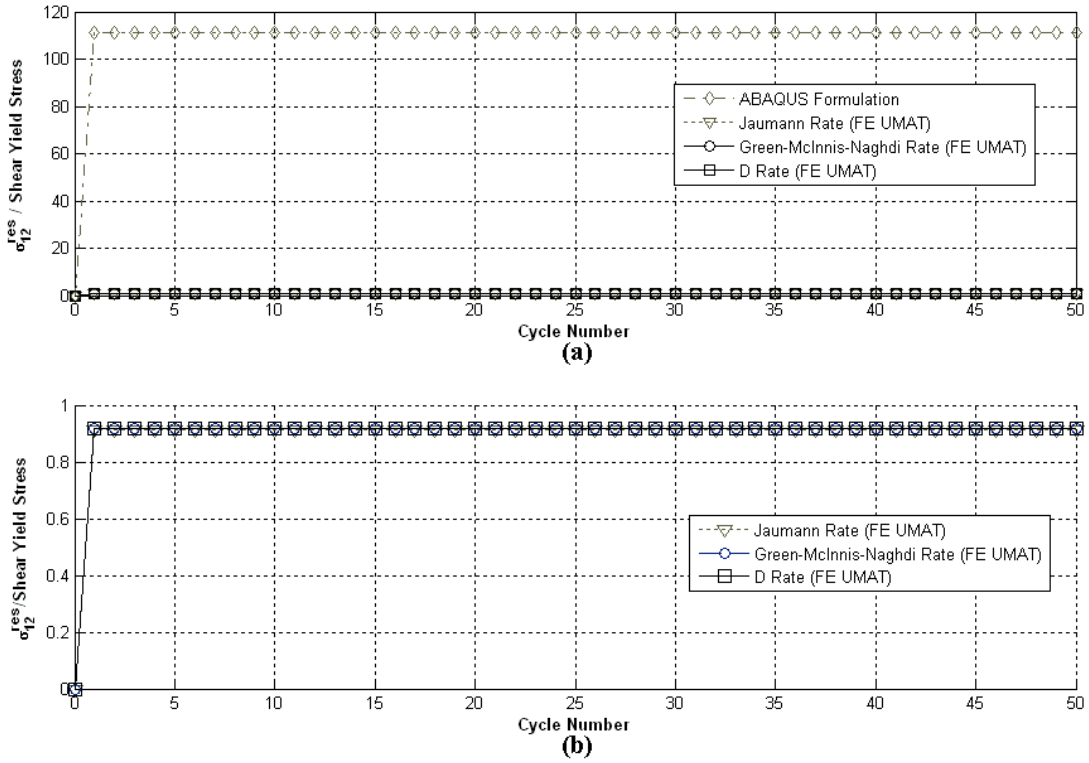

Figure 3-7- Cyclic simple shear results for 50 cycles, normalized residual shear stress using linear kinematic hardening rule, (a) UMAT results including ABAQUS results, (b) UMAT results only

3.6.2 Elliptical closed path loading

The problem of closed path cyclic loading has been discussed extensively in the literature. Recently, Meyers et al. [76] considered an elliptical loading path of a hypoelastic material for several cycles to study the effect of different rates on the elastic ratchetting response of the material. Here the same problem of elliptical loading is considered and the results are compared with those of Meyers et al. [76]. As shown in Figure 3-8 a square of side *H* is loaded using the elliptical loading path. The motion is described by [76]:

$$x_1 = X_1 + \alpha\beta \frac{1 - cos\,\phi}{1 + \alpha\, sin\,\phi} X_2$$
$$x_2 = (1 + \alpha\, sin\,\phi) X_2 \tag{3-62}$$

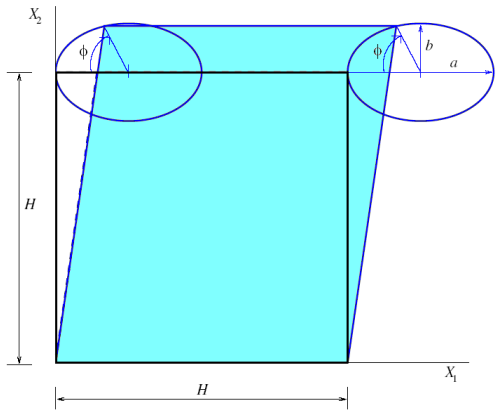

Figure 3-8- Cyclic closed path loading

where $\alpha = \frac{b}{H}$ and $\beta = \frac{a}{b}$. The material properties used for the simulation are given in Table 3-2. The problem is solved assuming $\alpha = 0.1$ and $\beta = 5$. The user defined subroutine DISP in ABAQUS was used to define the elliptical loading.

Table 3-2 Material properties for the elliptical cyclic loading problem

Elastic Modulus (GPa)	200
Shear Modulus (GPa)	77
Poisson's Ratio	0.3
Yield Stress (MPa)	800
Hardening Modulus (GPa)	20
Shear Yield Stress τ_Y (MPa)	462

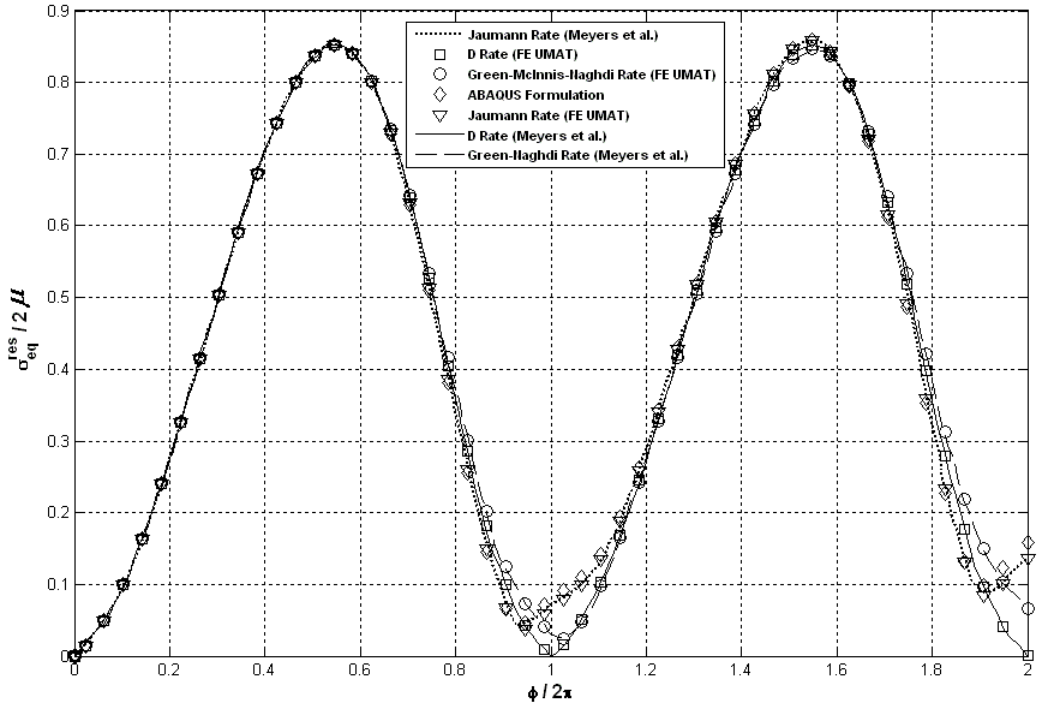

Figure 3-9- Elliptical cyclic loading, normalized Mises stress for 2 cycles, using 3 different stress rates, Jaumann, Green-McInnis-Naghdi, and D rates of stress (FE UMAT), ABAQUS formulation, and analytical solution

To examine elastic ratchetting, the same problem was solved for 50 cycles. Figure 3-10 shows the normalized residual elastic shear and residual normal stress components vs. cycle number.

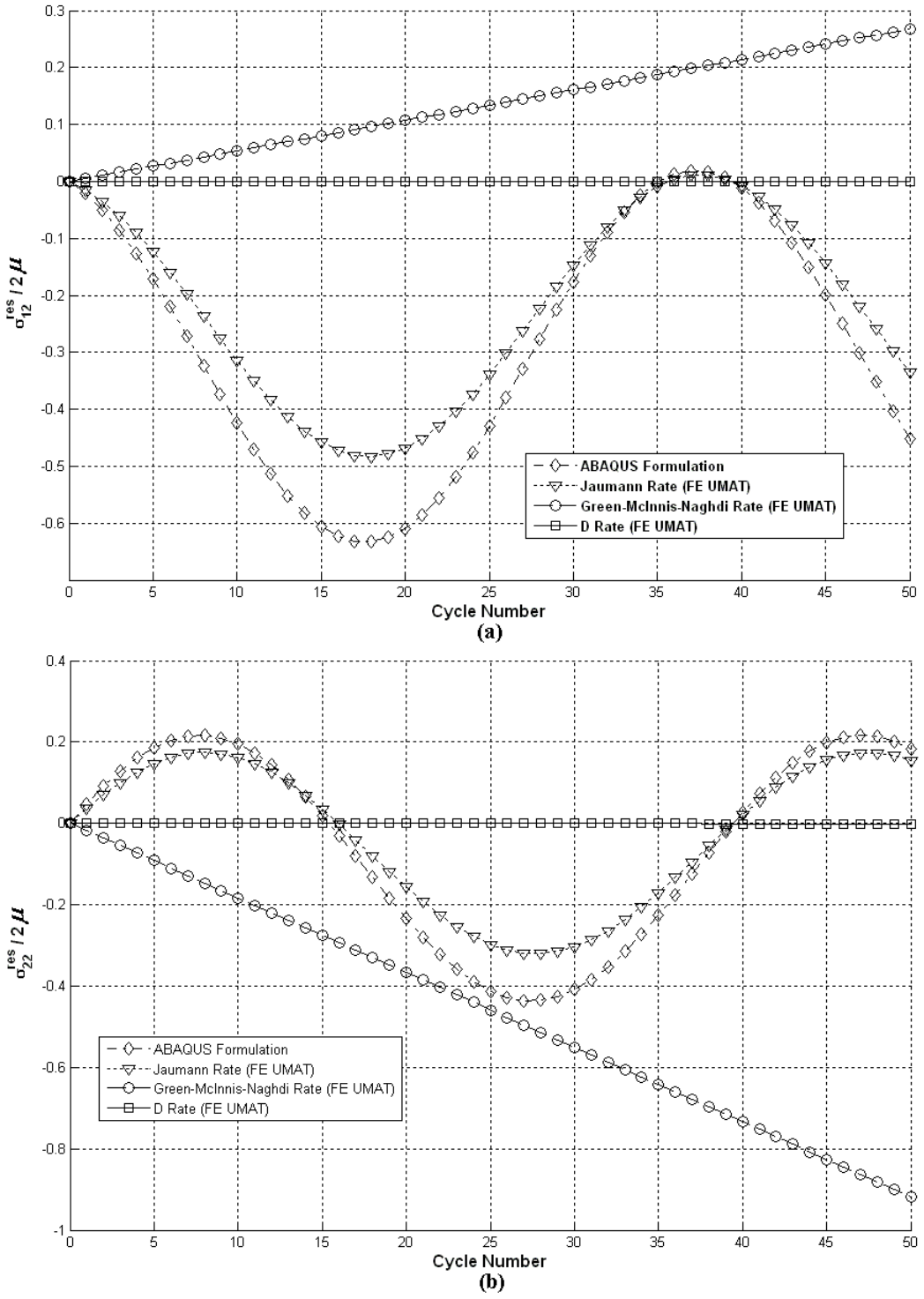

Figure 3-10- Elliptical cyclic loading results for 50 cycles using different rate formulations, (a) normalized residual elastic shear stress, (b) normalized residual elastic normal stress

As can be seen from Figure 3-10, the residual stress for the Green-McInnis-Naghdi rate shows an increasing pattern with cycles, while the Jaumann rate and the ABAQUS built-in formulation show an oscillatory pattern. Only the D rate of stress exhibits no residual stress. The strain-stress cyclic responses for each formulation are plotted in Figure 3-11. Strain-stress curves clearly show how the rate formulation affects the material response. For all the cases except the D rate of stress, elastic dissipation is evident. Similar to the results given in [76], only the D rate of stress shows the expected elastic behavior under cyclic loading, i.e. no elastic dissipation.

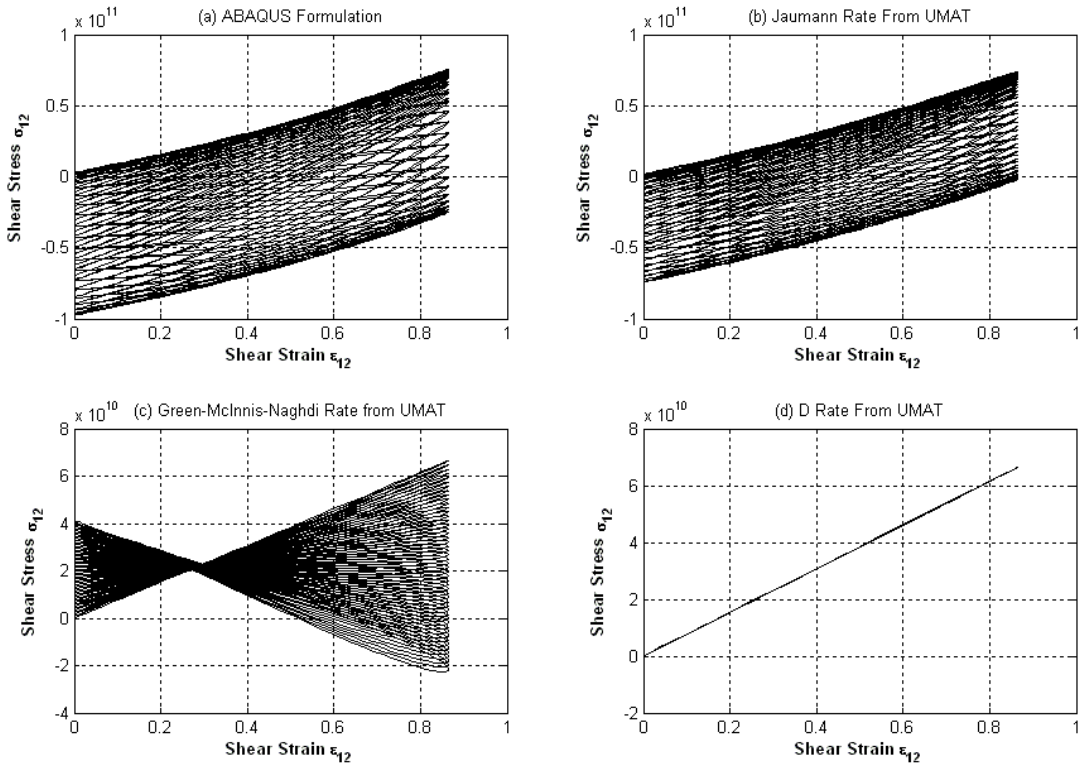

Figure 3-11- Strain-Stress curves for 50 cycles of egg-shaped cyclic loading using different rate formulations, (a) ABAQUS Formulation, (b) Jaumann rate UMAT, (c) Green-McInnis-Naghdi rate UMAT, (d) D rate UMAT

The problem of elliptical cyclic loading is further solved assuming Ziegler's linear kinematic hardening rule. The problem was solved for 50 cycles using different rate-type formulations. Figure 3-12 shows the normalized residual stress components at the end of each cycle for different rate formulations.

From Figure 3-12, the D rate shows a constant residual stress which is not affected by the cycles. The Green-McInnis-Naghdi rate shows monotonically increasing residual stress which becomes unrealistic for high numbers of cycles. The Jaumann and ABAQUS formulations show an oscillatory residual stress response.

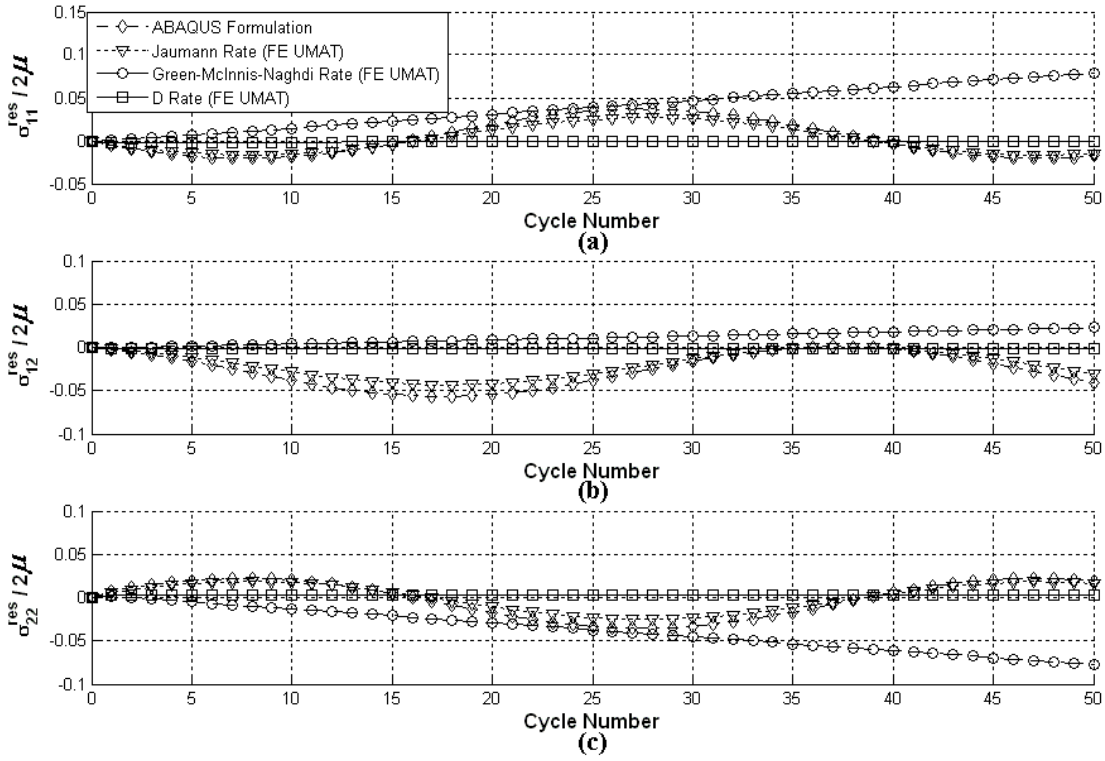

Figure 3-12- Elliptical cyclic loading results for 50 cycles, normalized residual (a), normal σ_{11}, (b) shear σ_{12}, and (c) normal σ_{22} stresses vs. cycle number for different rate formulations using a linear kinematic hardening (Ziegler) rule

Figure 3-13 shows the cyclic shear strain-stress curves for 50 cycles. From Figure 3-13 the Jaumann and ABAQUS formulations predict a profound cyclic softening material response, while the Green-McInnis-Naghdi rate formulation predicts a rather unusual but equally unrealistic response. Only the D rate formulation exhibits the expected stabilized hysteresis loop.

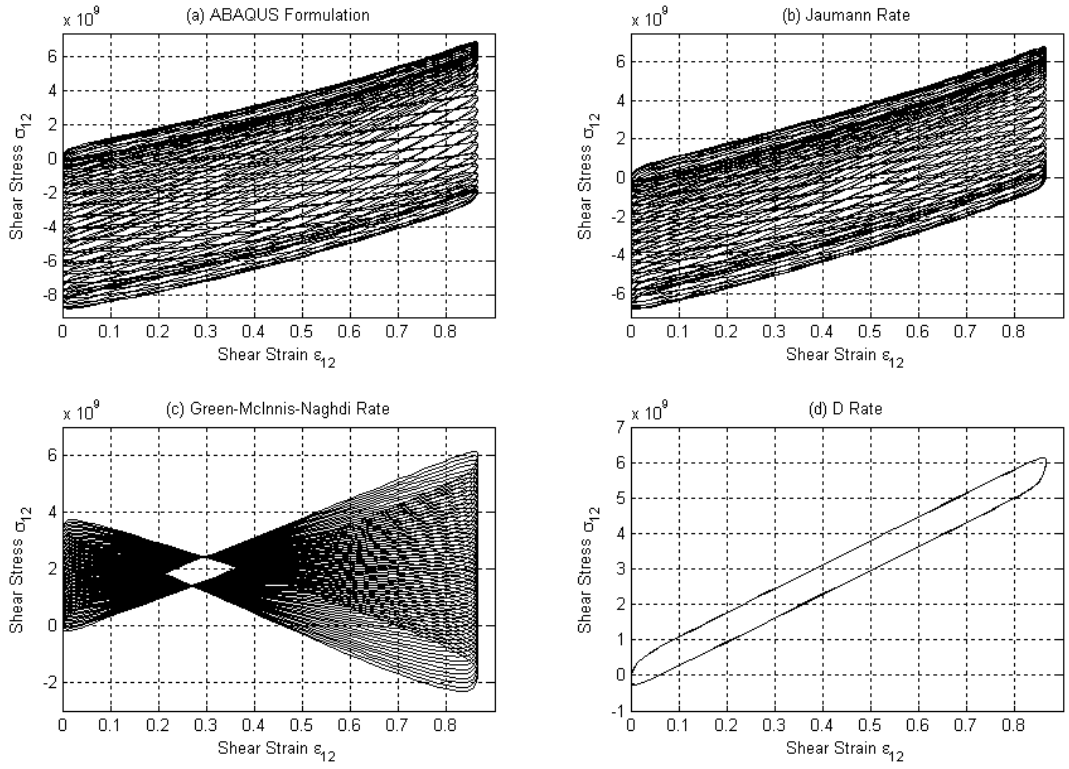

Figure 3-13- Elliptical cyclic loading results for 50 cycles, shear strain-stress curves using a linear kinematic hardening rule

3.6.3 Non-uniform four-step loading

The problem of four-step loading solved in Chapter 2 is considered next. Unlike the four-step loading discussed in Chapter 2, the deformation applied here is not homogeneous and therefore the FE solution requires use of discretized elements.

As illustrated in Figure 3-14, a 1*1 m^2 square is subjected to a closed path four-step loading at its top edge while the bottom edge is fixed. The loading path is shown in Figure 3-15. Material properties used for this problem is the same as those given in Table 3-2 for the problem of elliptical cyclic loading. First the problem was solved for 10 complete elastic cycles with the maximum extension and shear displacement magnitudes equal to 0.2 (m) each. Therefore, deformations are not large; only 20% of maximum extension and a maximum shear of 0.2. Since the stress field is not uniform in this problem, no analytical solution is available and use of the finite element method is required for a solution.

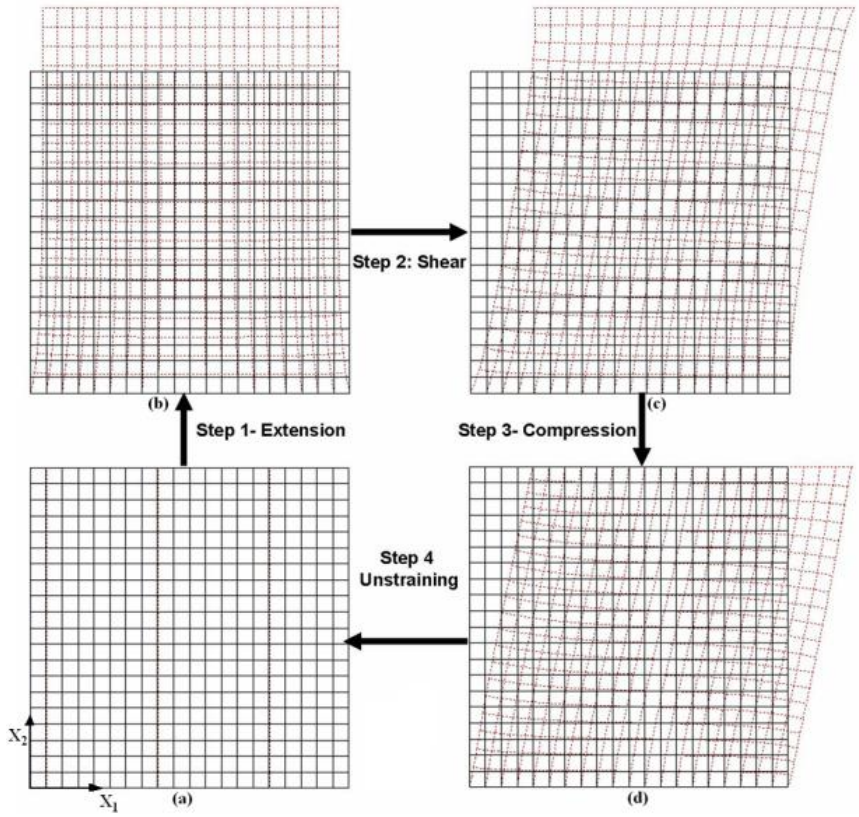

Figure 3-14- Four-step loading, (a) initial configuration (no extension and no shear), (b) after extension, (c) after added shear, (d) after removing extension

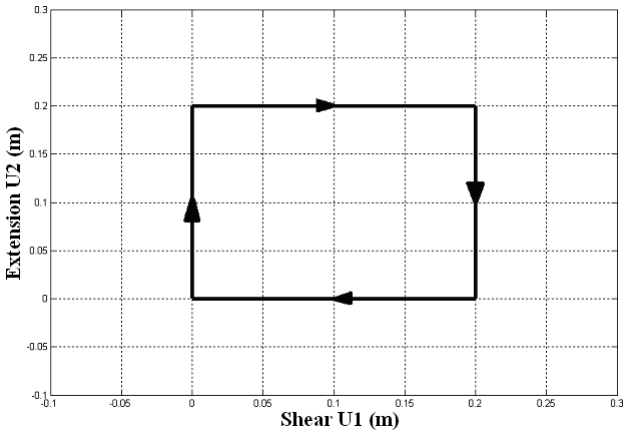

Figure 3-15-Four-step loading path

Quadrilateral 8 noded elements were used in the FE simulation. All of the results are reported at the centroid of the element shown in Figure 3-16.

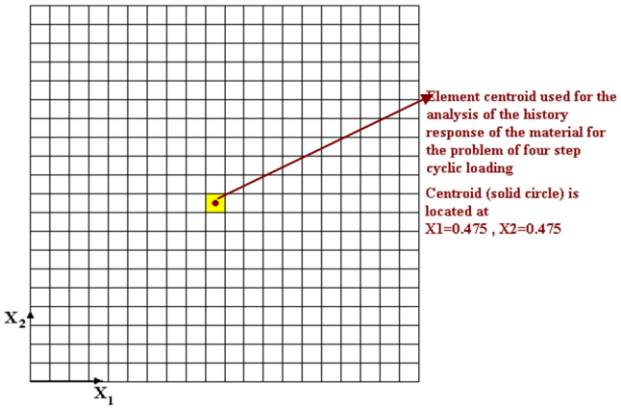

Figure 3-16- Location of the element and its centroid used for the results output

Figure 3-17 shows the residual elastic shear stresses at the end of each cycle for different rates of stress. Again, except for the D rate, all other rates show increasing residual stress over cycles. Figure 3-18 shows the strain-stress response using different rate formulations. The applied deformation is not large (20% extension), however, the error accumulation is considerable even after a few cycles.

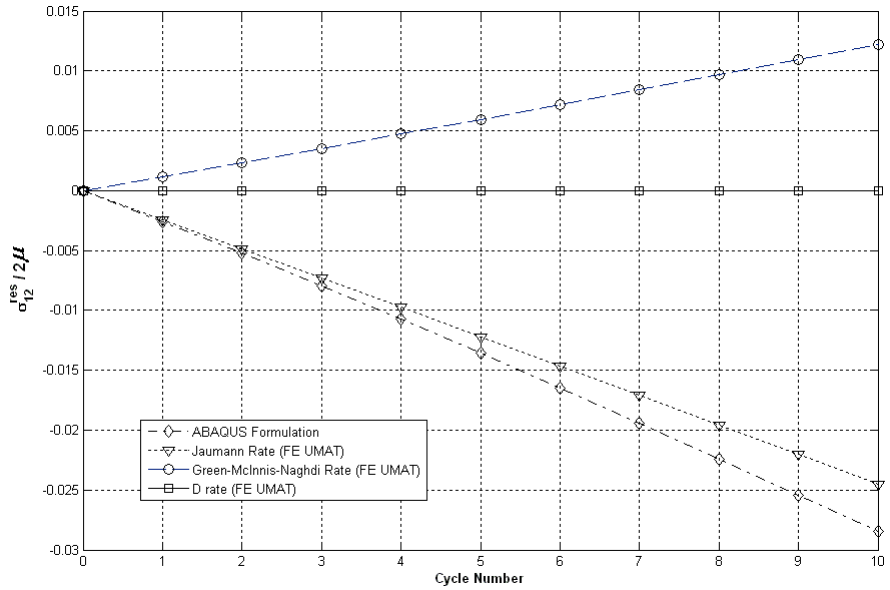

Figure 3-17- Four-step loading results for 10 cycles, normalized residual elastic shear stress using different rate formulations

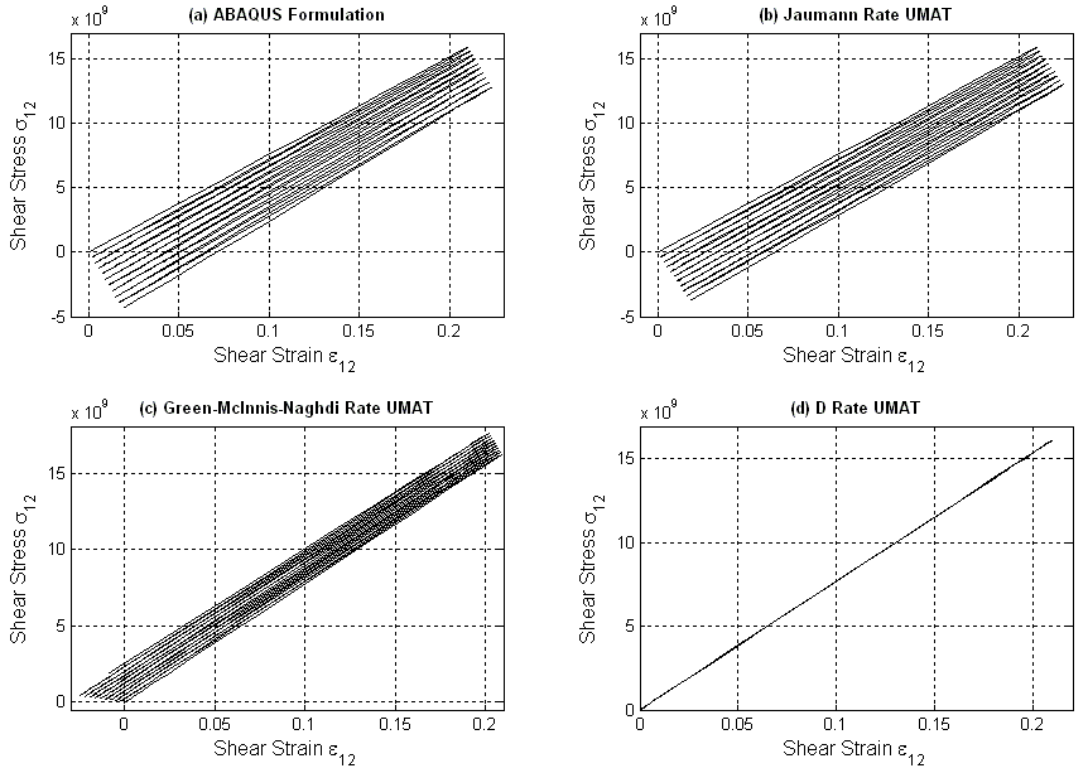

Figure 3-18- Four-step loading elastic response for 10 cycles, (a) ABAQUS Formulation, (b) Jaumann rate UMAT, (c) Green-McInnis-Naghdi rate UMAT, (d) D rate UMAT

The problem of closed path four-step loading was further solved assuming Ziegler's linear kinematic hardening rule. The same quadrilateral elements (8 noded) were used for this simulation. All the results are reported at the centroid of the element which was shown in Figure 3-16. The problem is solved for 10 cycles. Figure 3-19 shows the normalized residual stress components vs. cycle number for different rate-type formulations. Figure 3-20 also shows the shear strain-stress cyclic curves obtained for different rate type formulations.

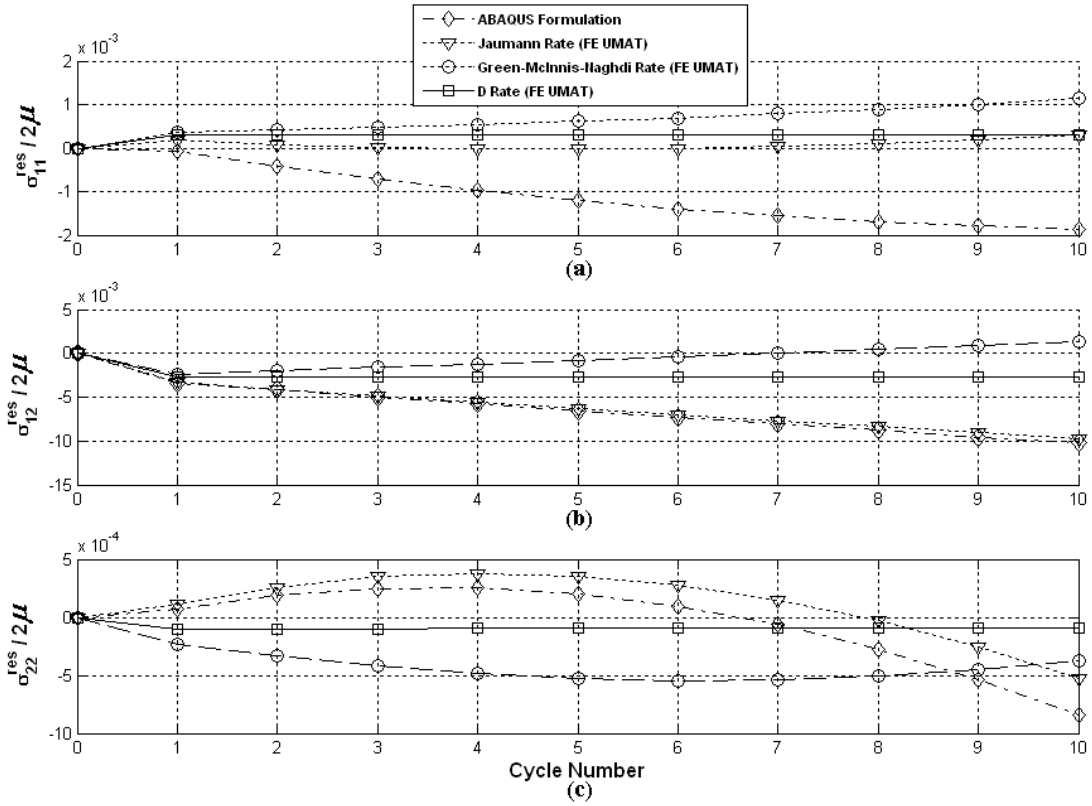

Figure 3-19- Four-step loading results for 10 cycles, assuming linear kinematic hardening rule, normalized residual stress components

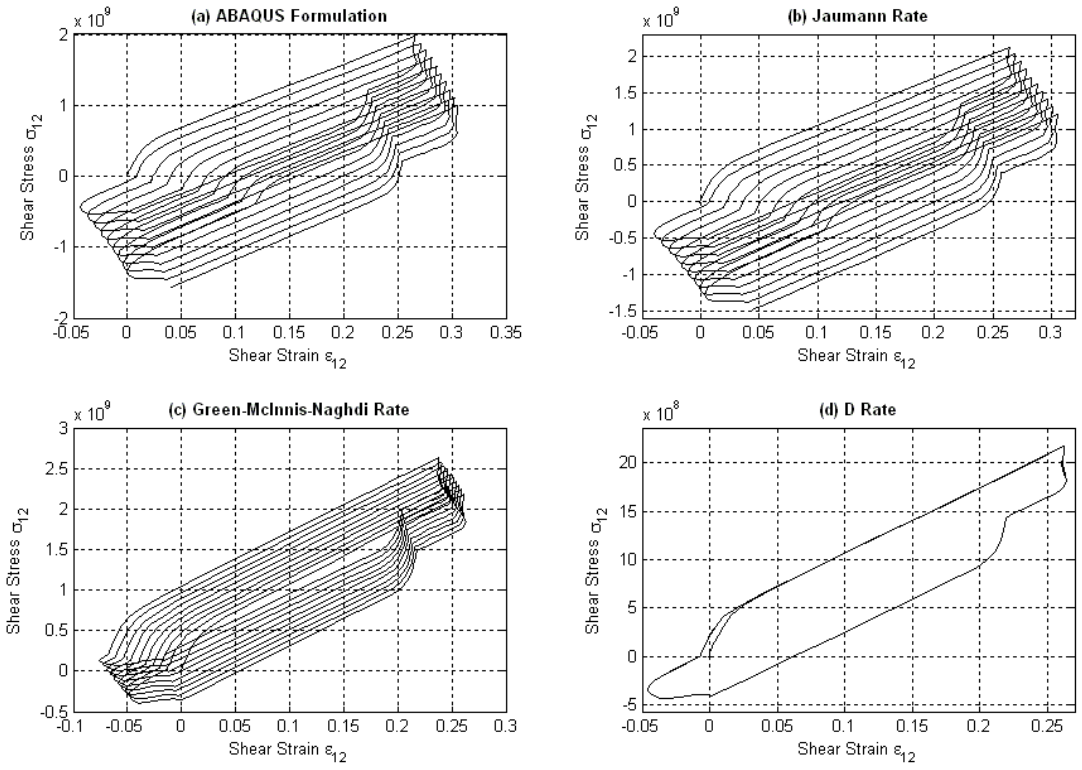

Figure 3-20- Four-step loading, shear strain-stress response, linear kinematic hardening rule, (a) ABAQUS formulation, (b) Jaumann rate, (c) Green-McInnis-Naghdi rate, (d) D rate

The deformation is not very large, however, differences in response of different rate formulations build up very fast and the results even after a few cycles deviate significantly. The D rate formulation exhibits a constant residual stress response as expected for a stabilized hysteresis loop. The residual stresses for the Jaumann, ABAQUS, and Green-McInnis-Naghdi formulations exhibit a mixture of oscillatory and monotonically increasing pattern. Also, the cyclic shear strain-stress curves for the Jaumann, Green-McInnis-Naghdi, and ABAQUS formulations are not stabilized, showing a mix cyclic strain ratchetting and stress hardening. Only, the D rate formulation exhibits the expected stabilized cyclic shear strain-stress curve.

It should be mentioned that the deformation path for this problem is non-uniform which necessitates a linearized form of the constitutive model at the end of each load increment. The algorithmic tangent modulus for this problem was based on the formulation given in [72,73] for the Jaumann and Green-McInnis-Naghdi rates, respectively. For the D rate however an exact algorithmic modulus was not implemented. The algorithmic modulus used for the Jaumann rate was used for the D rate as an approximation. While this approximation does not affect the accuracy of the converged solutions it might slow down the convergence rate or sometimes lead to the divergence of integration. As a result, the approximation used does not guarantee the convergence of the stress integration.

3.7 Summary

Extension of the infinitesimal plasticity models for finite deformation and their corresponding numerical integration were discussed in this chapter. The Eulerian rate-type plasticity models are based on the hypoelastic material models. As a result, certain considerations should be taken when such models are used.

Hypoelastic material models should be exactly integrable and consistent with the notion of hyperelasticity. Furthermore, Prager's yielding stationary requires use of objective corotational rates in evolution equations. Such conditions suggest the use of the D or logarithmic spin as the only consistent rate in the Eulerian rate models of elastoplasticity.

Numerical solutions obtained for different loading paths along with the analytical proof of hypoelastic model integrability given in Chapter 2 verify the uniqueness of the logarithmic (D) rate. As a result, only the Eulerian rate model of plasticity based on the logarithmic (D) rate of stress provides the consistent formulation of elastoplasticity for finite deformations. Physically, thermodynamics considerations regarding the recoverable and irrecoverable parts of the deformation can be satisfied if the logarithmic (D) rate is used in the formulation.

Chapter 4

Finite plasticity based on a unified Eulerian rate form of elasticity

Eulerian rate models of elastoplasticity are mostly based on the additive decomposition of the strain rate tensor and hypoelastic material models for the elastic part of the deformation and stress update. However, issues with hypoelasticity limit the applicability of hypoelastic models in Eulerian rate models to the use of a specific rate of stress, as discussed in Chapters 2 and 3.

In this chapter, an Eulerian rate form of elasticity is presented and used to set up a new Eulerian rate model for finite deformation plasticity. The model is based on the Eulerian Hencky (logarithmic) strain and additive decomposition of its objective

corotational rate. Integrability conditions of the proposed model for a general stress-dependent isotropic elasticity tensor are investigated and it is shown that the grade-zero form of the model is unconditionally integrable in the sense of hyperelasticity for any objective corotational rate.

The grade-zero form of the proposed model is used in an Eulerian rate form of elastoplasticity. Thermodynamic consistency of the model requires proper definition of the conjugate stress for the corotational rate of strain used in the model. Two cases of deformation, i.e. the cases of coaxiality and non-coaxiality of stress and strain, are discussed in the proposed model. Application of the proposed model to mixed nonlinear hardening behavior is further presented. Predicted results by the proposed model are in good agreement with the available experimental data of finite fixed-end torsional loading of SUS 304 stainless steel tubes [83]. Prediction of the axially induced strain (stress) under free-end (fixed-end) finite torsional loading (the Swift effect) is of importance since the axially induced strain (stress) remarkably affects the cyclic behavior of hardening materials for finite deformation [1].

The proposed model does not assign any preference to different objective rates and any corotational objective rate of stress can be successfully used in the model.

4.1 Eulerian rate form of elasticity

An incremental hyperelastic model can be given in Eulerian form by [47]

$$\delta e = \frac{\partial^2 \mathcal{Z}}{\partial t \partial t} : \delta t \tag{4-1}$$

where (e, t) is an Eulerian conjugate pair of stress and strain and $M^{-1}(t) = \frac{\partial^2 \mathcal{Z}}{\partial t \partial t}$ is the instantaneous (stress-dependent) compliance tensor.

The objectivity and rate homogeneity requirements of a rate model in a spinning background discussed in Chapter 2 require that an incremental form of the hyperelastic model (4-1) be written in terms of identical objective rates, i.e.:

$$\overset{*}{\dot{e}} = M^{-1}(t) : \overset{*}{\dot{t}} \tag{4-2}$$

Or equivalently

$$\overset{*}{\dot{t}} = M(t) : \overset{*}{\dot{e}} \tag{4-3}$$

According to Truesdell and Noll [6] all elastic materials are hypoelastic while the inverse statement is not true in general. Here, a more general question is asked: if a hyperelastic model given by equation (4-1) is derivable from equation (4-3). In other words, integrability of the Eulerian rate model (4-3) in the sense of Cauchy and Green elasticity is under question. This is investigated mathematically in the following sections.

4.1.1 Integrability of the Eulerian rate model of elasticity

Following the approach used by Bernstein [16,17] the integrability of the Eulerian rate model (4-3) is investigated here [77,78]. Rotating the Eulerian rate model (4-3) in its corresponding spinning frame with the rotation tensor R_* yields

$$\dot{\Sigma} = M(\Sigma):\dot{E} \tag{4-4}$$

in which $\Sigma = R_*^T t R_*$ and $E = R_*^T e R_*$ are the rotated counterparts of the Eulerian stress and strain tensors, respectively. In deriving (4-4) it is assumed that the elasticity tensor is isotropic, i.e. $M(R_*^T t R_*) = M(t)$. Equation (4-4) has the standard form of a first-order differential as follows:

$$\frac{\partial \Sigma}{\partial E} = M(\Sigma) \tag{4-5}$$

Integrability of equation (4-5) can be investigated by differentiating it with respect to E as follows:

$$\frac{\partial^2 \Sigma_{ij}}{\partial E_{mn}\partial E_{kl}} - \frac{\partial^2 \Sigma_{ij}}{\partial E_{kl}\partial E_{mn}} = \frac{\partial M_{ijkl}(\Sigma)}{\partial E_{mn}} - \frac{\partial M_{ijmn}(\Sigma)}{\partial E_{kl}} = 0 \tag{4-6}$$

Knowing that $\frac{\partial M_{ijkl}(\Sigma)}{\partial E_{mn}} = \frac{\partial M_{ijkl}(\Sigma)}{\partial \Sigma_{rs}}\frac{\partial \Sigma_{rs}}{\partial E_{mn}} = \frac{\partial M_{ijkl}(\Sigma)}{\partial \Sigma_{rs}} M_{rsmn}(\Sigma)$ and substituting it into equation (4-6) yields

$$\frac{\partial M_{ijkl}(\Sigma)}{\partial \Sigma_{rs}} M_{rsmn}(\Sigma) = \frac{\partial M_{ijmn}(\Sigma)}{\partial \Sigma_{rs}} M_{rskl}(\Sigma) \tag{4-7}$$

Since E and Σ are arbitrary stress and strain tensors and $M(\Sigma)$ is an isotropic tensor, equation (4-7) can be re-written in the fixed background as follows:

$$\frac{\partial M_{ijkl}\,(\boldsymbol{t})}{\partial \boldsymbol{t}_{rs}} M_{rsmn}\,(\boldsymbol{t}) = \frac{\partial M_{ijmn}\,(\boldsymbol{t})}{\partial \boldsymbol{t}_{rs}} M_{rskl}\,(\boldsymbol{t}) \tag{4-8}$$

Conditions (4-8) are necessary and sufficient conditions for the Eulerian rate model given by (4-3) to be integrable in the sense of Cauchy elasticity. Conditions (4-8) are similar to Bernstein's integrability conditions given by (2-86) except that conditions (4-8) are solely imposed on the spatial elasticity tensor. It is worth mentioning that, contrary to Bernstein's integrability conditions given by (2-86), the integrability conditions (4-8) are derived irrespective of any specific spin tensor.

Conditions (4-8) can be expressed in terms of the compliance tensor. Differentiating $M(\boldsymbol{t}) : M^{-1}(\boldsymbol{t}) = \mathbb{I}$ with respect to $\boldsymbol{t}$ yields:

$$\frac{\partial M^{-1}_{ijmn}}{\partial \boldsymbol{t}_{pq}} M_{mnkl} + M^{-1}_{ijmn} \frac{\partial M_{mnkl}}{\partial \boldsymbol{t}_{pq}} = 0 \tag{4-9}$$

Substituting (4-9) into (4-8) yields

$$\frac{\partial M^{-1}_{ijkl}}{\partial \boldsymbol{t}_{mn}} = \frac{\partial M^{-1}_{ijmn}}{\partial \boldsymbol{t}_{kl}} \tag{4-10}$$

Conditions (4-10) are an equivalent form of integrability conditions (4-8) and are applied on the compliance tensor. To satisfy (4-8) or (4-10) it is sufficient that the compliance tensor $M^{-1}(\boldsymbol{t})$ be an isotropic tensor valued function of $\boldsymbol{t}$, i.e.:

$$M^{-1}(\boldsymbol{t}) = \nabla \Psi(\boldsymbol{t}) \tag{4-11}$$

in which ∇ indicates the gradient of a tensor with respect to its argument.

For the Green integrability conditions of the Eulerian rate model (4-3), in addition to the conditions (4-8) or (4-10), a scalar function of stress, $\zeta(t)$, should exist such that:

$$\dot{\zeta}(t) = t : \overset{*}{\dot{e}} \tag{4-12}$$

where from the unified work conjugacy given by equation (2-41) equality $t : \overset{*}{\dot{e}} = \tau : d$ holds and (4-12) generates the same stress power in the spinning background. A similar approach used above is followed to investigate the existence of the scalar function $\zeta(t)$. Transferring equation (4-12) to the rotated configuration yields

$$\dot{\zeta}(\Sigma) = \Sigma : \dot{E} \tag{4-13}$$

in which $\dot{\zeta}(\Sigma) = \dot{\zeta}(R_*^T t R_*) = \dot{\zeta}(t)$ applies since $\dot{\zeta}(t)$ is a scalar function of stress. With the help of (4-4) equation (4-13) can be modified as follows:

$$\dot{\zeta}(\Sigma) = \Sigma : M^{-1}(\Sigma) : \dot{\Sigma} \tag{4-14}$$

Equation (4-14) has the standard form of a first order differential as follows:

$$\frac{\partial \zeta(\Sigma)}{\partial \Sigma} = \Sigma : M^{-1}(\Sigma) \tag{4-15}$$

Differentiating (4-15) with respect to Σ yields the conditions for which equation (4-15) is an exact differential:

$$\frac{\partial^2 \zeta(\Sigma)}{\partial \Sigma_{mn}\, \partial \Sigma_{kl}} - \frac{\partial^2 \zeta(\Sigma)}{\partial \Sigma_{kl}\, \partial \Sigma_{mn}} = \frac{\partial}{\partial \Sigma_{mn}} \left[\Sigma_{ij}\, M^{-1}_{ijkl} \right] - \frac{\partial}{\partial \Sigma_{kl}} \left[\Sigma_{ij}\, M^{-1}_{ijmn} \right] = 0 \tag{4-16}$$

And in the fixed background, equation (4-16) can be re-written as follows:

$$\frac{\partial}{\partial t_{mn}}\left[t_{ij}\, M^{-1}_{ijk\,l}(t)\right] = \frac{\partial}{\partial t_{kl}}\left[t_{ij}\, M^{-1}_{ijmn}\,(t)\right] \tag{4-17}$$

Conditions (4-17) are necessary and sufficient conditions for the Eulerian rate model given by (4-3), which is integrable as a Cauchy elastic material to be also integrable as a Green elastic one. A simplified form of conditions (4-17) can be obtained as a result of the Cauchy integrability of the model. Expanding (4-17) gives:

$$\frac{\partial t_{ij}}{\partial t_{mn}} M^{-1}_{ijkl} + t_{ij}\,\frac{\partial M^{-1}_{ijkl}}{\partial t_{mn}} = \frac{\partial t_{ij}}{\partial t_{kl}} M^{-1}_{ijmn} + t_{ij}\,\frac{\partial M^{-1}_{ijmn}}{\partial t_{kl}} \tag{4-18}$$

With the help of (4-10), equation (4-18) can be simplified as follows:

$$M^{-1}_{mnkl}\,(t) = M^{-1}_{klmn}\,(t) \tag{4-19}$$

So the compliance tensor should possess main diagonal symmetry as a consequence of the Green integrability conditions.

A special case applies to the grade-zero form of the Eulerian rate model (4-3) where the elasticity tensor is assumed to be constant and isotropic. In this case $\frac{\partial M}{\partial t} = \underset{\sim}{0}$ and the Cauchy and Green integrability conditions given by (4-8) and (4-19) are automatically satisfied. Such an unconditional integrability was expected since the grade-zero form of (4-3) trivially yields an exact differential of the following form:

$$\frac{d}{dt}(R_*^T t R_*) = M{:}\frac{d}{dt}(R_*^T e R_*) \Leftrightarrow t = M{:}\,e \tag{4-20}$$

A special case of the hypoelastic models can be obtained from (4-3) if the spinning frame is chosen to be a frame having the logarithmic spin and the strain measure is the Eulerian Hencky strain. In this case the logarithmic rate of the Eulerian Hencky strain and the Kirchhoff stress are work conjugate and $\overset{log}{\dot{\varepsilon}} = d$. Use of the Eulerian rate model (4-3) in the logarithmic frame yields:

$$\overset{log}{\dot{\tau}} = M(\tau): \overset{log}{\dot{\varepsilon}} = M(\tau): d \tag{4-21}$$

As a result, the same integrability conditions apply to hypoelastic models based on the logarithmic spin. This is in agreement with the integrability conditions derived by Xiao et al. [26] for the case of hypoelastic models based on the logarithmic spin.

4.1.2 Elastic potentials

Following Ericksen [18] and Xiao et al. [26] conditions for the existence of hypoelastic potentials given by equations (2-100) and (2-101), a similar approach can be used here for the Eulerian rate model (4-3). Since the Eulerian tensors t and e are work conjugate in an Ω_*-spinning frame, i.e. $t: \overset{*}{\dot{e}} = \tau: d$, equation (2-101) can be extended in the form of:

$$\tau: d = \Gamma \dot{\Pi} = \Gamma \frac{\partial \Pi}{\partial \tau}: \dot{\tau} = \Gamma \frac{\partial \Pi}{\partial \tau}: \overset{*}{\dot{\tau}} = \Gamma \frac{\partial \Pi}{\partial \tau}: \mathcal{M}(\tau): d = t: \overset{*}{\dot{e}} = \Gamma \frac{\partial \Pi}{\partial t}: M(t): \overset{*}{\dot{e}} \tag{4-22}$$

Therefore, elastic potentials exist for the Eulerian rate model (4-3) if conditions (2-100) are satisfied.

4.2 Extension to finite deformation plasticity

Similar to the additive decomposition of the strain rate tensor given by equation (3-42), in an Ω_*-spinning frame of reference an additive decomposition of the objective rate of Eulerian strain tensor can be given by [79]

$$\overset{*}{\dot{e}} = \overset{*}{\dot{e}}^{e} + \overset{*}{\dot{e}}^{p} \tag{4-23}$$

Such an additive decomposition is physically acceptable if the constitutive model used for the elastic part of the deformation generates the exact recoverable part of the stress power and the plastic part of the constitutive model generates the corresponding dissipative part, i.e.:

$$\boldsymbol{t} : \overset{*}{\dot{e}} = \boldsymbol{t} : \overset{*}{\dot{e}}^{e} + \boldsymbol{t} : \overset{*}{\dot{e}}^{p} \tag{4-24}$$

Since $(e, \boldsymbol{t})$ are Ω_*-frame work conjugate and the grade-zero form of the Eulerian rate model given by (4-3) is unconditionally integrable in the sense of hyperelasticity, the elastic part of equation (4-24) can be given by

$$\overset{*}{\dot{t}} = M : \overset{*}{\dot{e}}^{e} \tag{4-25}$$

where M is assumed to be constant. Therefore, decomposition (4-24) is physically acceptable since equation (4-25) is an elastic material and generates the recoverable part of the stress power [79].

In the Ω_*-spinning frame the plastic part of the deformation can be related to a flow potential based on associative plasticity (maximum plastic dissipation) by [79]

$$\dot{E}^p = \dot{\lambda}\frac{\partial \phi_*}{\partial \Sigma_*} \tag{4-26}$$

where $\dot{E}^p = R_*^T \overset{*}{\dot{e}}^p R_*$. The corresponding Kuhn-Tucker loading/unloading conditions are given by

$$\phi_* \leq 0\ ;\ \dot{\lambda} \geq 0\ ;\ \dot{\lambda}\phi_* = 0 \tag{4-27}$$

An observer in the Ω_*-spinning frame defines a yield limit by

$$f_*(\eta_*, \Upsilon_*) = \phi_* - \Upsilon_* \tag{4-28}$$

where $\eta_* = \mathrm{dev}\, t_* - \beta_*$ is the shift stress tensor. ϕ_* and Υ_* are scalar functions and therefore rotation-independent. As a result, the yield surface takes the following form in the fixed background:

$$f(\eta, \Upsilon) = \phi - \Upsilon \tag{4-29}$$

The evolution equations for the tensorial internal variables should be objective. To satisfy Prager's yielding stationary requirement, the same objective rate of stress must be used for the objective rates of tensorial internal variables (such as back stress tensor). Therefore, in the fixed background an evolution equation for the back stress tensor can be proposed with the following form [79]:

$$\overset{*}{\dot{\beta}} = \dot{\lambda}\hbar\left(\beta, \overset{*}{\dot{e}}^p\right) \tag{4-30}$$

Equations (4-23) to (4-30) define a unified Eulerian rate form of elastoplasticity for arbitrary objective corotational frames of reference.

It is worth mentioning that, if the Eulerian Hencky strain is used in the model, the Kirchhoff stress is conjugate to the logarithmic (D) rate of the Eulerian Hencky strain. As a result, the self-consistent Eulerian rate model of Bruhns et al. [27] is derivable from the proposed unified model given by equations (4-23) to (4-30).

In what follows it is assumed that only the Eulerian Hencky strain is used in the model and any evolution equation is based on this measure of strain.

4.2.1 Case of coaxial stress and total stretch

The stress power is scalar and therefore rotation-independent. The principal axis representation of the work conjugacy can be given by

$$\tau : d = \tau_E : d_E \tag{4-31}$$

where subscript *"E"* indicates components of a tensor on the principal axis of the left stretch tensor (Eulerian triad). If the Kirchhoff stress is coaxial with the left stretch tensor, the principal axis representation of the Kirchhoff stress is a diagonal tensor. Therefore, the rate of deformation tensor in equation (4-31) can be replaced by any arbitrary objective rate of the Eulerian Hencky strain and rotated back to the fixed background as follows:

$$\tau : d = \tau_E : d_E = \tau_E : \overset{*}{\dot{\varepsilon}}_E = \tau : \overset{*}{\dot{\varepsilon}} \tag{4-32}$$

which states that the conjugate Eulerian stress t is equivalent to the Kirchhoff stress irrespective of the chosen spinning frame of reference.

One example for which the principal axes coincide is the case of isotropic elasticity. In this case equation (4-25) yields the following rate form of elasticity:

$$\overset{*}{\dot{\tau}} = M : \overset{*}{\dot{\varepsilon}} \tag{4-33}$$

which is an exact differential and trivially yields the following integrated form for arbitrary objective rates:

$$\tau = M : \varepsilon \tag{4-34}$$

In Appendices A and B details of direct integrations of the rate form (4-33) under simple shear deformation path and four-step closed path loading are given for different objective corotational rates.

4.2.2 Case of non-coaxial stress and total stretch

In this case the principal axes do not coincide and as a result the Kirchhoff stress is not work conjugate to different objective rates of the Eulerian Hencky strain. Therefore, use of equation (4-25) requires proper definition of the conjugate stress t to the Hencky strain in different spinning backgrounds. Here the case of isotropic plasticity for which the elastic part of the deformation is assumed to be isotropic (i.e. constant isotropic elasticity tensor) is considered.

Transferring the unified work conjugacy on the Eulerian triad yields:

$$\tau : d = \tau_E : d_E = \mathit{t}_E : \overset{*}{\dot{\varepsilon}}_E \tag{4-35}$$

According to Xiao et al. [56] (see also Reinhardt and Dubey [21], Lehmann et al. [25], Hill [39], Lehmann and Liang [49], and Scheidler [80]), objective corotational rates of strain can be related to the strain rate tensor through a linear transformation given by

$$\overset{*}{\dot{\varepsilon}} = \mathbb{L}_*: d \tag{4-36}$$

where $\mathbb{L}_* = \mathbb{L}_*(b)$ is a fourth order transformation tensor function of the left Cauchy-Green tensor b. Use of (4-35) and (4-36) yields

$$\tau = \mathbb{L}_*: t \tag{4-37}$$

On the principal axis of the left stretch tensor, simple forms of the transformation function can be found for different objective rates. In what follows we consider only the cases of the Jaumann and Green-McInnis-Naghdi frames without loss of generality. Following the work of Reinhardt and Dubey [21], Lehmann et al. [25], Hill [39], and Scheidler [80] for an Eulerian measure of strain $e = f(V)$, the following can be obtained on the Eulerian triad:

$$\begin{aligned} \overset{J}{\dot{e}}_{E,ij} &= \overset{J}{\dot{f}}(V)_{E,ij} = \frac{\lambda_{ij}^2 + 1}{\lambda_{ij}^2 - 1} f(\lambda_{ij}) d_{E,ij} \; ; \; \lambda_{ij} \neq 1 \\ \overset{GMN}{\dot{e}}_{E,ij} &= \overset{GMN}{\dot{f}}(V)_{E,ij} = \frac{2\lambda_{ij}}{\lambda_{ij}^2 - 1} f(\lambda_{ij}) d_{E,ij} \; ; \; \lambda_{ij} \neq 1 \end{aligned} \tag{4-38}$$

where $\mathfrak{\lambda}_{ij} = \frac{\lambda_j}{\lambda_i}$ and λ_i's are the principal stretches. The normal components are the same as the normal components of the strain rate tensor on the Eulerian triad. Use of the Hencky strain measure, i.e. $\varepsilon = \ln(V)$, in (4-35) and (4-38) yields:

$$\mathfrak{t}_{*E,ij} = \hbar_*(\mathfrak{\lambda}_{ij})\tau_{E,ij} \quad ; \quad \mathfrak{\lambda}_{ij} \neq 1 \tag{4-39}$$

where $\hbar_*(\mathfrak{\lambda}_{ij})$ is a scalar scale function and is dependent on the selected spinning frame. For the J and GMN frames the scaling function is given by

$$\begin{aligned} \hbar_J(\mathfrak{\lambda}_{ij}) &= \frac{\mathfrak{\lambda}_{ij}^2 - 1}{\mathfrak{\lambda}_{ij}^2 + 1}\frac{1}{ln\,\mathfrak{\lambda}_{ij}} \; ; \; \mathfrak{\lambda}_{ij} \neq 1 \\ \hbar_{GMN}(\mathfrak{\lambda}_{ij}) &= \frac{\mathfrak{\lambda}_{ij}^2 - 1}{2\mathfrak{\lambda}_{ij}}\frac{1}{ln\,\mathfrak{\lambda}_{ij}} \; ; \; \mathfrak{\lambda}_{ij} \neq 1 \end{aligned} \tag{4-40}$$

The scale function for the special case of the logarithmic rate of the Eulerian Hencky strain is given by $\hbar_{\log}(\mathfrak{\lambda}_{ij}) = 1$. For all of the corotational rates $\mathfrak{\lambda}_{ii} = 1$ (normal components) and the scale function is given by $\hbar_*(\mathfrak{\lambda}_{ii}) = 1$ and therefore $\mathfrak{t}_{*E,ii} = \tau_{E,ii}$ (no sum on *i*). The same thing applies to the case of coincident eigenvalues of the stretch tensor. Basis-free expressions for (4-39) have been obtained for specific objective rates by different researchers (cf. Asghari et al. [54] and references therein).

4.2.2.1 Application to the simple shear problem

The problem of simple shear using a bilinear material model based on Ziegler's linear kinematic hardening is considered here as a case of non-coaxial stress and total stretch tensors.

Defining the shift stress tensor by $\eta_{*E} = \mathcal{t}_{*E} - \beta_{*E}$ and considering the normality rule on the principal axis of the left stretch tensor (Eulerian triad) yields:

$$\begin{aligned} \overset{rel}{\dot{\varepsilon}}{}_E^p &= \dot{\lambda}\frac{\partial \phi_*}{\partial \mathcal{t}_{*E}} \\ \overset{rel}{\dot{\beta}} &= H\overset{rel}{\dot{\varepsilon}}{}_E^p \end{aligned} \tag{4-41}$$

where H is the hardening modulus and is assumed to be constant. On the Eulerian triad the Mises yield function can be given by

$$\phi_* = \sqrt{2\eta_{*E,11}^2 + 2\hbar_*^2\eta_{*E,12}^2} - \tau_0 \tag{4-42}$$

where $\tau_0 = \sqrt{\frac{2}{3}}\sigma_0$ and σ_0 is the uniaxial yield limit and is assumed to be constant. In equation (4-41) a superposed "*rel*" indicates the objective rate of a tensor relative to the Eulerian triad and is given by

$$\overset{rel}{\dot{s}}_E = \dot{s}_E + s_E\Omega_{rel} - \Omega_{rel}s_E = R_E^T\overset{*}{\dot{s}}R_E \tag{4-43}$$

And the relative spin is defined by $\Omega_{rel} = R_E^T(\Omega_* - \Omega_E)R_E$. Use of equations (4-23), (4-25), and (4-41-1) on the Eulerian triad yields

$$\overset{rel}{\dot{\mathcal{t}}}_{*E} = 2\mu\left(\overset{rel}{\dot{\varepsilon}}_E - \dot{\lambda}\frac{\partial \phi_*}{\partial \mathcal{t}_{*E}}\right) \tag{4-44}$$

And therefore the shift stress tensor is given by

$$\overset{rel}{\dot{\eta}}_{*E} = 2\mu\overset{rel}{\dot{\varepsilon}}_E - (2\mu + H)\dot{\lambda}\frac{\partial \phi_*}{\partial \boldsymbol{t}_{*E}} \tag{4-45}$$

Equations (4-41), (4-42), and (4-45) can be used for the solution of the problem of simple shear on the Eulerian triad. The plastic multiplier $\dot{\lambda}$ can be found using the consistency condition $\dot{\phi}_* = 0$. The spin tensors for this motion are given by

$$\begin{aligned}
\Omega_J &= \frac{\dot{\gamma}}{2}(N_1 \otimes N_2 - N_2 \otimes N_1) \\
\Omega_{GMN} &= \frac{2\dot{\gamma}}{4+\gamma^2}(N_1 \otimes N_2 - N_2 \otimes N_1) \\
\Omega_E &= \frac{\dot{\gamma}}{4+\gamma^2}(N_1 \otimes N_2 - N_2 \otimes N_1) \\
\Omega_{log} &= \left[\frac{1}{4+\gamma^2} + \frac{\gamma}{4\sqrt{4+\gamma^2}\, asinh\left(\frac{\gamma}{2}\right)}\right]\dot{\gamma}(N_1 \otimes N_2 - N_2 \otimes N_1)
\end{aligned} \tag{4-46}$$

All the kinematics variables such as spin tensors and the total stretch and its corresponding Hencky strain are known since the motion is uniform. Therefore, $\boldsymbol{\lambda}_{12}$ and the orientation of the Eulerian triad are also known during stress integration. From the consistency condition one can obtain the plastic multiplier function of the shift stress components and eigenvalues of the left stretch tensor, i.e. $\dot{\lambda} = \dot{\gamma} g\left(\eta_{*E,11}, \eta_{*E,12}, \boldsymbol{\lambda}_{12}; \gamma\right)$. As a result, the following differentials can be obtained from (4-41), (4-45), and (4-46):

$$\frac{d\eta_{*E,11}}{d\gamma} = 2\frac{d\Omega_{rel,12}}{d\gamma}\eta_{*E,12} + 2\mu\frac{d\overset{rel}{\dot{\varepsilon}}_{E,11}}{d\gamma} - (2\mu + H)\frac{\eta_{*E,11}}{\tau_0}g\left(\eta_{*E,11}, \eta_{*E,12}, \lambda_{12}\right)$$

$$\frac{d\eta_{*E,12}}{d\gamma} = -2\frac{d\Omega_{rel,12}}{d\gamma}\eta_{*E,11} + 2\mu\frac{d\overset{rel}{\dot{\varepsilon}}_{E,12}}{d\gamma} - (2\mu + H)\hbar_*^2\frac{\eta_{*E,12}}{\tau_0}g\left(\eta_{*E,11}, \eta_{*E,12}, \lambda_{12}\right) \quad (4\text{-}47)$$

where $\eta_{*E,11}^2 + \hbar_*^2\eta_{*E,12}^2 = \frac{\tau_0^2}{2}$. Equations (4-47) can be numerically integrated for the cases of the J and GMN rates. A fourth-order Runge-Kutta integration scheme is used here for such a purpose. Values of $\frac{\mu}{\tau_0} = \frac{30}{\sqrt{6}}$, $\tau_0 = 200$ MPa, and $H = \sqrt{\frac{2}{3}}\tau_0$ are used during the numerical integration of (4-47).

Once the components of the shift stress tensor η_{*E} are found for each spinning frame, the components of the back stress tensor on the Eulerian triad can be integrated by the following approach. Defining the complex variable $z(\gamma) = \beta_{E,12} + i\beta_{E,11}$ and substituting for back stress components from (4-41-2) into $\frac{dz(\gamma)}{d\gamma} = \frac{d\beta_{E,12}}{d\gamma} + i\frac{d\beta_{E,11}}{d\gamma}$ yields:

$$\frac{dz(\gamma)}{d\gamma} - i2\frac{d\Omega_{rel}}{d\gamma}z(\gamma) = \frac{H}{\tau_0}\left(\hbar_*^2\eta_{*E,12} + i\eta_{*E,11}\right)g(\gamma) \quad (4\text{-}48)$$

which has a solution of the following form:

$$z(\gamma) = \frac{H}{\tau_0}exp[i\mathcal{G}(\gamma)]\int_{\gamma_p}^{\gamma} exp[-i\mathcal{G}(\gamma)]\left(\hbar_*^2\eta_{*E,12} + i\eta_{*E,11}\right)g(\gamma)d\gamma \quad (4\text{-}49)$$

where $\mathcal{G}(\gamma) = \int_{\gamma_p}^{\gamma} 2\dot{\Omega}_{rel,12}\, d\gamma$. Separating the real and imaginary parts of (4-49) yields the following integrals for the back stress components:

$$\beta_{E,11}(\gamma) = \frac{H}{\tau_0} sin[\mathcal{G}(\gamma)] \int_{\gamma_p}^{\gamma} P(\gamma)\, d\gamma - \frac{H}{\tau_0} cos[\mathcal{G}(\gamma)] \int_{\gamma_p}^{\gamma} R(\gamma)\, d\gamma$$
$$\beta_{E,12}(\gamma) = \frac{H}{\tau_0} cos[\mathcal{G}(\gamma)] \int_{\gamma_p}^{\gamma} P(\gamma)\, d\gamma + \frac{H}{\tau_0} sin[\mathcal{G}(\gamma)] \int_{\gamma_p}^{\gamma} R(\gamma)\, d\gamma \tag{4-50}$$

in which $\gamma_p = 2\sinh\left(\frac{\sqrt{2}\tau_0}{4\mu}\right)$ is the amount of shear for which plastic yielding starts and:

$$P(\gamma) = g(\gamma)\{\hbar_*^2 \eta_{*E,12}\, cos[\mathcal{G}(\gamma)] + \eta_{*E,11}\, sin[\mathcal{G}(\gamma)]\}$$
$$R(\gamma) = g(\gamma)\{\hbar_*^2 \eta_{*E,12}\, sin[\mathcal{G}(\gamma)] - \eta_{*E,11}\, cos[\mathcal{G}(\gamma)]\} \tag{4-51}$$

Equations (4-51) can be integrated using a trapezoidal integration scheme. Having obtained the back stress components, the conjugate stress corresponding to each corotational frame can be obtained on the Eulerian triad using $t_{*E,ij} = \eta_{*E,ij} + \beta_{*E,ij}$.

Figure 4-1 and Figure 4-2 show the fixed components of the conjugate stress and its equivalent Kirchhoff stress for the J and GMN rates. Using the proposed formulation both the J and GMN rates return identical Kirchhoff stress responses as compared to that of the self-consistent Eulerian rate model of Bruhns et al. [27] based on the logarithmic rate.

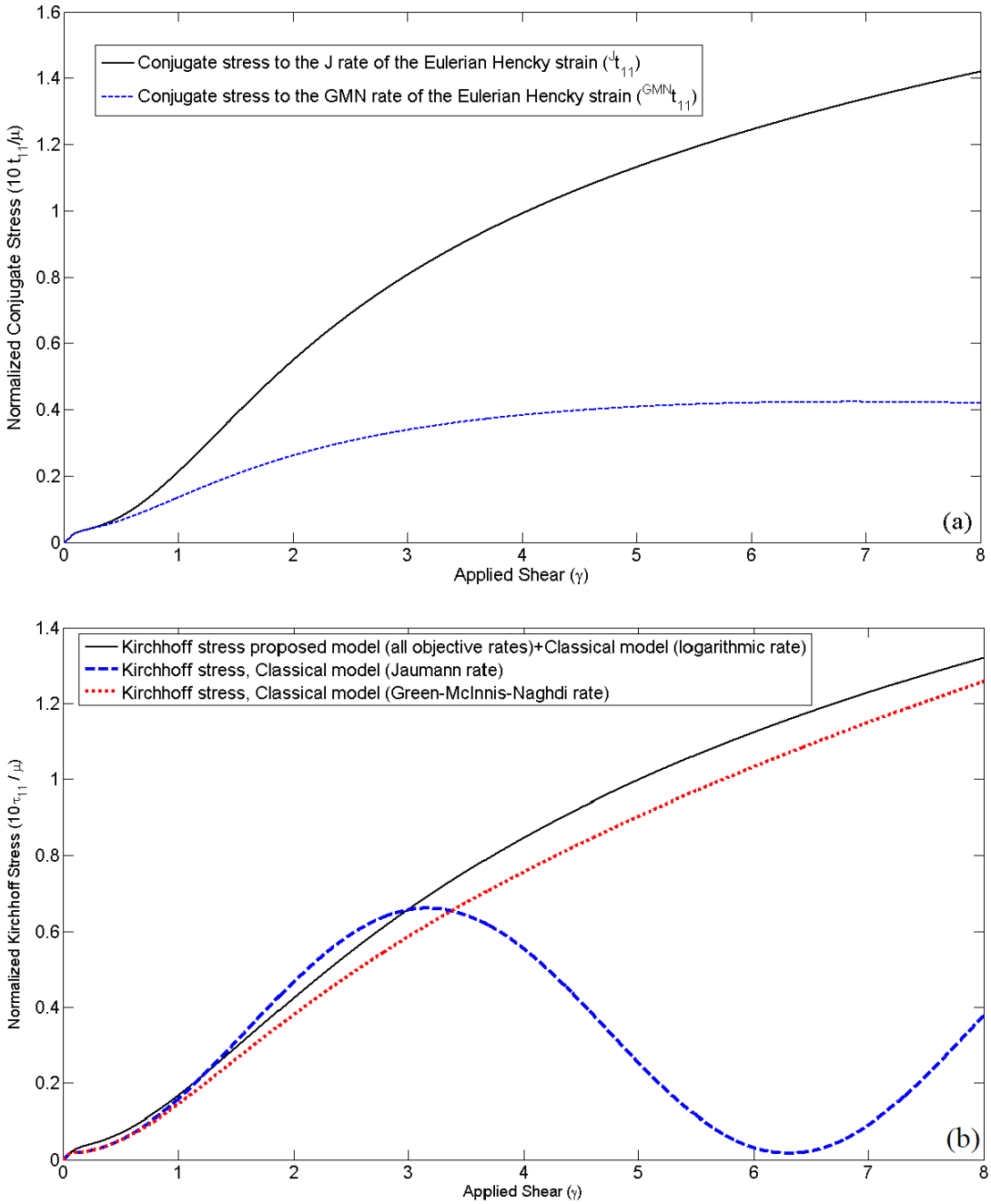

Figure 4-1- Normal stress component, (a): conjugate stress for the J and GMN rates of the Hencky strain (proposed model), (b): equivalent Kirchhoff stress (proposed model, J and GMN rates) and classical hypoe-based model (J, GMN, and logarithmic rates), linear kinematic hardening behavior

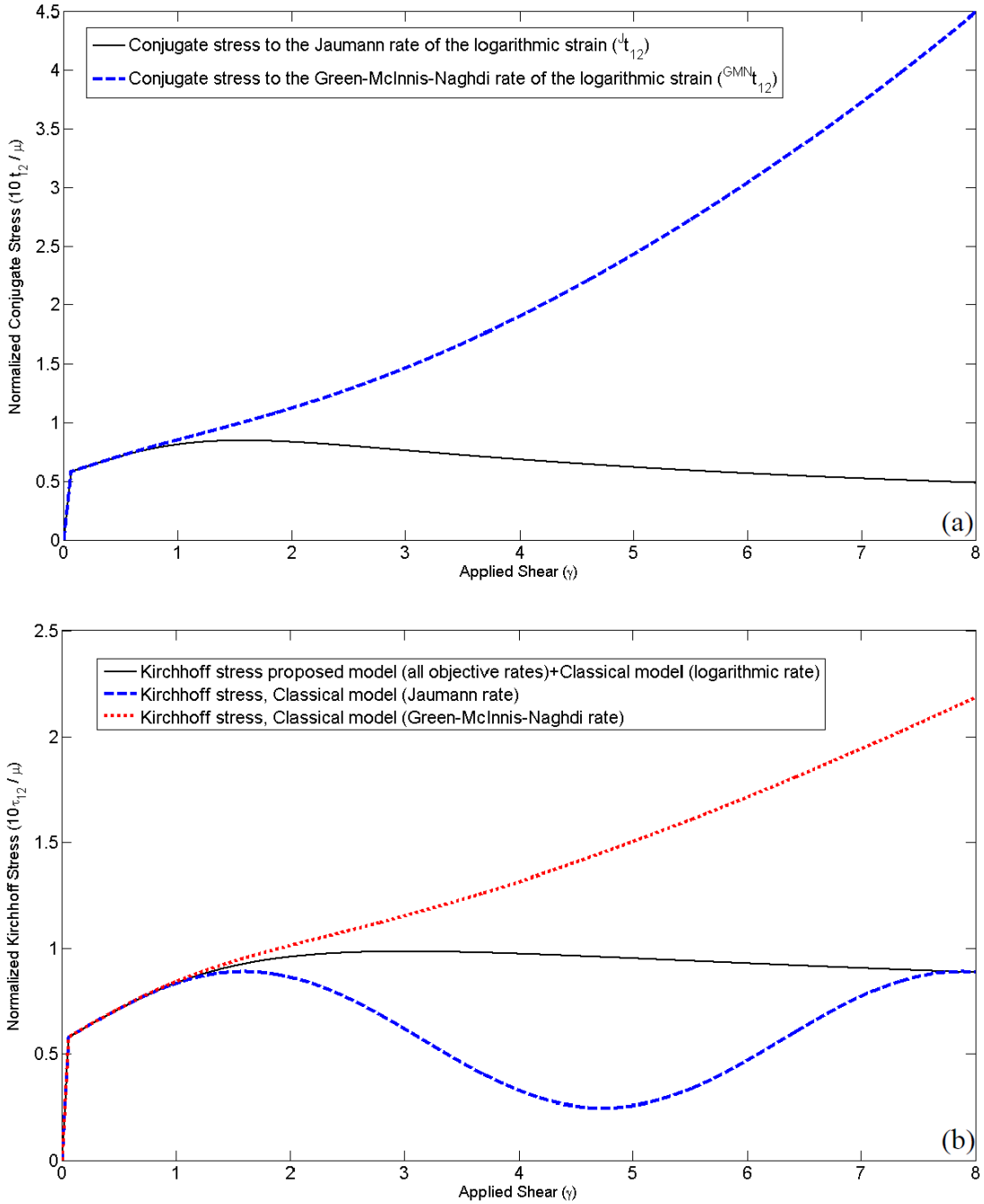

Figure 4-2- Shear stress component, (a): conjugate stress for the J and GMN rates of the Hencky strain (proposed model), (b): equivalent Kirchhoff stress (proposed model, J and GMN rates) and classical hypoe-based model (J, GMN, and logarithmic rates), linear kinematic hardening behavior

4.3 Application of the proposed model to nonlinear mixed hardening

An extension of the proposed model to the case of nonlinear mixed hardening is used here to predict the hardening behaviour of SUS 304 stainless steel thin tubes under fixed end finite torsional loading. With the help of the Armstrong-Frederick (A-F) nonlinear hardening model [81] the proposed back stress evolution equation given by (4-41-2) can be extended as follows:

$$\overset{rel}{\dot{\beta}_E} = A_f \overset{rel}{\dot{\varepsilon}_E^p} - B_f \dot{E}^{p,eq} \beta_E \tag{4-52}$$

where A_f and B_f are the A-F material parameters and $\dot{E}^{p,eq}$ is a scalar parameter representing the rate of the equivalent plastic strain and will be defined later in this section. The yield surface of a strain hardening material can expand and translate nonlinearly in the stress space. Therefore, a modified Mises yield surface under simple shear motion can be given by

$$\phi_* = \sqrt{3\eta_{*E,11}^2 + 3\hbar_*^2 \eta_{*E,12}^2} - \Upsilon \tag{4-53}$$

where Υ is a scalar parameter function of the plastic internal variables representing the subsequent yield surface size during plastic loading. An exponential form of the yield surface size based on the original model of Voce [82] can be used here as follows:

$$\Upsilon = \sigma_{Y0} + (\sigma_{Ys} - \sigma_{Y0})[1 - exp(-bE^{p,eq})] \tag{4-54}$$

where σ_{Y0} is the initial yield surface size, σ_{Y_S} is the saturation value of the yield surface size, and b is a parameter which controls the rate of saturation.

A modified plastic work can be used to derive an expression for the equivalent plastic strain. The plastic work in relative spinning frame can be given by

$$\dot{W}^p = \eta_{*E} : \overset{rel}{\dot{\varepsilon}_E^p} = \Upsilon \dot{E}^{p,eq} \tag{4-55}$$

in which $\Upsilon = \sqrt{3\eta_{*E,11}^2 + 3\hbar_*^2\eta_{*E,12}^2}$ is the equivalent Mises shift stress. Use of equations (4-41-1) and (4-55) yields the following definition for the equivalent plastic strain:

$$\dot{E}^{p,eq} = \sqrt{\frac{2}{3\hbar_*^2}\overset{rel}{\dot{\varepsilon}_E^p} : \overset{rel}{\dot{\varepsilon}_E^p}} \tag{4-56}$$

It is worth mentioning that definition (4-56) is similar to the classical definition of the equivalent plastic strain rate. For the special case of the logarithmic rate $\hbar_{log}^2(\mathfrak{z}_{ij}) = 1$ and (4-56) yields $\dot{E}^{p,eq} = d^{p,eq} = \sqrt{\frac{2}{3}d^p : d^p} = \sqrt{\frac{2}{3}d_E^p : d_E^p}$.

Similar to the case of the Ziegler's linear hardening discussed in section 4.2.2, the governing equations (4-52) to (4-56) are numerically integrated using the fourth order Runge-Kutta integration method for three different objective rates, i.e. the J, GMN, and logarithmic rates. The stress responses from the proposed model are plotted in Figure 4-3 using the material parameters given in [83] for SUS 304 stainless steel, which are summarized in Table 4-1. Also, the stress responses for the J

and GMN rates using the classical hypo-based model are plotted for comparison. From Figure 4-3, the proposed model gives identical results to those of the self-consistent classical model of Bruhn's et al. [27] based on the logarithmic rate. Unlike the classical model response, the Jaumann stress response of the proposed model does not show any shear oscillation.

Table 4-1 Parameters used for the mixed hardening behaviour of SUS 304 stainless steel [83]

Shear Modulus	$\mu = 78$ GPa
Exponential Isotropic Hardening Parameters	$\sigma_{Y0} = 285.6$ MPa ; $\sigma_{Ys} = 680$ MPa ; $b = \frac{5}{3}$
Armstrong-Frederick Model Parameters	$A_f = 20$ MPa ; $B_f = 0.2$

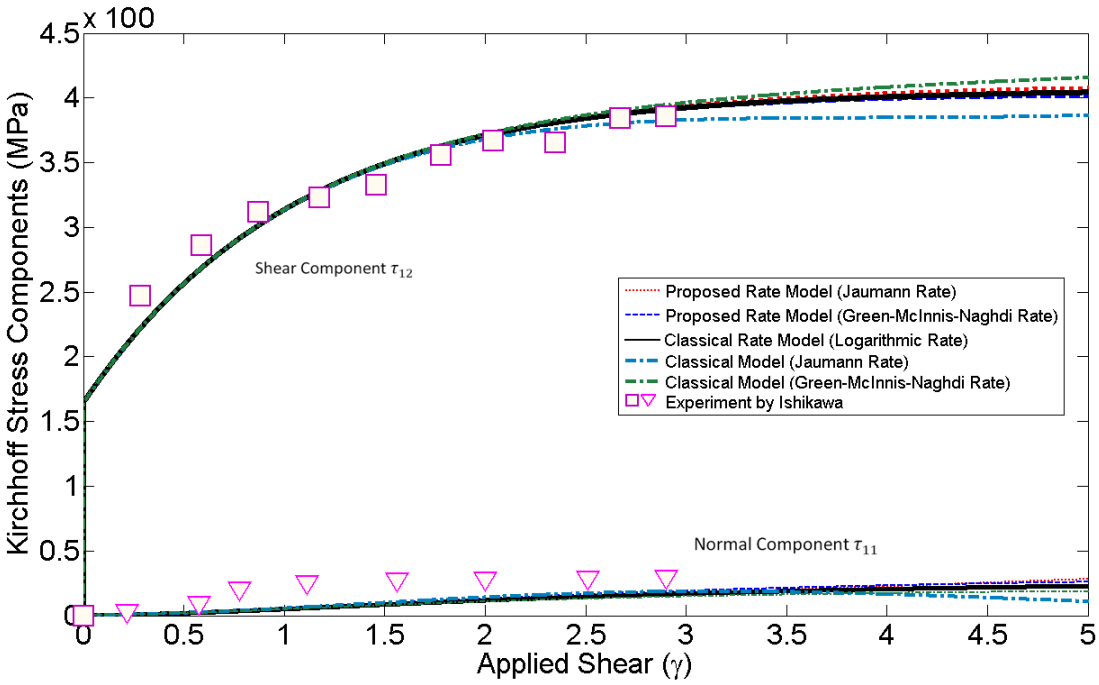

Figure 4-3- Stress components for SUS 304 stainless steel under fixed end torsion using the proposed mixed hardening model

Figure 4-4 shows the evolution of the yield surface size vs. the applied shear. It is clear that the radius of the yield surface is not affected by the corotational rates used in the model.

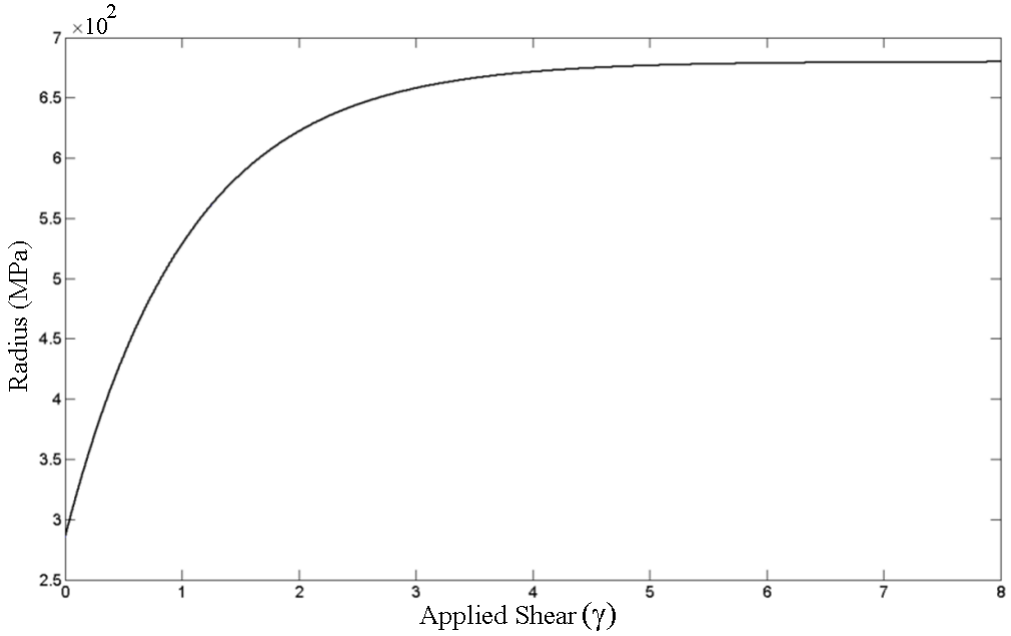

Figure 4-4- Radius of the subsequent yield surfaces as predicted by the proposed model using any corotational rates with the mixed hardening rule

4.4 Summary

An Eulerian rate form of elasticity was used for setting up a unified Eulerian rate model for finite strain elastoplasticity. The grade-zero model was shown to be unconditionally integrable for its elastic part and was consistent with hyperelasticity in its integrated form irrespective of the objective rate of stress used in the model. Conjugate measure of stress to each objective corotational rate of the Eulerian strain was obtained based on the unified work conjugacy theorem. An additive

decomposition of the arbitrary objective rate of the Eulerian strain was proposed which was consistent with thermodynamic considerations. A modified flow rule in each spinning background was used in the model. Furthermore, a new evolution equation for the back stress tensor was proposed and used in the model. The model was successfully integrated on the Eulerian axes of the total stretch tensor which were known during the time integration process.

Results obtained for the simple shear problem and the case of linear kinematic hardening using different objective corotational rates, such as the Jaumann and Green-McInnis-Naghdi rates, were identical to those of the self-consistent Eulerian rate model of Bruhn's et al. [27] based on the logarithmic (D) rate of stress. Therefore, the proposed model assigns no preference on the choice of objective rates for its consistency and is unified for all of the objective corotational rates.

The unified model was further extended to the mixed nonlinear hardening behavior. Application of the proposed unified model to fixed-end finite torsional loading of SUS 304 stainless steel tubes showed that the model predicts the second order effect (Swift effect) accurately and obtained results were in good agreement with the available experimental data done for this material.

The unified Eulerian model is a good candidate for Eulerian rate models for finite strain elastoplasticity and can be successfully implemented in the displacement-based formulation of the finite element method.

Chapter 5
Phenomenological plasticity models based on multiplicative decomposition

In Chapter 3 and Chapter 4 respectively, Eulerian rate models of plasticity based on the additive decomposition of the strain rate tensor and arbitrary objective rates of the Hencky strain tensor were presented. These models are mainly based on rate-type material models and need objective integration schemes for their numerical implementation.

Another class of plasticity models has been formulated based on the multiplicative decomposition of the deformation gradient. Such decomposition has been physically validated based on observations made in crystal plasticity. Plastic

flow of material can be viewed as the flow of material through the crystal lattice by the movement of dislocations [30]. This physical interpretation is given in the work of Taylor and Elam [84,85] and Taylor [86]. A detail review of micromechanical description of plastic flow is given in the review work of Asaro and Rice [87] and Asaro [88]. As shown in Figure 3-19 for a single crystal having a single slip system defined by $\{s, m\}$ the plastic flow can be characterized by [30]

$$F^P = I + \gamma s \otimes m \tag{5-1}$$

where γ is the plastic shearing parameter in the crystallographic slip system. Such a plastic deformation results into an intermediate stress-free configuration as shown in Figure 5-1.

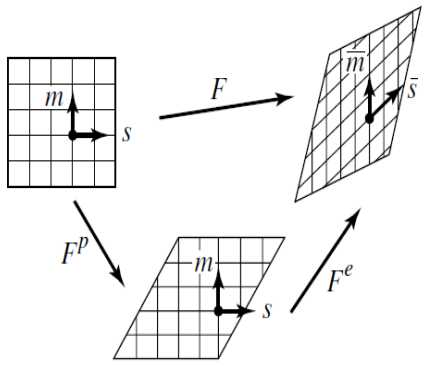

Figure 5-1- Micromechanical representation of deformations in a crystall lattice [30]

Next, the elastic part of the deformation stretches and rotates the crystal lattice. The total deformation can therefore be split into plastic and elastic parts using

$$F = F^e F^p \tag{5-2}$$

Constitutive models based on the decomposition (5-2) are mostly formulated in the Lagrangian framework of elastoplasticity and are based on hyperelastic material models; as a result, they do not require any rate-type material model for the elastic part of deformation. However, this does not preclude the use of decomposition (5-2) in the Eulerian framework of elastoplasticity; rate-type Eulerian formulations of finite elastoplasticity based on the multiplicative decomposition have been proposed by several authors [43].

In this chapter a review of phenomenological plasticity models based on multiplicative decomposition (5-2) is presented first. A modified decomposition based on the right stretch tensor is then introduced. Using this modified decomposition, a unified Lagrangian model of plasticity based on the right plastic stretch tensor is proposed. A hyperelastic function is used to relate the rotated Kirchhoff stress to the Lagrangian Hencky strain. The proposed model is integrated on the Lagrangian triad of the plastic stretch tensor using a modified back stress evolution equation. Results obtained for the problem of simple shear for a Ziegler kinematic hardening material are identical to those of the self-consistent Eulerian rate model of Bruhn's et al. [27] discussed in Chapter 3 and Chapter 4. The proposed model is further extended to mixed nonlinear hardening behavior. Predicted results by the proposed model for SUS 304 stainless steel under fixed-end finite torsion are in good agreement with the corresponding experimental observations.

5.1 Continuum formulation of multiplicative plasticity

The Green-Lagrange strain tensor is defined relative to the reference configuration by

$$\varrho = \frac{1}{2}(C - Z)$$
$$\varrho^P = \frac{1}{2}(C^P - Z) \tag{5-3}$$

where $C = F^T F$ and $C^P = F^{P^T} F^P$ are the total and plastic right Green-Cauchy deformation tensors, respectively and Z is the metric tensor of the reference configuration and is equal to the Kronecker delta in a Cartesian coordinate system. Similarly on the current configuration the Almansi-Euler strain tensor is defined by

$$\xi = \frac{1}{2}(z - b^{-1})$$
$$\xi^e = \frac{1}{2}\left(z - b^{e\,-1}\right) \tag{5-4}$$

where $b^{-1} = F^{-T} F^{-1}$ and $b^{e\,-1} = F^{e\,-T} F^{e\,-1}$ are the total and elastic Finger deformation tensors, respectively, and z is the spatial metric tensor of the current configuration. The spatial metric tensor is the push-forward of the Green deformation tensor and is given by

$$C_{AB} = F_A^i z_{ij} F_B^j \tag{5-5}$$

Similarly, the intermediate plastic configuration has the following coordinate transformation:

$$C_{IJ}^{p} = (F^{p})_{I}^{A} Z_{AB} (F^{p})_{J}^{B} \tag{5-6}$$

By definition the Eulerian plastic strain tensor can be defined by

$$\xi^{p} = \xi - \xi^{e} = \frac{1}{2}\left(b^{e\,-1} - b^{-1}\right) \tag{5-7}$$

which shows that $b^{e\,-1}$ serves as the plastic metric tensor [35] and the following relations define the coordinate transformation:

$$\begin{aligned} C^{p} &= F^{T} b^{e\,-1} F \\ \varrho^{p} &= F^{T} \xi^{p} F \end{aligned} \tag{5-8}$$

The Eulerian strain rate tensor can be related to the Lie derivative of the spatial metric tensor by

$$L_{v} z = \phi_{*} \frac{d}{dt} \phi^{*} z = F^{-T} \dot{C} F^{-1} = 2d \tag{5-9}$$

And the Lie derivative of the Finger deformation tensor is given by

$$L_{v} b^{-1} = \phi_{*} \frac{d}{dt} \phi^{*} b^{-1} = F^{-T} \frac{d}{dt} [F^{T} F^{-T} F^{-1} F] F^{-1} = \underset{\sim}{0} \tag{5-10}$$

A unique definition cannot be derived for the elastic and plastic parts of the strain rate tensor from kinematic analysis [89]. Different definitions for the elastic and plastic parts might be used in constitutive models, which result in different flow rules and stress responses. Simo and Ortiz [90] proposed the following definitions for elastic and plastic parts of the strain rate tensor:

$$d^e = L_v \xi^e$$
$$d^p = L_v \xi^p = \frac{1}{2} L_v b^{e\,-1} \tag{5-11}$$

Contrary to equation (5-11-1), one can define the elastic part by:

$$d^e = sym[l^e] = \frac{1}{2}\left(\dot{F}^e F^{e\,-1} + F^{e\,-T} \dot{F}^{e^T}\right) \tag{5-12}$$

Using the spatial velocity gradient tensor, i.e. $l = \dot{F} F^{-1}$, and decomposition (5-2) the following kinematic relation can be obtained:

$$l = \dot{F} F^{-1} = \dot{F}^e F^{e\,-1} + F^e \left(\dot{F}^p F^{p\,-1}\right) F^{e\,-1} \tag{5-13}$$

Similarly it is possible to define the plastic velocity gradient $\bar{L}^p = \dot{F}^p F^{p\,-1}$ on the intermediate stress-free configuration and introduce a modified additive decomposition of the velocity gradient by

$$l = \dot{F} F^{-1} = l^e + F^e \bar{L}^p F^{e\,-1} = l^e + l^p \tag{5-14}$$

Using equation (5-14), different definitions for the plastic part of the strain rate tensor and plastic spin on the intermediate configuration can be obtained as follow:

$$\bar{d}^p = sym[\bar{L}^p]$$
$$\bar{w}^p = skew[\bar{L}^p] \tag{5-15}$$

And the pull-back of the elastic velocity gradient tensor on the intermediate configuration, i.e. $\bar{L}^e = F^{e^T} \dot{F}^e F^{e\,-1} F^e = F^{e^T} \dot{F}^e$, yields the elastic part of the deformation by

$$\bar{d}^e = sym[\bar{L}^e]$$
$$\bar{w}^e = skew[\bar{L}^e] \tag{5-16}$$

Equations (5-15) and (5-16) are different definitions for the elastic and plastic parts of the strain rate tensor on the intermediate plastic configuration.

Another possibility for the definition of the elastic and plastic parts of deformation on the intermediate configuration is first to pull-back the velocity gradient on the intermediate plastic configuration by

$$\bar{L} = F^{e^T}\left(\dot{F}F^{-1}\right)F^e = \bar{L}^e + \bar{C}^e\bar{L}^p \tag{5-17}$$

where $\bar{L}^e = F^{e^T}\dot{F}^e$ is the pull-back of the elastic velocity gradient and $\bar{C}^e = F^{e^T}F^e$ is the right Cauchy-Green deformation tensor on the intermediate configuration. Use of equation (5-17) results in a different definition for the plastic part of the strain rate tensor as follows [91-93]:

$$\bar{d}^p = sym[\bar{C}^e\bar{L}^p] \tag{5-18}$$

Simo [35] introduced a framework of finite strain elastoplasticity based on the principle of maximum plastic dissipation, which bypassed the need for an explicit definition of the plastic strain rate in the formulation. Equivalent material (convected) and spatial forms of the formulation were derived in his formulation. Simo [35] assumed two functionals representing the free energy of the system in the convected and spatial frames and derived a hyper-based stress-strain relationship by

$$S = 2\rho_0 \frac{\partial \bar{\Psi}(C, C^p, \mathcal{Q})}{\partial C} = \rho_0 \frac{\partial \bar{\Psi}(\varrho, \varrho^p, \mathcal{Q})}{\partial \varrho}$$

$$\tau = 2\rho_0 \frac{\partial \hat{\Psi}\left(z, b^{e\,-1}, F, q_{\mathcal{Q}}\right)}{\partial z} = \rho_0 \frac{\partial \hat{\Psi}(\xi, \xi^p, F, q_{\mathcal{Q}})}{\partial \xi} \tag{5-19}$$

where S and τ are the second Piola-Kirchhoff and Kirchhoff stress tensors, and $\bar{\Psi}$ and $\hat{\Psi}$ are the free energy potentials in the material and spatial frames, respectively. Flow potentials and their corresponding hardening rules were given in the material and spatial frames by

$$\bar{\phi}\left(z, b^{e\,-1}, F, q_{\mathcal{Q}}\right) \leq 0\,; L_v q_{\mathcal{Q}} = \dot{\lambda} \hbar\left(z, b^{e\,-1}, F, q_{\mathcal{Q}}\right)$$

$$\bar{\phi}(C, C^p, \mathcal{Q}) \leq 0\,; \dot{\mathcal{Q}} = \dot{\lambda} \mathcal{H}(C, C^p, \mathcal{Q}) \tag{5-20}$$

where $\mathcal{Q}$ and $q_{\mathcal{Q}}$ are the vectors of the material and spatial hardening parameters and $\mathcal{Q} = \phi^* q_{\mathcal{Q}}$ is the pull-back of the spatial hardening tensor on the convected background. Using the principle of maximum plastic dissipation, Simo derived the following flow rules on the material and spatial configurations:

$$L_v \tau^p = 2\dot{\lambda} \frac{\partial \bar{\phi}\left(z, b^{e\,-1}, F, q_{\mathcal{Q}}\right)}{\partial z} = \dot{\lambda} \frac{\partial \bar{\phi}(\xi, \xi^p, F, q_{\mathcal{Q}})}{\partial e}$$

$$\dot{S}^p = 2\dot{\lambda} \frac{\partial \bar{\phi}(C, C^p, \mathcal{Q})}{\partial Z} = \dot{\lambda} \frac{\partial \bar{\phi}(\varrho, \varrho^p, \mathcal{Q})}{\partial \varrho} \tag{5-21}$$

A complete volumetric/deviatoric decoupled form of the model was further derived by Simo. Details of the decoupled formulation and its algorithmic implementation for the case of the J_2 flow theory can be found in Simo [35,36].

A modified multiplicative decomposition based on the left stretch tensor was used by Metzger and Dubey [43]. The hypoelastic model was integrated on the principal axis of the elastic stretch tensor and results were independent of the choice of objective rates. An isotropic flow rule based on the modified multiplicative decomposition of the left stretch tensor was used to solve the problem of simple shear. The left stretch tensor decomposition used in their formulation was given by

$$\Gamma = \Lambda\Pi \tag{5-22}$$

where Γ, Π, and Λ are the total, plastic, and elastic left stretch tensors on the principal axis of the elastic stretch tensor, respectively. The Z rate of these tensors was used in developing the kinematic relations in the formulation. Integration of the model needed the current orientation of the principal axis of the elastic stretch. Therefore, additional equations were needed for the evolution of the principal elastic directions. The integrated model returned equivalent stress responses for the problem of simple shear for different objective rates of stress.

Eterovic and Bathe [94] and Gabriel and Bathe [32] proposed a finite strain model based on the decomposition of the right stretch tensor and integrated their model on the mid-configuration. The case of isotropic plasticity was assumed in their proposed model and the effect of plastic spin was neglected. Recently, Montans and Bathe [95] extended the original formulation of Eterovic and Bathe [94] and included the effect of plastic spin. They expressed the modified stress power on the intermediate configuration by

$$\tau : l = \bar{S} : \bar{l} = \bar{S} : \left(\bar{l}^e + \bar{C}^e \bar{l}^p\right) = \bar{S} : \left(\bar{d}^e + \bar{w}^e\right) + \bar{C}^e \bar{S} : \left(\bar{d}^p + \bar{w}^p\right) \tag{5-23}$$

where $\bar{S} = F^{e\,-1} \tau F^{e\,-T}$ is the pull-back of the Kirchhoff stress tensor on the intermediate configuration. In equation (5-23) the term $\Xi = \bar{C}^e \bar{S}$ is defined as the non-symmetric Mandel [96] stress tensor. Symmetry of $\bar{S}$ requires that the elastic spin have no contribution in the stress power. Therefore:

$$\tau : l = \bar{S} : \bar{l} = \bar{S} : \bar{d}^e + \Xi_{sym} : \bar{d}^p + \Xi_{skew} : \bar{w}^p \tag{5-24}$$

Montans and Bathe [95] concluded that the symmetric part of the Mandel stress tensor generates power on the modified plastic strain rate while the skew part of it generates power on the modified plastic spin. They further showed that for the case of isotropic plasticity, where the principal axes of the stress and elastic stretch coincide, the skew-symmetric part of the Mandel stress tensor vanishes and as a result the plastic spin has no contribution to plastic dissipation. In this case $F^e = R^e U^e$ and as a result:

$$\Xi_{sym} = U^e \bar{S} U^e = R^{e\,T} \tau R^e = \bar{\tau} \tag{5-25}$$

which shows that for isotropic plasticity the rotated Kirchhoff stress defines the work conjugacy on the intermediate configuration. The dissipation inequality on the intermediate configuration is given by

$$\dot{\phi} = \bar{S} : \bar{d}^e + \Xi_{sym} : \bar{d}^p + \Xi_{skew} : \bar{w}^p - \dot{\psi} \geq 0 \tag{5-26}$$

If the free energy potential is assumed to be a function of the elastic strain rate $\bar{d}^e$ and other tensorial and scalar internal variables such as $\bar{\beta}$ and Υ, the dissipation inequality (5-26) and the assumption of maximum plastic dissipation yield the following relationships:

$$\bar{S} = \frac{\partial \psi\left(\bar{d}^e, \bar{\beta}, \Upsilon\right)}{\partial \bar{E}^e}$$
$$\bar{d}^p = \dot{\lambda}\frac{\partial f}{\partial \Xi_{sym}} \; ; \; \bar{w}^p = \dot{\lambda}\frac{\partial f}{\partial \Xi_{skew}} \; ; \; \dot{\vartheta}_\beta = \dot{\lambda}\frac{\partial f}{\partial \bar{\beta}} \; ; \; \dot{\vartheta}_\Upsilon = \dot{\lambda}\frac{\partial f}{\partial \Upsilon} \tag{5-27}$$

where $f = f\left(\Xi, \bar{\beta}, \Upsilon\right)$ is a convex plastic potential, and ϑ_β and ϑ_Υ are the conjugate tensor and scalar variables to $\bar{\beta}$ and Υ in the dual strain space, respectively. For the case of isotropic plasticity the elastic strain energy function was assumed to be given by the following hyperelastic function (cf. [32,95,97]):

$$W(\lambda_1, \lambda_2, \lambda_3) = u(J) + \mu \sum_{i=1}^{3} \left(ln\, \hat{\lambda}_i\right)^2 \tag{5-28}$$

where $\hat{\lambda}_i = J^{-\frac{1}{3}}\lambda_i$ are the principal values of the deviatoric stretch tensor, J is the Jacobian of the deformation, $u(J)$ is the volumetric part of the strain energy, and μ is the material shear modulus. Therefore the symmetric Mandel stress tensor, which is the same as the rotated Kirchhoff stress, can be derived from the stored energy by

$$\Xi_{sym} = \bar{\tau} = \frac{\partial W(\lambda_1, \lambda_2, \lambda_3)}{\partial \bar{E}^e} = Ju^{'}(J)I + 2\mu \bar{E}^e_{dev} \tag{5-29}$$

where $\bar{E}^e_{dev} = \bar{E}^e - \frac{1}{3}(\ln J)I = \ln\left(J^{-\frac{1}{3}}U^e\right)$ is the deviatoric elastic strain. Details of the numerical integration of the above formulation based on the exponential mapping algorithm are given in [32,95,97].

Reinhardt and Dubey [98] developed a rate form model based on the multiplicative decomposition of the left stretch tensor. The deformation gradient was decomposed based on the left stretch tensor by

$$F = V^e F^p = V^e V^p R^p R \tag{5-30}$$

Using the left stretch decomposition (5-30) they proposed the following additive decomposition of the velocity gradient:

$$l = l^e + V^e\left(l^p_* - \Omega_R\right)V^{e\,-1} \tag{5-31}$$

where $l^e = \left(\dot{V}^e + V^e\Omega_R\right)V^{e\,-1}$ and l^p_* is given by

$$l^p_* = V^e\left[\dot{V}^p V^{p\,-1} + V^p\left(\Omega_p + \Omega_*\right)V^{p\,-1}\right]V^{e\,-1} = d^p_* + w^p_* \tag{5-32}$$

where $\Omega_p = \dot{R}^p R^{p\,T}$ and $\Omega_* = R^p\Omega_R R^{p\,T}$. Following the approach used by Metzger and Dubey [43], Reinhardt and Dubey [98] further derived a relationship for the modified plastic spin based on the known kinematic variables. The complete field of equations and the corresponding Eulerian rate constitutive model based on the modified additive decomposition given by (5-31) were derived and integrated with different objective rates of stress. Recently, Ghavam and Naghdabadi [99] have used a modified decomposition of the left stretch tensor originally proposed by Metzger

and Dubey [43] and applied it to nonlinear mixed kinematic/isotropic hardening material models.

5.2 Proposed Lagrangian formulation

In the Lagrangian formulations of elastoplasticity based on multiplicative decomposition, a right stretch decomposition is often used. However, the left stretch tensor decomposition can also be used in constitutive models which would result in an Eulerian rate formulation as discussed in the previous section. While the left stretch decomposition-based formulations require use of an objective rate of the Kirchhoff stress (or more generally a covariant rate) and a neutrally objective integration scheme, the right stretch decomposition-based formulations use a total relation between the rotated Kirchhoff stress and Hencky strain through a hyperelastic strain energy function and bypass the need for objective rate quantities as discussed in the previous section.

Assuming that the total symmetric right stretch tensor can be decomposed into a symmetric elastic part and a non-symmetric plastic part, one can write:

$$F = RU = RU^e\chi^p$$
$$U = U^e\chi^p \tag{5-33}$$

Polar decomposition of the non-symmetric plastic tensor χ^p into a symmetric plastic stretch tensor U^p and an orthogonal transformation tensor Q^p yields:

$$\chi^p = Q^p U^p \tag{5-34}$$

As a result, the modified plastic velocity gradient $\bar{L}^p$ can be defined by

$$\bar{L}^p = \dot{\chi}^p \chi^{p\,-1} = \dot{Q}^p Q^{p\,T} + Q^p \left(\dot{U}^p U^{p\,-1}\right) Q^{p\,T} = \Omega^Q + Q^p \left(\dot{U}^p U^{p\,-1}\right) Q^{p\,T} \tag{5-35}$$

Figure 5-2 shows a schematic representation of the proposed decomposition:

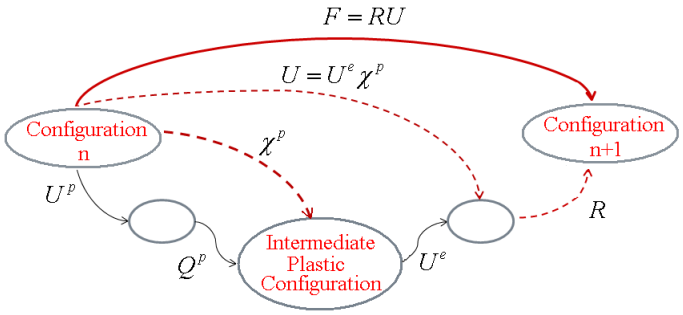

Figure 5-2- Schematic representation of the proposed multiplicative decomposition

In Figure 5-2, the non-symmetric plastic deformation χ^p maps the old configuration "*n*" onto the stress-free intermediate plastic configuration. This mapping induces no stress in the body and is assumed to be an isochoric mapping. The symmetric elastic stretch tensor then deforms the mid-configuration into a stressed body. Finally, the rigid rotation *R* maps the stretched body onto the current configuration "*n+1*". Taking the symmetric and skew-symmetric parts of equation (5-35) yields [100]:

$$\begin{aligned} \bar{d}^p &= \frac{1}{2} Q^p \left(\dot{U}^p U^{p\,-1} + U^{p\,-1} \dot{U}^p\right) Q^{p\,T} \\ \bar{w}^p &= \Omega^Q + \frac{1}{2} Q^p \left(\dot{U}^p U^{p\,-1} - U^{p\,-1} \dot{U}^p\right) Q^{p\,T} \end{aligned} \tag{5-36}$$

With the rotation of the Lagrangian axis of the right plastic stretch tensor, R_L^p, the diagonalized form of the plastic stretch tensor can be obtained by the following transformation:

$$U^p = R_L^p \Lambda_d^p {R_L^p}^T \tag{5-37}$$

Similarly, the diagonalized plastic stretch tensor, Λ_d^p, can be rotated back to the left plastic stretch tensor using the rotation of the Eulerian axis as follows:

$$V^p = R_E^p \Lambda_d^p {R_E^p}^T \tag{5-38}$$

in which R_E^p is the rotation of the Eulerian axis of the plastic stretch tensor and V^p is the symmetric left plastic stretch tensor satisfying: $\chi^p = Q^p U^p = V^p Q^p$.

The relation between the Lagrangian and Eulerian axes is given by

$$R_E^p = Q^p R_L^p \tag{5-39}$$

The orthogonal plastic rotation and the rotations of the Lagrangian and Eulerian triads are related to their corresponding spin tensors by

$$\begin{aligned} \dot{Q}^p &= \Omega^Q Q^p \\ \dot{R}_E^p &= R_E^p \Omega_E \\ \dot{R}_L^p &= R_L^p \Omega_L \end{aligned} \tag{5-40}$$

in which Ω_E^p and Ω_L^p are the spins of the Eulerian and Lagrangian triads satisfying the equality $\Omega^Q = R_E^p \left(\Omega_E^p - \Omega_L^p\right) {R_E^p}^T$, respectively.

Transferring equation (5-36) to the Lagrangian axis of the plastic stretch tensor yields:

$$\bar{d}_E^p = \dot{\Lambda}_d^p \Lambda_d^{p\,-1} + \frac{1}{2}\left(\Lambda_d^{p\,-1}\Omega_L^p \Lambda_d^p - \Lambda_d^p \Omega_L^p \Lambda_d^{p\,-1}\right)$$
$$\bar{w}_E^p = \Omega_E^p - \frac{1}{2}\left(\Lambda_d^{p\,-1}\Omega_L^p \Lambda_d^p + \Lambda_d^p \Omega_L^p \Lambda_d^{p\,-1}\right) \tag{5-41}$$

in which $\bar{d}_E^p = R_E^{p\,T}\bar{d}^p R_E^p$ and $\bar{w}_E^p = R_E^{p\,T}\bar{w}^p R_E^p$ are the Eulerian representations of the plastic strain rate and plastic spin, respectively. Following the method of the principal axis (cf. Hill [39], Reinhardt and Dubey [98], and Eterovic and Bathe [101]), the symmetric and skew-symmetric parts of equation (5-41-1) give the following relations for the diagonalized plastic stretch tensor and its corresponding Lagrangian spin:

$$\frac{\left(\dot{\Lambda}_d^p\right)_{ii}}{\lambda_i^p} = \left(\bar{d}_E^p\right)_{ii} \quad ; \quad (no\ sum)$$
$$\left(\Omega_L^p\right)_{ij} = \frac{2\lambda_j^p \lambda_i^p}{\lambda_j^{p\,2} - \lambda_i^{p\,2}}\left(\bar{d}_E^p\right)_{ij} \quad ; (i \neq j) \tag{5-42}$$

Similarly, use of equations (5-41-2) and (5-42-2) gives the following relation for the evolution of the Eulerian triad of the plastic stretch:

$$\left(\Omega_E^p\right)_{ij} = \left(\bar{w}_E^p\right)_{ij} + \frac{\lambda_j^{p\,2} + \lambda_i^{p\,2}}{\lambda_j^{p\,2} - \lambda_i^{p\,2}}\left(\bar{d}_E^p\right)_{ij} \quad ; (i \neq j) \tag{5-43}$$

in which λ_i^p's are the principal plastic stretches.

The rotated Kirchhoff stress, $\bar{\tau}$, is work conjugate to the Lagrangian Hencky strain for the case of isotropic plasticity. Defining $\bar{\bar{\tau}}_L$ and $\bar{\bar{U}}_L^e$ as the Lagrangian representations of the rotated Kirchhoff stress and elastic right stretch tensors on the Lagrangian triad, we have:

$$\begin{aligned}\bar{\bar{\tau}}_L &= \left(Q^p R_L^p\right)^T \bar{\tau}\left(Q^p R_L^p\right) = R_E^{pT} \bar{\tau} R_E^p \\ \bar{\bar{U}}_L^e &= \left(Q^p R_L^p\right)^T \bar{U}^e \left(Q^p R_L^p\right) = R_E^{pT} \bar{U}^e R_E^p\end{aligned} \tag{5-44}$$

in which a superposed double bar along with a subscript "*L"* indicate the components of a tensor on the Lagrangian axis of the plastic stretch tensor. The Lagrangian rotated Kirchhoff stress, $\bar{\bar{\tau}}_L$, can be related to the Lagrangian rotated elastic Hencky strain through a hyperelastic function as follows:

$$\bar{\bar{\tau}}_L = M : \left(R_E^{pT}\, ln\, \bar{U}^e\, R_E^p\right) = M : ln\left(R_E^{pT} \bar{U}^e R_E^p\right) = M : ln\, \bar{\bar{U}}_L^e \tag{5-45}$$

In equation (5-45) the fourth-order elasticity tensor M is assumed to be isotropic and constant. Equation (5-45) defines the elastic part of the proposed constitutive model on the Lagrangian axis of the plastic stretch.

The shift stress tensor on the intermediate configuration $\bar{\eta} = \text{dev}\bar{\tau} - \bar{\beta}$, where $\bar{\beta}$ is the deviatoric back stress tensor and "dev" denotes the deviatoric part of a symmetric tensor, can be rotated to the Lagrangian axis of plastic stretch by

$$\bar{\bar{\eta}}_L = \left(Q^p R_L^p\right)^T \bar{\eta}\left(Q^p R_L^p\right) = R_E^{pT} \bar{\eta} R_E^p = dev\bar{\bar{\tau}}_L - \bar{\bar{\beta}}_L \tag{5-46}$$

Furthermore, the following evolution equation for the back stress tensor on the Lagrangian axis is proposed [100]:

$$\dot{\bar{\beta}}_L = H\dot{\bar{E}}_L^p \tag{5-47}$$

Similar expressions can be proposed for a nonlinear back stress evolution equation, and will be discussed in the next section. In equation (5-47), H is the hardening modulus and $\dot{\bar{E}}_L^p$ is the material time rate of the Lagrangian plastic Hencky strain and is related to the plastic strain rate tensor by

$$\left[\dot{\bar{E}}_L^p\right]_{ij} = \hbar_{ij}^{log}\left[\bar{d}_E^p\right]_{ij} \quad ; \textit{(no sum on i and j)} \tag{5-48}$$

$\hbar_{ij}^{\log}$ in equation (5-48) is a scaling function defined by

$$\hbar_{ij}^{log} = \begin{cases} 1 & ; if\ \lambda_j^p = \lambda_i^p \\ \dfrac{2\ ln\left(\dfrac{\lambda_j^p}{\lambda_i^p}\right)\lambda_j^p\lambda_i^p}{\lambda_j^{p\,2} - \lambda_i^{p\,2}} & ; otherwise \end{cases} \tag{5-49}$$

A Mises plastic potential on the Lagrangian axis of plastic stretch is used here. The yield surface for the case of associative J_2 flow of plasticity is given by [100]

$$\phi = \sqrt{\frac{3}{2}\bar{\eta}_L : \bar{\eta}_L} - \Upsilon = 0 \tag{5-50}$$

in which Υ is a scalar parameter function of the equivalent plastic strain representing the current size of the yield surface.

With the assumption of maximum plastic dissipation (cf. Simo and Hughes [30] and Lemaitre and Chaboche [7]) the plastic strain rate tensor can be related to the normal to the yield surface by

$$\bar{d}^p = \dot{\lambda}\frac{\partial \phi}{\partial \bar{\tau}} \rightarrow \bar{d}_E^p = \dot{\lambda}\frac{\partial \phi}{\partial \bar{\bar{\tau}}_L} \tag{5-51}$$

in which $\dot{\lambda}$ is the plastic multiplier which can be found from the consistency condition $\dot{\phi} = 0$. The Kuhn-Tucker loading/unloading conditions for the proposed model can therefore be given by

$$\bar{\bar{E}}_L^p = \dot{\lambda}\hbar^{log}\frac{\partial \phi}{\partial \bar{\bar{\tau}}_L}$$
$$\dot{\lambda} \geq 0\ ;\ \phi \leq 0\ ;\ \dot{\lambda}\phi = 0 \tag{5-52}$$

The plastic spin $\bar{w}^p$ can be related to the known kinematics parameters, and will be discussed in detail in the next section.

5.3 Solution of the simple shear problem

The deformation gradient of the simple shear motion is given by:

$$F = N_1 \otimes N_1 + N_2 \otimes N_{2+} \gamma N_1 \otimes N_2 \tag{5-53}$$

in which γ is the applied shear. Polar decomposition of the deformation gradient leads to equation (2-64) for the rigid rotation and the total left and right stretch tensors. The rotated Lagrangian Kirchhoff stress tensor is given by:

$$\bar{\bar{\tau}}_L = \bar{\bar{\tau}}_{L,11}(N_1 \otimes N_1 - N_2 \otimes N_2) + \bar{\bar{\tau}}_{L,12}(N_1 \otimes N_2 + N_2 \otimes N_1) \tag{5-54}$$

Use of the proposed constitutive model yields the following for the elastic part of the model under the simple shear motion:

$$\bar{\bar{U}}_L^e = exp\left(\frac{\bar{\bar{\tau}}_L}{2\mu}\right) = \mathfrak{B}N_1 \otimes N_1 + \mathfrak{C}N_2 \otimes N_{2+}\mathfrak{J}(N_1 \otimes N_2 + N_2 \otimes N_1) \tag{5-55}$$

in which μ is the shear modulus of the material and $\mathfrak{B}$, $\mathfrak{C}$, and $\mathfrak{J}$ are given by [99]

$$\mathfrak{B} = \frac{1}{2GT}\left[T(1+G^2) - \bar{\bar{\tau}}_{L,11}(1-G^2)\right]$$

$$\mathfrak{J} = \frac{1}{2GT}\left[\bar{\bar{\tau}}_{L,12}(G^2-1)\right] \tag{5-56}$$

$$\mathfrak{C} = \frac{1}{2GT}\left[T(1+G^2) + \bar{\bar{\tau}}_{L,11}(1-G^2)\right]$$

in which $T = \sqrt{\bar{\bar{\tau}}_{L,11}^2 + \bar{\bar{\tau}}_{L,12}^2}$ and $G = \exp\left(\frac{T}{2\mu}\right)$.

The Mises plastic potential for a pure kinematic hardening behavior under simple shear motion is given by

$$\phi = \sqrt{3\left(\bar{\bar{\eta}}_{L,11}^2 + \bar{\bar{\eta}}_{L,12}^2\right)} - \sigma_0 = 0 \tag{5-57}$$

in which σ_0 is the initial yield surface size and is assumed to be constant during plastic deformation. Plastic incompressibility requires that the third invariant of the plastic stretch tensor be 1, i.e. $\det \chi^p = \det U^p = 1$. Such an incompressibility condition specifies the following form for the diagonalized plastic stretch tensor under simple shear motion [100]:

$$\Lambda_d^p = \ell^p N_1 \otimes N_1 + \frac{1}{\ell^p} N_2 \otimes N_2 \tag{5-58}$$

The rotations of the Lagrangian and Eulerian axes of the right plastic stretch tensor for the case of the simple shear motion are given by:

$$\begin{aligned} R_L^p &= cos\,\theta_L^p\,(N_1 \otimes N_1 + N_2 \otimes N_2) + sin\,\theta_L^p\,(N_1 \otimes N_2 - N_2 \otimes N_1) \\ R_E^p &= cos\,\theta_E^p\,(N_1 \otimes N_1 + N_2 \otimes N_2) + sin\,\theta_E^p\,(N_1 \otimes N_2 - N_2 \otimes N_1) \end{aligned} \tag{5-59}$$

in which θ_L^p and θ_E^p are the angles of the Lagrangian and Eulerian axes with respect to the fixed coordinate system, respectively.

Using the proposed decomposition given by equations (5-33) and (5-34), equations (5-39) and (5-44-2) yield the following for the rotated Lagrangian elastic stretch:

$$\bar{\bar{U}}_L^e = {R_E^p}^T U R_L^p {\Lambda_d^p}^{-1} \tag{5-60}$$

The time derivative of equation (5-60) yields the following for the components of time rate of the Lagrangian elastic right stretch tensor:

$$\begin{aligned} \frac{d\bar{\bar{U}}_{L,11}^e}{d\gamma} &= \mathcal{F}_1\left(\ell^p, \theta_E^p, \theta_L^p; \gamma\right)\frac{d\lambda}{d\gamma} + \mathcal{G}_1\left(\ell^p, \theta_E^p, \theta_L^p; \gamma\right) \\ \frac{d\bar{\bar{U}}_{L,12}^e}{d\gamma} &= \mathcal{F}_2\left(\ell^p, \theta_E^p, \theta_L^p; \gamma\right)\frac{d\lambda}{d\gamma} + \mathcal{G}_2\left(\ell^p, \theta_E^p, \theta_L^p; \gamma\right) \end{aligned} \tag{5-61}$$

On the other hand, equations (5-55) and (5-56) yield the following for the components of the time rate of the Lagrangian elastic right stretch tensor:

$$\dot{\bar{\bar{U}}}_L^e = \frac{d}{dt}\left[exp\left(\frac{\bar{\bar{\tau}}_L}{2\mu}\right)\right] = \left[\dot{\mathfrak{B}}N_1\otimes N_1 + \dot{\mathfrak{C}}N_2\otimes N_{2+}\dot{\mathfrak{J}}(N_1\otimes N_2 + N_2\otimes N_1)\right] \tag{5-62}$$

Therefore, the following are derived for the material time rate of the Lagrangian rotated Kirchhoff stress with the help of equations (5-61) and (5-62):

$$\begin{aligned}\frac{d\bar{\bar{\tau}}_{L,11}}{d\gamma} &= \mathcal{A}_1\left(\ell^p, \theta_E^p, \theta_L^p, \mathfrak{B}, \mathfrak{J}, \mathfrak{C}; \gamma\right)\frac{d\lambda}{d\gamma} + \mathcal{B}_1\left(\ell^p, \theta_E^p, \theta_L^p, \mathfrak{B}, \mathfrak{J}, \mathfrak{C};\right)\\ \frac{d\bar{\bar{\tau}}_{L,12}}{d\gamma} &= \mathcal{A}_2\left(\ell^p, \theta_E^p, \theta_L^p, \mathfrak{B}, \mathfrak{J}, \mathfrak{C}; \gamma\right)\frac{d\lambda}{d\gamma} + \mathcal{B}_2\left(\ell^p, \theta_E^p, \theta_L^p, \mathfrak{B}, \mathfrak{J}, \mathfrak{C};\right)\end{aligned} \tag{5-63}$$

Details of the derivation of the component form of equations (5-61), (5-62), and (5-63) and their corresponding coefficients $\mathcal{F}_1$, $\mathcal{F}_2$, $\mathcal{G}_1$, $\mathcal{G}_2$, $\mathcal{A}_1$, $\mathcal{A}_2$, $\mathcal{B}_1$, and $\mathcal{B}_2$ are given in Appendix C.

Use of the proposed constitutive model for the evolution of the back stress tensor given by (5-47) results in the following differential equations for the simple shear problem:

$$\begin{aligned}\frac{d\bar{\bar{\beta}}_{L,11}}{d\gamma} &= \sqrt{\frac{3}{2}}H\bar{\bar{\bar{N}}}_{L,11}\frac{d\lambda}{d\gamma}\\ \frac{d\bar{\bar{\beta}}_{L,12}}{d\gamma} &= \sqrt{\frac{3}{2}}H\hbar_{12}^{log}\ \bar{\bar{\bar{N}}}_{L,12}\frac{d\lambda}{d\gamma}\end{aligned} \tag{5-64}$$

in which $\bar{\bar{\bar{N}}}_L = \sqrt{\frac{2}{3}}\frac{\partial\phi}{\partial\bar{\bar{\eta}}_L} = \frac{\bar{\bar{\eta}}_L}{\|\bar{\bar{\eta}}_L\|}$ is the unit normal to the yield surface.

Use of equations (5-63) and (5-64) and the consistency condition, which requires that $\dot{\phi} = 0$ during plastic loading, the plastic multiplier can be obtained as follows:

$$\frac{d\lambda}{d\gamma} = \frac{\bar{\bar{\eta}}_{L,11}\mathcal{B}_1 + \bar{\bar{\eta}}_{L,12}\mathcal{B}_2}{\sqrt{\frac{3}{2}}H\left(\bar{\bar{N}}_{L,11}\bar{\bar{\eta}}_{L,11} + \hbar_{12}^{log}\ \bar{\bar{N}}_{L,12}\bar{\bar{\eta}}_{L,12}\right) - \left(\mathcal{A}_1\bar{\bar{\eta}}_{L,11} + \mathcal{A}_2\bar{\bar{\eta}}_{L,12}\right)} \tag{5-65}$$

In summary the governing differential equations for the problem of simple shear using the proposed constitutive model and the case of linear kinematic hardening are given as follows:

$$\begin{aligned}
\frac{d\bar{\bar{\tau}}_{L,11}}{d\gamma} &= \mathcal{A}_1\left(\ell^p, \theta_E^p, \theta_L^p, \mathfrak{B}, \mathfrak{J}, \mathfrak{C}; \gamma\right)\frac{d\lambda}{d\gamma} + \mathcal{B}_1\left(\ell^p, \theta_E^p, \theta_L^p, \mathfrak{B}, \mathfrak{J}, \mathfrak{C}; \gamma\right) \\
\frac{d\bar{\bar{\tau}}_{L,12}}{d\gamma} &= \mathcal{A}_2\left(\ell^p, \theta_E^p, \theta_L^p, \mathfrak{B}, \mathfrak{J}, \mathfrak{C}; \gamma\right)\frac{d\lambda}{d\gamma} + \mathcal{B}_2\left(\ell^p, \theta_E^p, \theta_L^p, \mathfrak{B}, \mathfrak{J}, \mathfrak{C}; \gamma\right) \\
\frac{d\bar{\bar{\beta}}_{L,11}}{d\gamma} &= \sqrt{\frac{3}{2}}H\bar{\bar{N}}_{L,11}\frac{d\lambda}{d\gamma} \\
\frac{d\bar{\bar{\beta}}_{L,12}}{d\gamma} &= \sqrt{\frac{3}{2}}H\hbar_{12}^{log}\ \bar{\bar{N}}_{L,12}\frac{d\lambda}{d\gamma} \\
\frac{d\theta_E^p}{d\gamma} &= \mathfrak{T}_1\left(\ell^p, \theta_E^p, \theta_L^p; \gamma\right)\frac{d\lambda}{d\gamma} + \mathfrak{T}_2\left(\ell^p, \theta_E^p, \theta_L^p; \gamma\right) \\
\frac{d\theta_L^p}{d\gamma} &= -\sqrt{\frac{3}{2}}\bar{\bar{N}}_{L,12}\frac{2{\ell^p}^2}{{\ell^p}^4 - 1}\frac{d\lambda}{d\gamma}
\end{aligned} \tag{5-66}$$

$$\frac{d\ell^p}{d\gamma} = \sqrt{\frac{3}{2}}\bar{\bar{N}}_{L,11}\ell^p\frac{d\lambda}{d\gamma}$$

$$\frac{d\lambda}{d\gamma} = \frac{\bar{\bar{\eta}}_{L,11}\mathcal{B}_1 + \bar{\bar{\eta}}_{L,12}\mathcal{B}_2}{\sqrt{\frac{3}{2}}H\left(\bar{\bar{N}}_{L,11}\bar{\bar{\eta}}_{L,11} + \hbar_{12}^{log}\ \bar{\bar{N}}_{L,12}\bar{\bar{\eta}}_{L,12}\right) - \left(\mathcal{A}_1\bar{\bar{\eta}}_{L,11} + \mathcal{A}_2\bar{\bar{\eta}}_{L,12}\right)}$$

Evolution equation (5-66-5) is used to update the Eulerian triad angle during time integration instead of equation (5-43), which needs a separate evolution equation for the plastic spin. This is due to the fact that the plastic spin is a function of the known kinematic variables and does not require a separate evolution equation to be specified (see Appendix C for a detailed derivation of the evolution equations).

The set of differential equations given in (5-66) is numerically integrated for a maximum applied shear of $\gamma = 8$ using a fourth-order Runge-Kutta numerical integration scheme. The amount of shear at which the plastic yielding starts is $\gamma_p = 2\sinh\left(\frac{\sigma_0}{\sqrt{12}\mu}\right)$ and the initial conditions at this amount of shear are given by

$$\tau_{12}(\gamma_p) = \frac{4\mu\, asinh\left(\frac{\gamma_p}{2}\right)}{\sqrt{4+\gamma_p^2}}\ ;\ \tau_{11}(\gamma_p) = \sqrt{\frac{\sigma_0^2}{3} - \tau_{12}^2}$$

$$\bar{\bar{\beta}}_{L,11}(\gamma_p) = \bar{\bar{\beta}}_{L,12}(\gamma_p) = 0 \qquad (5\text{-}67)$$

$$\ell^p(\gamma_p) = 1$$

$$\theta_E^p(\gamma_p) = \theta_L^p(\gamma_p) = \theta(\gamma_p) = atan\left(\frac{\gamma_p}{2}\right)$$

Figure 5-3 and Figure 5-4 show the evolution of the Kirchhoff stress using the proposed constitutive model for the problem of simple shear. Values of $\tau_0 = \sqrt{\frac{2}{3}}\sigma_0 = 200$ MPa, $H = \sqrt{\frac{2}{3}}\tau_0$, and $\mu = \frac{30\tau_0}{\sqrt{6}}$ were used for the size of the yield surface, hardening modulus, and shear modulus of the material, respectively. The stress response of the same problem using the self-consistent Eulerian rate model of Bruhns et al. [27] based on the logarithmic (D) rate is also plotted. The stress responses of the original and modified formulations by Gabriel and Bathe [32], as well as the stress response of the decoupled volumetric/deviatoric model of Simo [35], are also plotted for comparison. Details of the numerical implementations of the original and modified formulation of Gabriel and Bathe and the decoupled volumetric/deviatoric formulation of Simo are given in [32,36]. Figure 5-5 and Figure 5-6 also show the evolution of the back stress components using the proposed constitutive model, and models presented in [27,32,36,95]. It should be noted that in Figure 5-5 and Figure 5-6 the back stress components of the model proposed by Simo [36] are the decoupled deviatoric components used in the spatial representation of the model. The response of the model is identical to those of the self-consistent Eulerian rate model of Bruhns et al. [27]. However, unlike the self-consistent Eulerian rate model of Bruhns et al. which is based on the specific logarithmic rate of the Kirchhoff stress, the proposed model is integrated without making any reference to any specific rate of stress. No objective rate of stress is used in the proposed model and a total hyperelastic stress function relates the Kirchhoff stress to the Hencky strain.

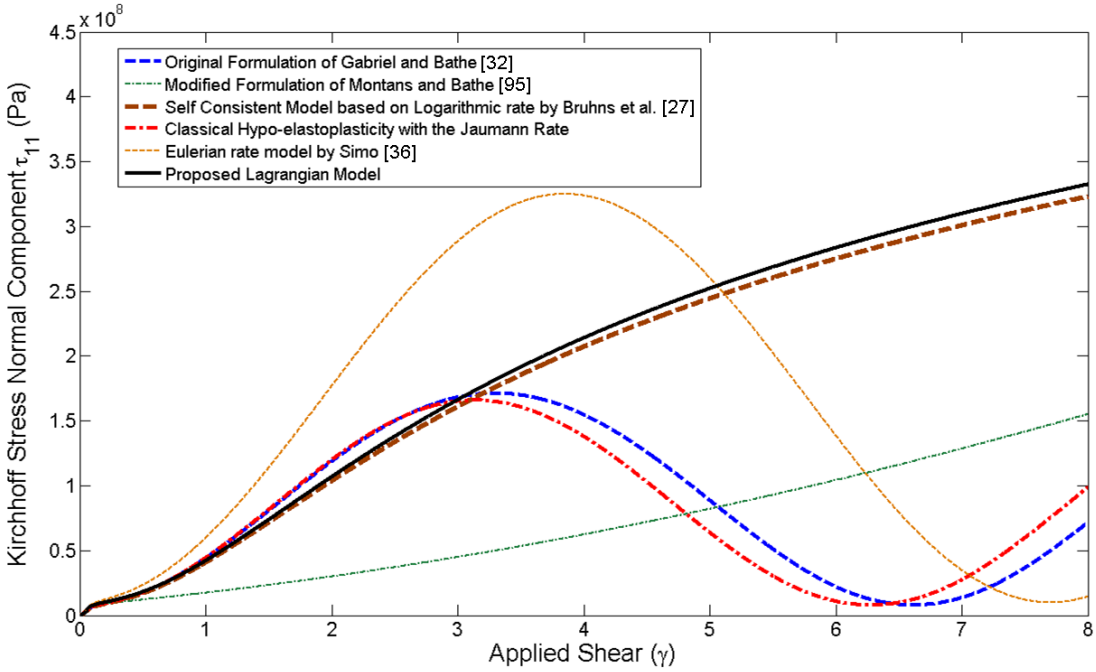

Figure 5-3- Normal component of the Kirchhoff stress using different models

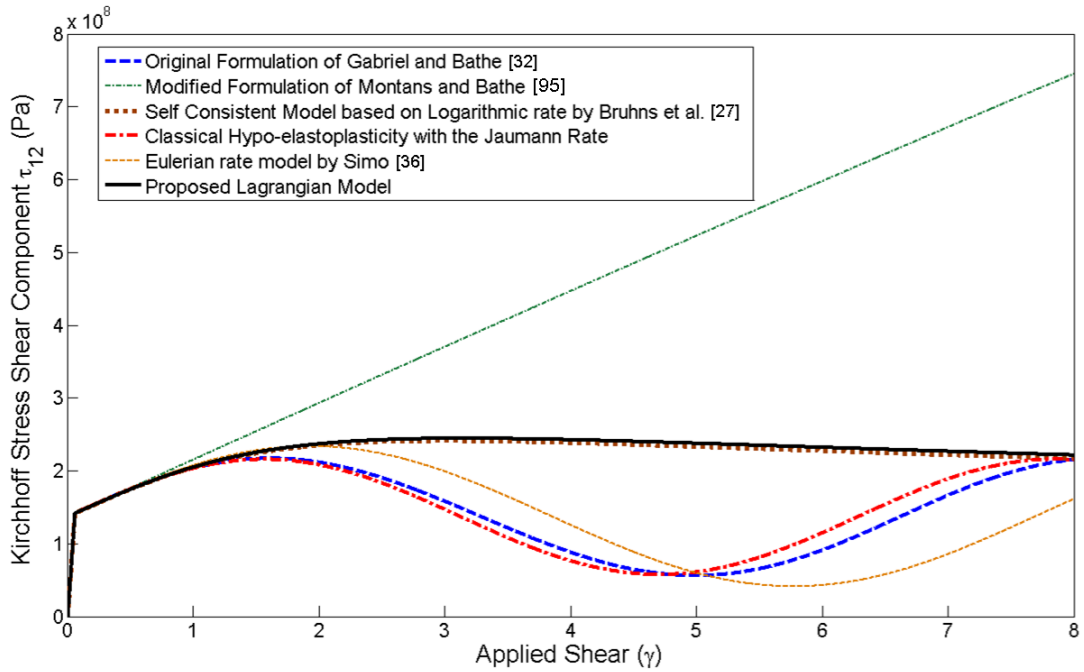

Figure 5-4- Shear component of the Kirchhoff stress using different models

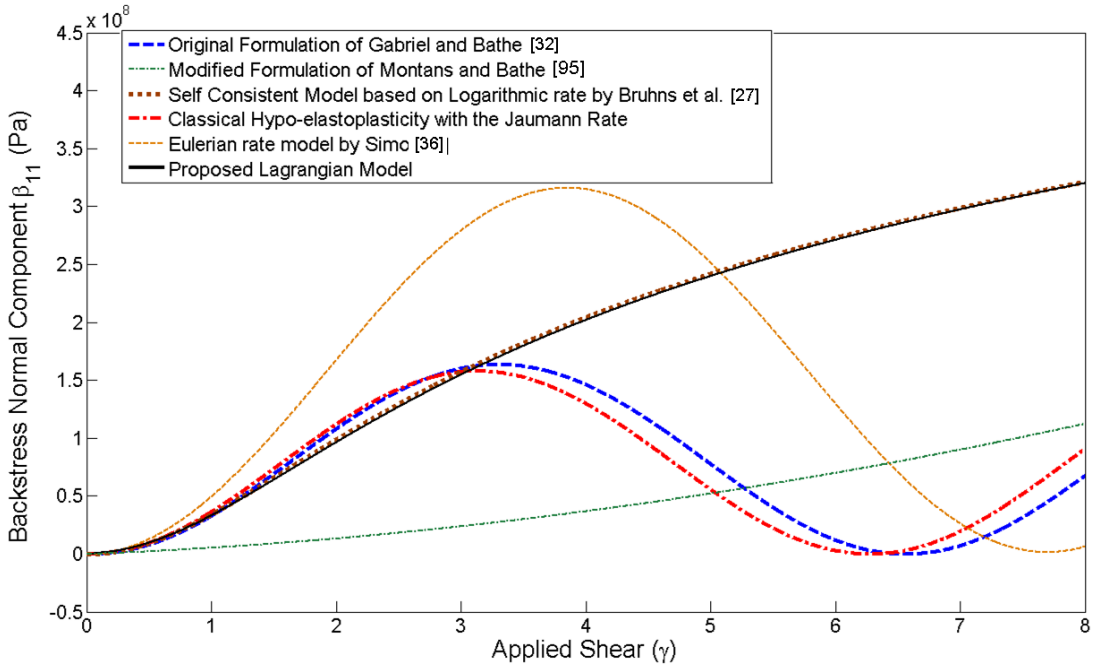

Figure 5-5- Normal component of the back stress using different models

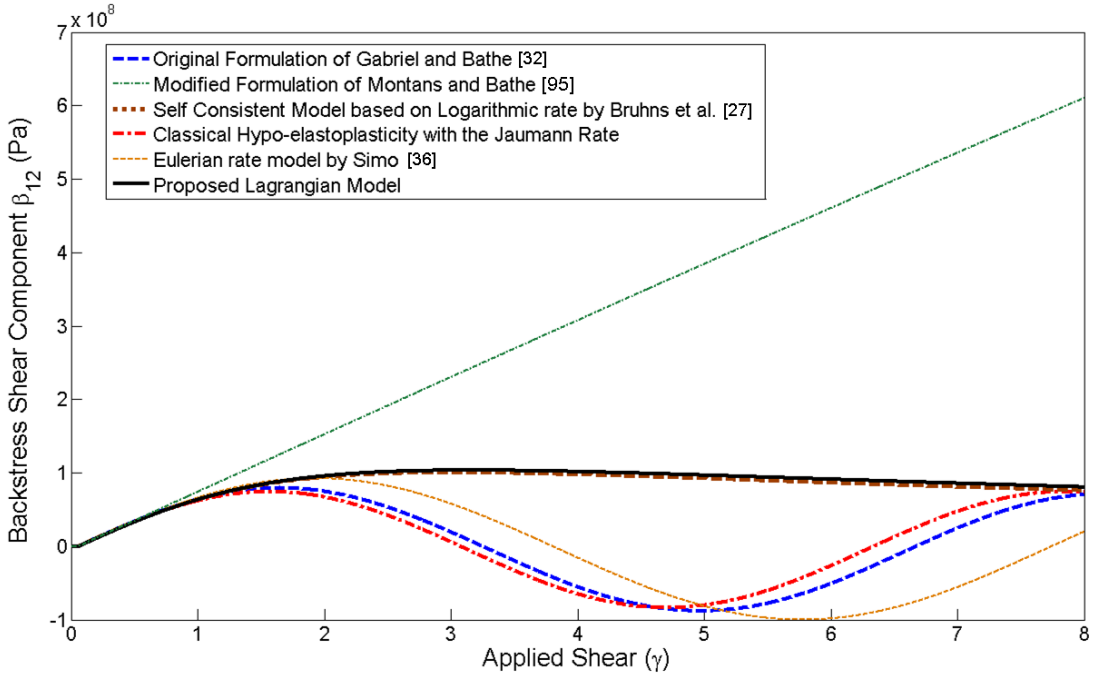

Figure 5-6- Shear component of the back stress using different models

Figure 5-7 shows the evolution of the principal plastic stretches for the proposed model only.

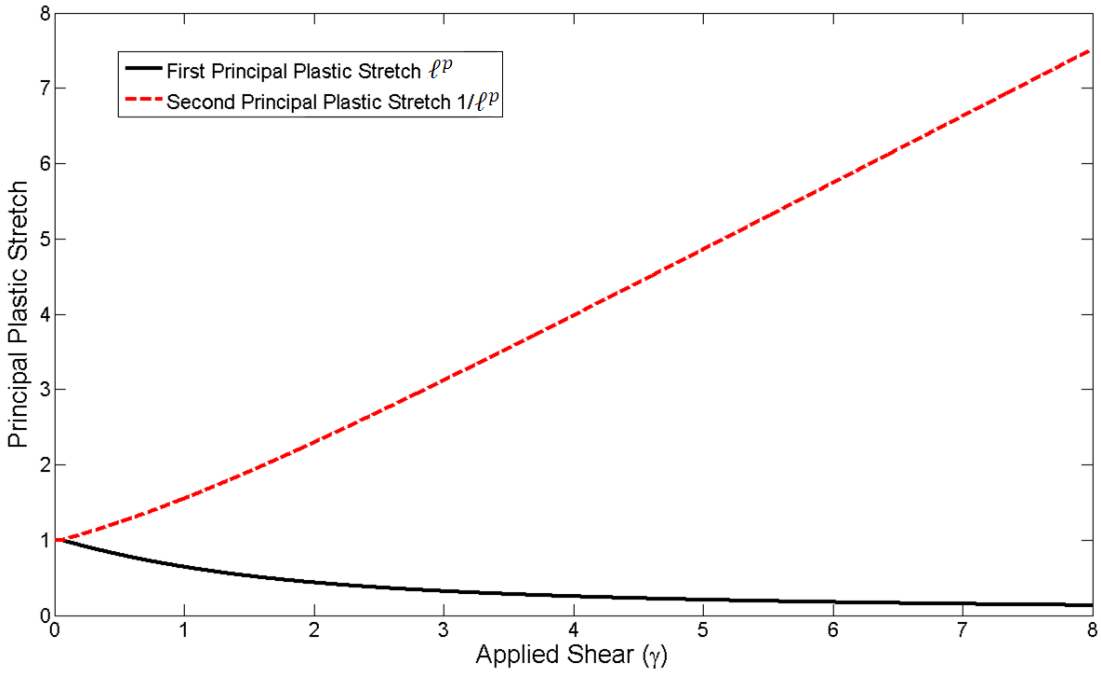

Figure 5-7- Evolution of the principal plastic stretches (Proposed Model only)

5.4 Application of the proposed model to the mixed nonlinear hardening behavior of SUS 304 stainless steel

In this section the proposed constitutive model is extended to a mixed nonlinear kinematic/isotropic hardening. The model is then used to predict the behavior of SUS 304 stainless steel under fixed-end finite torsional loading.

With the help of the Armstrong-Frederick nonlinear kinematic hardening model [81], the proposed backstress evolution equation given in (5-47) can be modified as follows:

$$\dot{\bar{\beta}}_L = A_f \dot{\bar{E}}_L^p - B_f \bar{\beta}_L \dot{E}^{p,eq} \tag{5-68}$$

in which A_f and B_f are the A-F material parameters and $\dot{E}^{p,eq}$ is the rate of the equivalent plastic strain which will be defined later in this section.

The Mises flow potential given in equation (5-50) is extended for a nonlinear mixed hardening by

$$\phi = \sqrt{\frac{3}{2}\bar{\eta}_L : \bar{\eta}_L} - \Upsilon = 0 \tag{5-69}$$

in which Υ is a scalar function of the equivalent plastic strain which represents the current size of the yield surface, and is related to the equivalent plastic strain through an exponential form as follows [82]:

$$\Upsilon = \sigma_{Y0} + (\sigma_{Ys} - \sigma_{Y0})[1 - exp(-bE^{p,eq})] \tag{5-70}$$

In equation (5-70) σ_{Y0} is the initial yield surface size, σ_{Ys} is the saturation value for the subsequent yield stress, b is a material parameter which controls the rate of saturation, and $E^{p,eq} = \int_0^t \dot{E}^{p,eq}\,\mathrm{d}t$ is the accumulated equivalent plastic strain.

To derive a relation for the equivalent plastic strain, a modified plastic work is used here as follows:

$$\dot{W}^p = \bar{\bar{\eta}}_L : \dot{\bar{\bar{E}}}_L^p = \Upsilon \dot{E}^{p,eq} \tag{5-71}$$

in which $\Upsilon = \sqrt{\frac{3}{2}\bar{\bar{\eta}}_L : \bar{\bar{\eta}}_L}$. Equations (5-48) and (5-71) yield the following expression for the rate of the equivalent plastic strain for the case of the simple shear problem:

$$\frac{dE^{p,eq}}{d\gamma} = \frac{2\left(\bar{\bar{\eta}}_{L,11}^2 + \hbar_{12}^{log}\ \bar{\bar{\eta}}_{L,12}^2\right)}{\|\bar{\bar{\eta}}_L\|^2}\frac{d\lambda}{d\gamma} \tag{5-72}$$

Similar to the case of the linear kinematic hardening discussed in section 5.3, the governing equations given in (5-66) are modified as follows for the case of nonlinear mixed hardening. The evolution equations for the stress components remain the same as given by equations (5-66). The evolution equations for the back stress tensor should be modified as follows:

$$\begin{aligned}
\frac{d\bar{\bar{\beta}}_{L,11}}{d\gamma} &= \left[\sqrt{\frac{3}{2}}A_f \bar{\bar{N}}_{L,11} - \frac{2\left(\bar{\bar{\eta}}_{L,11}^2 + \hbar_{12}^{log}\ \bar{\bar{\eta}}_{L,12}^2\right)}{\|\bar{\bar{\eta}}_L\|^2} B_f \bar{\bar{\beta}}_{L,11}\right]\frac{d\lambda}{d\gamma} \\
\frac{d\bar{\bar{\beta}}_{L,12}}{d\gamma} &= \left[\sqrt{\frac{3}{2}}A_f \hbar_{12}^{log}\ \bar{\bar{N}}_{L,12} - \frac{2\left(\bar{\bar{\eta}}_{L,11}^2 + \hbar_{12}^{log}\ \bar{\bar{\eta}}_{L,12}^2\right)}{\|\bar{\bar{\eta}}_L\|^2} B_f \bar{\bar{\beta}}_{L,12}\right]\frac{d\lambda}{d\gamma}
\end{aligned} \tag{5-73}$$

And the consistency condition for the evolution of the plastic multiplier should be modified as follows:

$$\frac{d\lambda}{d\gamma} = \frac{\bar{\bar{N}}_{L,11}\mathcal{B}_1 + \bar{\bar{N}}_{L,12}\mathcal{B}_2}{T_1 - T_2 - T_3 + T_4} \tag{5-74}$$

in which:

$$T_1 = \sqrt{\frac{3}{2}} A_f \left(\bar{\bar{N}}_{L,11} \bar{\bar{\eta}}_{L,11} + \hbar_{12}^{log} \ \bar{\bar{N}}_{L,12} \bar{\bar{\eta}}_{L,12} \right)$$

$$T_2 = \left(\mathcal{A}_1 \bar{\bar{N}}_{L,11} + \mathcal{A}_2 \bar{\bar{N}}_{L,12} \right) \tag{5-75}$$

$$T_3 = \frac{2B_f \left(\bar{\bar{\eta}}_{L,11}^2 + \hbar_{12}^{log} \ \bar{\bar{\eta}}_{L,12}^2 \right)}{\| \bar{\bar{\eta}}_L \|^2} \left(\bar{\bar{\beta}}_{L,11} \bar{\bar{\eta}}_{L,11} + \bar{\bar{\beta}}_{L,12} \bar{\bar{\eta}}_{L,12} \right)$$

$$T_4 = \frac{b(\sigma_{Ys} - Y)}{\sqrt{6}}$$

Similar to the case of the linear kinematic hardening model, the governing equations given by (5-66) with their corresponding modified equations given by equations (5-73) to (5-75) are numerically integrated using the fourth-order Runge-Kutta method for a maximum applied shear of $\gamma = 4$. The stress responses from the proposed model are plotted in Figure 5-8 using the material parameters given in [83] for SUS 304 stainless steel, which were summarized in Table 4-1. The model prediction for the fixed-end finite torsional loading of SUS 304 is in good agreement with the experimental data reported by Ishikawa [83]. Furthermore, from Figure 5-8, the proposed model gives identical results to those of the self-consistent Eulerian rate model of Bruhns et al. [27], based on the logarithmic (D) rate. Figure 5-9 and Figure 5-10 also show the evolution of the back stress tensor and subsequent yield surface size vs. the applied shear, respectively.

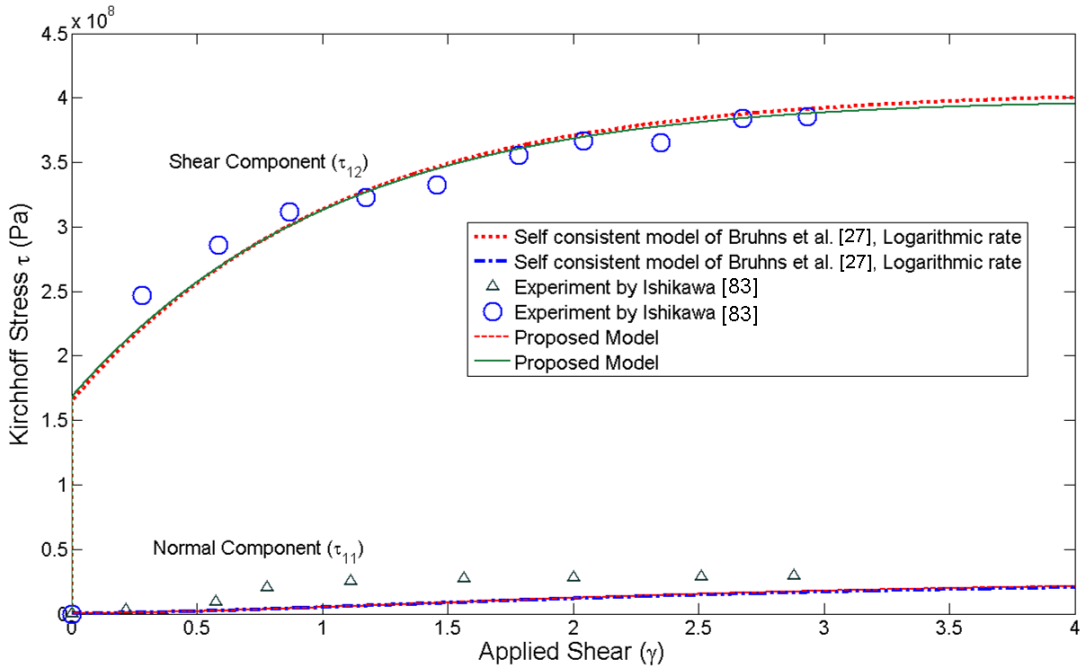

Figure 5-8- Stress components for SUS 304 stainless steel under fixed end finite torsional loading using the proposed mixed hardening model, self-consistent model based on logarithmic rate, and experimental data

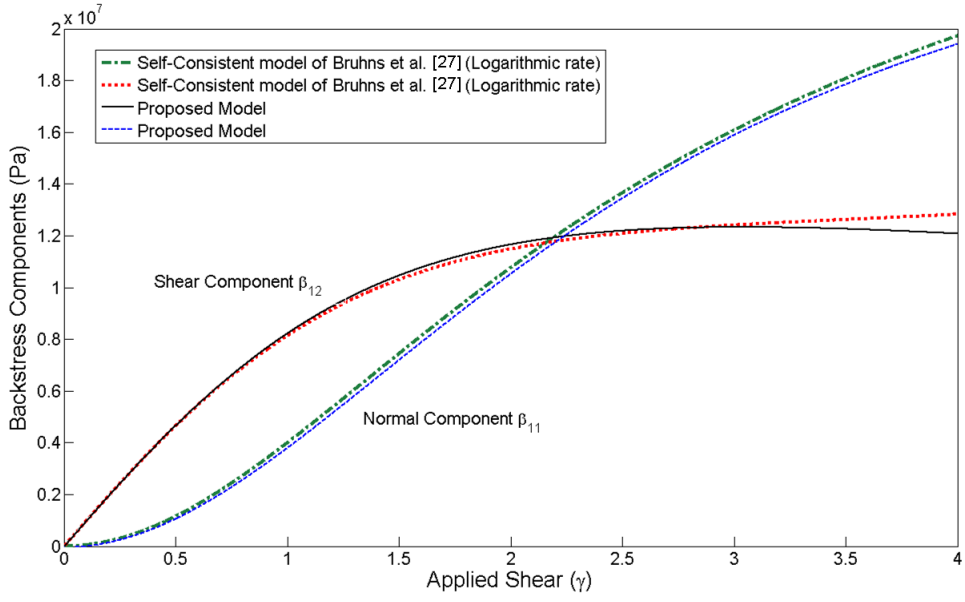

Figure 5-9- Evolution of back stress components for SUS 304 stainless steel under fixed end torsion using the proposed mixed hardening model and self consistent model based on logarithmic rate

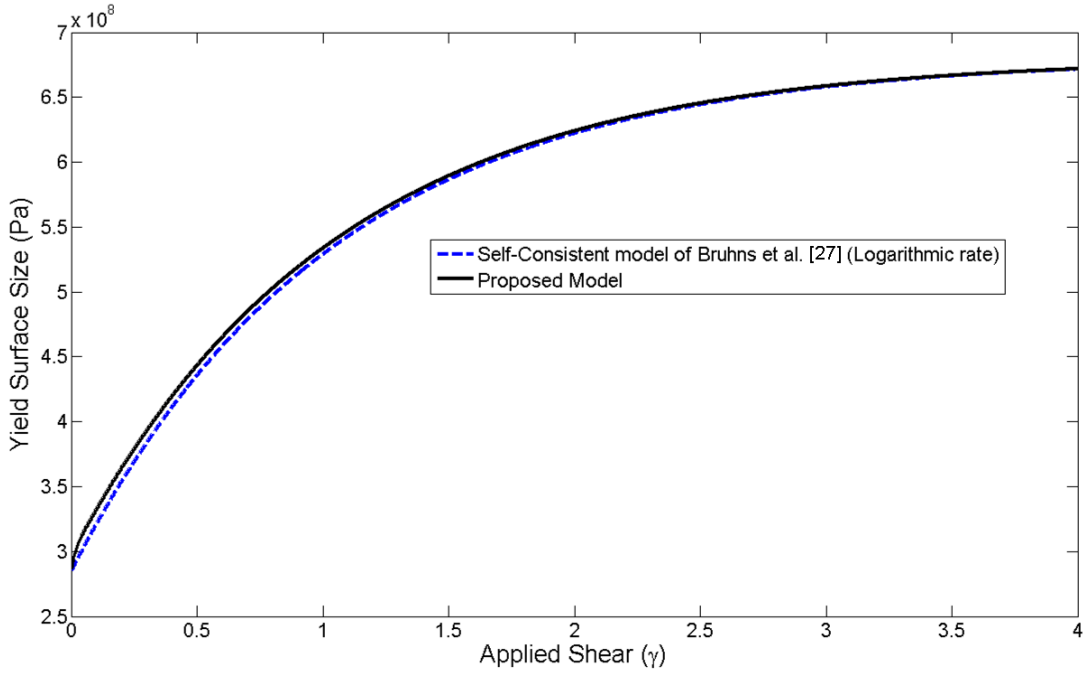

Figure 5-10- Evolution of subsequent yield surface size for SUS 304 stainless steel under fixed end torsional using the proposed mixed hardening model and the self-consistent model based on the logarithmic rate

5.5 Summary

A new kinematic decomposition of the deformation gradient based on the right stretch tensor was proposed in this chapter. The total right stretch tensor was decomposed into a symmetric elastic stretch tensor and a non-symmetric plastic deformation tensor. The plastic deformation tensor was further decomposed into an orthogonal plastic rotation and a symmetric right plastic stretch tensor. Based on this decomposition, a new Lagrangian model for finite strain elastoplasticity was proposed. The rotated Kirchhoff stress was related to the Lagrangian logarithmic strain for the elastic part of the deformation through a hyperelastic potential. The flow

rule was modified based on the logarithmic measure of the right plastic stretch tensor. Furthermore, a new evolution equation for the back stress tensor was proposed based on the Hencky plastic strain tensor. The proposed model was successfully integrated on the Lagrangian axis of the plastic stretch tensor.

Results obtained for the problem of simple shear and linear kinematic hardening of the material were identical to those of the self-consistent Eulerian rate model of Bruhns et al. [27]. The model was integrated with no reference to any objective rate of stress.

The proposed Lagrangian model was extended to mixed nonlinear hardening behavior. Application of the proposed Lagrangian model to fixed-end finite torsional loading of SUS 304 stainless steel tubes showed that the model predicts the second order effect (Swift effect) accurately and results obtained were in good agreement with the available experimental data for this material. Therefore, the Lagrangian model is an equivalent framework of the unified Eulerian model proposed in Chapter 4.

The proposed Lagrangian model is a good candidate for the Lagrangian framework of finite strain elastoplasticity and can be successfully implemented in the displacement-based formulation of the finite element method.

Chapter 6

Conclusions and Recommendations

6.1 Summary and Conclusions

Both approaches for finite strain elastoplasticity have issues arising from inconsistent formulations. Eulerian formulations, which mostly have adopted hypoelastic material models for the elastic part of deformation, have faced issues such as shear oscillation, elastic dissipation, and elastic ratchetting because of the hypoelastic material models non-integrability. Issues regarding hypoelastic models non-integrability found in the existing hypo-based Eulerian rate formulation for finite strain elastoplasticity, which have questioned the physical applicability of such models, have been addressed thoroughly. The oscillatory shear stress response for

simple shear motion is one drawback of hypoelastic material models non-integrability in the sense of elasticity. Elastic dissipation in closed path loading when different rates of stress, such as the Jaumann and Green-McInnis-Naghdi rates, are used is another issue of hypoelasticity. In addition, elastic ratchetting under application of cyclic loading happens as a result of inconsistency of hypoelastic material models with the notion of Green elasticity. Previous attempts at resolving such issues have been focused on examining different objective rates of stress (e.g., Green-McInnis-Naghdi and logarithmic rates) and/or solution techniques such as the principal axes integration technique in the literature of finite strain analysis. Analytical and numerical results obtained from classical finite hypo-elastoplastic models have shown that the use of hypoelastic material models is limited to the specific case of the logarithmic (D) rate of stress. Grade-zero hypoelastic material models have been shown to be exactly integrable only if the logarithmic (D) rate of stress is used. Therefore, Hypo-based Eulerian rate models for finite strain elastoplasticity are not physically consistent when objective rates other than the logarithmic (D) rate of stress is used in their evolution equations. Applicability of other physical objective rates, such as the Jaumann and Green-McInnis-Naghdi rates, for setting up a consistent Eulerian model for finite strain analysis has remained unanswered.

On the other hand, existing Lagrangian formulations bypassed the need for hypoelastic material models for the elastic part of the deformation, by adopting a hyperelastic strain energy function. As a result, the requirement of spatial covariance (objectivity) and the need for covariant (objective) rates of stress were bypassed using

hyperelasticity. The elastic response of the existing Lagrangian models was therefore non-oscillatory and non-dissipative, consistent with the physical requirements of elasticity. However, a large degree of disagreement exists on a unique definition for the plastic part of deformation in the existing Lagrangian hyper-based models. Different definitions for plastic part of deformation have led to different flow rules and evolution equations for plastic internal variables. Such definitions were mostly based on the plastic part of the strain rate tensor in different reference configurations. In most of the existing Lagrangian models, the elastic part of the right stretch tensor has been used for stress update, while the plastic part of the strain rate tensor on the intermediate configuration has been used for the evolution of the plastic internal variables. The integrated form of the plastic part of the strain rate tensor does not necessarily represent the plastic part of the stretch tensor. Such a mismatch between the elastic and plastic parts of the deformation is not physically acceptable and it does not necessarily decompose the stress power into its reversible and irreversible parts. This has resulted in shear oscillation of the back stress and in cases the stress tensors. Several attempts, such as introducing the effect of plastic spin and/or formulations which bypassed the need for a definition of the plastic part of deformation, have been made to remove the oscillatory response. However, the mismatch between the elastic and plastic parts of deformation has yet to be resolved.

Issues of finite strain elastoplasticity enforce restrictions on the choice of objective rates and decomposition of the deformation for a physically consistent formulation. Furthermore, the non-unique decomposition of deformation used in

setting up Lagrangian and Eulerian models has led to different responses from different models and as a result currently available Eulerian and Lagrangian formulations for finite strain elastoplasticity are not transferable into each other.

In the current work, constitutive models for finite strain analysis have been formulated in both Lagrangian and Eulerian frameworks based on additive and/or multiplicative decompositions of deformation. It is shown that within the context of rate-independent isotropic plasticity, there should be no preference in the Lagrangian or Eulerian formulations for finite strain analysis since the two formulations are transformable into each other by proper transformations.

In this research, the unified Eulerian rate model for finite strain elastoplasticity has been presented based on an additive decomposition of deformation for arbitrary corotational rates of the Eulerian strain tensor into its elastic and plastic parts in the corresponding spinning background. Based on the presented additive decomposition, for the first time, an Eulerian rate form of elasticity was used for the stress update. Integrability conditions of the Eulerian rate form of elasticity were mathematically investigated and it was shown that the grade-zero form of the model was unconditionally integrable and consistent with hyperelasticity. As a result, the new additive decomposition was shown to be physically sound and led to an exact decomposition of the stress power into its reversible and irreversible parts. In this way, the flow rule and the yield surface were unified based on the plastic part of the objective corotational rate of the Eulerian strain. Depending on the objective rate used

in the model, flow rules and the corresponding yield surfaces were defined in each spinning background. Using the unified work conjugacy, conjugate measures of stress to different objective rates of the Eulerian strain, such as the Jaumann and Green-McInnis-Naghdi rates, have been obtained. The unified Eulerian rate model was successfully integrated on the principal axes of the total left stretch tensor. Any objective corotational rate of the Eulerian strain tensor can be used in the unified model provided the consistent conjugate measure of the Eulerian stress tensor is employed. The unified model returned identical stress responses irrespective of the chosen corotational rate of stress. Results obtained from the new unified model were identical for all of the classical objective rates of stress including the Jaumann, Green-McInnis-Naghdi, and logarithmic (D) rates of stress.

An equivalent Lagrangian framework for the unified Eulerian rate model was presented based on the multiplicative decomposition of the right stretch tensor for the case of isotropic plasticity. The presented right stretch tensor decomposition led to the definition of the non-symmetric right plastic stretch tensor. A quadratic hyperelastic function was used to relate the rotated Kirchhoff stress tensor to the Lagrangian Hencky strain tensor. This relationship is the transformed integrated form of the Eulerian rate model of elasticity used in the unified Eulerian model which was presented in Chapter 4 of this thesis. The flow rule was expressed in terms of the material time rate of the Hencky measure of the plastic stretch tensor instead of the plastic part of the strain rate tensor. Such a logarithmic type of flow is consistent with the Lagrangian Hencky strain measure used for the elastic part of the model; as a

result, the mismatch between the elastic and plastic parts of deformation is resolved and a unique decomposition of the deformation is employed in the presented Lagrangian model. The presented Lagrangian model was successfully integrated on the principal axes of the Lagrangian plastic stretch tensor. Results obtained were identical to those of the unified Eulerian rate model for the problem of simple shear. Assumption of isotropy bypassed the need for additional evolution equations for the plastic spin.

Both the unified Eulerian rate model and the Lagrangian model were extended to predict mixed nonlinear hardening behavior of materials. Results using the new unified models were in good agreement with experimental data for SUS 304 stainless steel tubes under fixed-end finite torsional loading. The well-known second order Swift effect was accurately predicted by the unified Eulerian and Lagrangian models.

Results from the new unified Eulerian and Lagrangian models show the equivalency of these models. As a result, the novel models formulated in the Lagrangian and Eulerian frameworks are equivalent and transformable to each other through proper transformations and no preference exists in order to have a consistent model for finite strain elastoplasticity.

A summary of the current research contributions to the field of finite strain elastoplasticity is given as follows:

1- An Eulerian rate form of elasticity was implemented for setting up the unified Eulerian rate formulation for finite strain elastoplasticity.

Integrability conditions of the new model were mathematically investigated and showed that the grade-zero form of the model is unconditionally integrable and consistent with the notion of elasticity. It is shown for the first time that instead of hypoelastic material models an exactly integrable rate form of elasticity for arbitrary corotational rate of stress can be used for setting up the unified Eulerian rate model and its corresponding stress update. As a result, the unified Eulerian rate model does not require hypoelastic material models for its stress update and is not limited to any specific rate of stress.

2- An additive decomposition of the objective rate of the Eulerian logarithmic strain tensor into elastic and plastic parts was used for the kinematic decomposition. Such an additive decomposition was shown to be in accordance with the thermodynamic principle. Based on the presented additive decomposition, the stress power was shown to be physically separable into its reversible and irreversible parts. The flow rule was derived based on the principle of maximum plastic dissipation for the plastic part of the stress power. This is in accordance with the second principle of thermodynamics which requires elastic reversibility and plastic irreversibility. As a result, maximization of the plastic part of the stress power to derive the corresponding flow rule for the unified Eulerian rate model in different spinning background is physically acceptable.

3- The new unified Eulerian rate model assigned no preference on the choice of objective corotational rates of stress and was thermodynamically consistent with the definition of stress power in arbitrary spinning background. Using the principle of maximum plastic dissipation, the flow rule was expressed in arbitrary spinning frame of reference for the plastic part of the objective rate of the Eulerian logarithmic strain. Since the stress power is invariant in different spinning background and it was shown that the stress power in the unified Eulerian rate model was exactly separable into its elastic and plastic parts irrespective of the chosen objective rate, maximization of the plastic part of the stress power returns identical flow rules for arbitrary objective rates of stress. The back stress evolution equation was accordingly modified in the arbitrary spinning background for a consistent definition of the back stress evolution equation.

4- The unified Eulerian rate model was successfully integrated on the principal axes of the total stretch tensor. Results were validated for the problem of simple shear assuming linear kinematic hardening behavior. Identical stress responses were obtained for arbitrary corotational rates of strain using the unified Eulerian rate model. The unified model assigned no preference on the choice of objective corotational rates of stress.

5- The unified Eulerian rate model was extended to nonlinear mixed hardening behavior. The extended model was used to predict the stress response of the

SUS 304 stainless steel tubes under fixed-end finite torsional loading. Predicted results were in good agreement with the available experimental data for SUS 304 stainless steel under fixed-end torsion. The well-known second order Swift effect was accurately predicted by the unified Eulerian rate model.

6- A novel equivalent Lagrangian framework for the unified Eulerian rate model was presented in the current research and it was shown for the first time that an exactly equivalent Lagrangian framework for the unified Eulerian rate model exists. The same thermodynamic principles were used for setting up the equivalent Lagrangian model. Based on the assumption of isotropic plasticity, the rotated Kirchhoff stress was used for setting up the stress power in the Lagrangian background. Because of this assumption, plastic spin has no contribution in stress power and is a function of known kinematic variables. The equivalent Lagrangian model is currently limited to the case of rate-independent isotropic plasticity. For the case of anisotropic plasticity, the rotated Kirchhoff stress is no longer work conjugate to the Lagrangian logarithmic strain and plastic spin contributes in plastic dissipation.

7- A new multiplicative decomposition of the right stretch tensor was presented for a unique definition for the elastic and plastic parts of the deformation. The total right stretch tensor was multiplicatively decomposed into a

symmetric right elastic stretch tensor and a non-symmetric plastic deformation tensor. The non-symmetric plastic deformation tensor was further decomposed into a symmetric right plastic stretch tensor and its corresponding orthogonal rotation. The logarithmic (Hencky) measures of the symmetric right elastic and plastic stretch tensors were used as unique definitions for the elastic and plastic parts of the deformation. The plastic strain rate tensor has no contribution in the current definition for the plastic part of the deformation in the presented Lagrangian model. The flow rule in the presented Lagrangian model was modified based on the Lagrangian logarithmic plastic strain tensor. As a result, contrary to the existing Lagrangian models, the flow rule used in the presented Lagrangian model returns exactly the plastic part of the stretch tensor in its integrated form. Back stress evolution equation was further modified based on the logarithmic plastic strain tensor instead of plastic strain rate tensor in order to be consistent with the presented flow rule.

8- The equivalent Lagrangian model was successfully integrated on the Lagrangian axes of the plastic stretch tensor for the problem of simple shear using linear kinematic hardening material model. Results obtained showed that the presented Lagrangian model returns the same stress response as compared to those of the presented unified Eulerian rate model. No shear oscillation was observed for the back stress response under simple shear motion from the presented Lagrangian model.

9- The equivalent Lagrangian model was further extended to mixed nonlinear hardening material behavior. The extended model was used to predict the stress response of the SUS 304 stainless steel tube under finite fixed-end torsional loading. Predicted results were in good agreement with the available experimental data for this material. The second order Swift effect was accurately predicted by the presented Lagrangian model.

10- Obtained results validate the equivalency of the presented unified Eulerian rate model and its equivalent Lagrangian framework. The presented models return equivalent stress responses for the same finite deformation loading path. The unified Eulerian and Lagrangian frameworks presented in this work for the first time, are transformable to each other and physically well-grounded based on the thermodynamic principles for the case of rate-independent isotropic plasticity.

6.2 Recommendations for future work

In the present work, a unified Eulerian rate model and its corresponding consistent Lagrangian form has been presented for large strain elastoplasticity. The following recommendations are suggested for the future work based on the present study:

1- Currently, the unified model is limited to rate-independent isotropic plasticity. Applications involving rate dependency and viscoplastic behavior

of hardening materials need to be properly implemented in the proposed models. Extension of the proposed models to rate-dependent plasticity is straightforward.

2- The unified Eulerian rate model is currently integrated on the principal axes of the total left stretch tensor. While integration on the principal axes simplifies the integration process, eigenvalue extraction is required at each material point during stress integration, which is not numerically efficient for finite element applications. Deriving basis-free expressions for each conjugate Eulerian stress tensor to the corresponding objective rate of the Eulerian strain tensor allows integration of the unified model on the fixed background. For some corotational rates, such as the Jaumann rate, such basis-free expressions are available [54]; however, the possibility of deriving basis-free expressions for other corotational rates must be investigated in more detail.

3- Covariance requirement (objectivity) limits the use of the proposed unified Eulerian rate model to the case of material isotropy. Generalization of the Eulerian rate model to the elastically anisotropic material is therefore required. Such generalization seems to be convenient since an incremental form of elasticity is used in the unified formulation. Generalization to anisotropy is feasible by introducing material symmetry groups into the

fourth-order stress-dependent spatial elasticity tensor. Integrability conditions for the case of anisotropy should be further investigated in detail.

4- The presented Lagrangian model is currently integrated on the principal axes of the right plastic stretch tensor. This was done because the flow rule was specified on the principal axes of the plastic stretch tensor. Integration of the model on the intermediate fixed configuration simplifies the integration process; however, it requires that the flow rule be specified on the fixed background. To do this, a basis-free expression for the evolution of the Hencky plastic strain is required which leads to a flow rule expressed on the fixed intermediate configuration.

5- The presented equivalent Lagrangian model is limited to isotropic plasticity. Extension of the proposed Lagrangian model to the case of anisotropic plasticity seems to be more convenient since limitations due to covariance requirement do not exist in the presented Lagrangian model. However, additional evolution equations for the evolution of the plastic spin should be specified for the case of anisotropic plasticity. Proper phenomenological models for the plastic spin can be obtained through experimental observations. Furthermore, for anisotropic elasticity the rotated Kirchhoff stress is no longer work conjugate to the Lagrangian Hencky strain and as a result a complicated measure of stress should be used instead of the rotated

Kirchhoff stress. Use of such a complicated measure of stress in the proposed Lagrangian model should be investigated in more detail.

6- The developed Eulerian and Lagrangian models should be implemented into a finite element code for engineering applications. This requires an algorithmic integration of the unified Eulerian and Lagrangian models. For the unified Eulerian model the integration scheme should be objective and neutral under superposed rigid rotation while for the Lagrangian model this requirement is bypassed. From a numerical point of view, some of objective rates of stress, such as the Jaumann rate, are preferred since they are obtainable from direct kinematic analysis and have simple kinematic representations. Contrary to the classical Eulerian rate model of elastoplasticity which is limited to the specific logarithmic (D) rate of stress, use of simpler corotational rates in the proposed Eulerian rate model is possible and therefore numerically efficient. However, applicability of the well-known radial return mapping scheme for the unified Eulerian model should be investigated in more detail. The general return mapping method can be used for the integration of the proposed Eulerian rate model in cases where the radial return mapping is not applicable.

7- Algorithmic linearization (used to derive the consistent tangent modulus) should be based on the strain and stress measures used in the Eulerian rate model instead of the strain rate tensor. Therefore, modifications must be

applied to the discretized momentum equations for finite element implementation. Existence of a closed form linearization for the consistent tangent modulus depends on the type of objective rate used in the model, which should be investigated in more detail.

8- Numerical implementation of the proposed Lagrangian model is also required for a finite element implementation. Algorithmic integration of the proposed Lagrangian model is not currently available. The radial return mapping method can be used for stress integration of the proposed Lagrangian model. Consistent linearization of the integrated form of the proposed Lagrangian model is also required for a quadratic norm of convergence of the Newton-Raphson method. Existence of such linearization is strongly dependent on the integration method which should be investigated in more detail.

9- Experimental verification for finite strain elastoplasticity under multiaxial non-proportional cyclic loading is still deficient. Especially, the influence of the axially induced strain (stress) under free-end (fixed-end) torsion of cylindrical bars on their cyclic response should be explored in more detail. A biaxial tension-torsion testing machine with independent axial and torsional load cells is suitable for such experimental verifications. However, contrary to infinitesimal measurement techniques, a suitable technique for measuring large torsional strains for finite strain should be developed first. There are

some techniques proposed in the literature which might be suitable for this task [1,83]. Extension of the proposed Eulerian and Lagrangian models to cyclic plasticity under multiaxial non-proportional loading should be done based on the observed experimental data. The problem of error accumulation over cycles reported in the classical hypo-based models of elastoplasticity does not exist in the unified model. As a result, the unified Eulerian model and its equivalent Lagrangian form are good candidates for extension to multiaxial non-proportional cyclic applications for finite strain elastoplasticity.

10- Smart materials such as shape memory alloys (SMA) and bio-related materials exhibit large recoverable elastic and viscoelastic responses. The proposed Eulerian and Lagrangian models are good candidates for applications related to this class of materials.

Appendix A.

Closed form solution of the simple shear problem using the proposed Eulerian rate form of elasticity

The deformation gradient of this motion is given by

$$F = N_1 \otimes N_1 + N_2 \otimes N_2 + \gamma N_1 \otimes N_2 \tag{A-1}$$

For this isochoric motion $J=\det F=1$ and therefore the Cauchy and Kirchhoff stresses are the same. The spin tensors corresponding to the J and GMN frames are given by

$$\Omega_J = \frac{\dot{\gamma}}{2}(N_1 \otimes N_2 - N_2 \otimes N_1)$$
$$\Omega_{GMN} = \dot{\theta}(N_1 \otimes N_2 - N_2 \otimes N_1) \quad \text{(A-2)}$$

in which $\dot{\theta} = \frac{2\dot{\gamma}}{4+\gamma^2}$. The logarithmic strain tensor for this deformation can be found as follows:

$$\varepsilon = \gamma\eta(N_1 \otimes N_1 - N_2 \otimes N_2) + 2\eta(N_1 \otimes N_2 + N_2 \otimes N_1) \quad \text{(A-3)}$$

in which $\eta = \frac{\operatorname{asinh}\left(\frac{\gamma}{2}\right)}{\sqrt{4+\gamma^2}}$. Time derivative of the logarithmic strain has the following components:

$$\frac{d\varepsilon}{d\gamma} = \frac{\gamma + 4\eta}{4+\gamma^2}(N_1 \otimes N_1 - N_2 \otimes N_2) + \frac{2(1-\gamma\eta)}{4+\gamma^2}(N_1 \otimes N_2 + N_2 \otimes N_1) \quad \text{(A-4)}$$

Use of the J rate form of the proposed grade-zero Eulerian rate model given by equation (4-3) leads to the following coupled first order differential equations:

$$\frac{d\tau_{11}}{d\gamma} - \tau_{12} = 2\mu\left(\frac{d\varepsilon_{11}}{d\gamma} - \varepsilon_{12}\right)$$
$$\frac{d\tau_{12}}{d\gamma} + \tau_{11} = 2\mu\left(\frac{d\varepsilon_{12}}{d\gamma} + \varepsilon_{11}\right) \quad \text{(A-5)}$$

Similarly, the following system of differentials is obtained for the GMN form of the proposed model:

$$\frac{d\tau_{11}}{d\gamma} - \frac{4}{4+\gamma^2}\tau_{12} = 2\mu\left(\frac{d\varepsilon_{11}}{d\gamma} - \frac{4}{4+\gamma^2}\varepsilon_{12}\right) \quad \text{(A-6)}$$

$$\frac{d\tau_{12}}{d\gamma} + \frac{4}{4+\gamma^2}\tau_{11} = 2\mu\left(\frac{d\varepsilon_{12}}{d\gamma} + \frac{4}{4+\gamma^2}\varepsilon_{11}\right)$$

To solve the above system of differentials, these equations are first decoupled. Assigning vector $X = \begin{Bmatrix} X_1 \\ X_2 \end{Bmatrix} = \begin{Bmatrix} \tau_{11} \\ \tau_{12} \end{Bmatrix}$, the coupled equations (A-5) and (A-6) can now be re-written in matrix form by $\dot{X} = AX + B$, in which $A = \begin{bmatrix} 0 & 1 \\ -1 & 0 \end{bmatrix}$, $B = \{B_1(\gamma), B_2(\gamma)\}^T = 2\mu\left\{\frac{d\varepsilon_{11}}{d\gamma} - \varepsilon_{12}, \frac{d\varepsilon_{12}}{d\gamma} + \varepsilon_{11}\right\}^T$ in (A-5) and $A = \begin{bmatrix} 0 & \cos^2\theta \\ -\cos^2\theta & 0 \end{bmatrix}$, $B = \{B_1(\gamma), B_2(\gamma)\}^T = 2\mu\left\{\frac{d\varepsilon_{11}}{d\gamma} - \varepsilon_{12}\cos^2\theta, \frac{d\varepsilon_{12}}{d\gamma} + \varepsilon_{11}\cos^2\theta\right\}^T$, and $\cos^2\theta = \frac{4}{4+\gamma^2}$ in (A-6).

Here, the differential equations (A-5) corresponding to the J spin are solved first. Using the eigenvalues of the coefficient matrix *A*, i.e. $\lambda_{1,2} = \pm i$, the decoupled system of equations can be found as follows:

$$\begin{Bmatrix} \dot{Y}_1 \\ \dot{Y}_2 \end{Bmatrix} = \begin{Bmatrix} iY_1 \\ -iY_2 \end{Bmatrix} - \sqrt{2}\mu\begin{Bmatrix} iB_1 + B_2 \\ iB_1 - B_2 \end{Bmatrix} \tag{A-7}$$

in which $Y = S^{-1}X$ and S is the matrix of the eigenvectors of *A*. The general solution of this system is given by:

$$\begin{aligned} Y_1 &= C_1\, exp(\lambda_1\gamma) - \sqrt{2}\mu\, exp(\lambda_1\gamma)\int exp(-\lambda_1\gamma)\,(iB_1 + B_2)d\gamma \\ Y_2 &= C_2\, exp(\lambda_2\gamma) - \sqrt{2}\mu\, exp(\lambda_2\gamma)\int exp(-\lambda_2\gamma)\,(iB_1 - B_2)d\gamma \end{aligned} \tag{A-8}$$

Solution of the above decoupled first order differentials is given by

$$Y_1 = C_1\, exp(i\gamma) - \sqrt{2}\mu(i\gamma + 2)\eta$$
$$Y_2 = C_2\, exp(-i\gamma) - \sqrt{2}\mu(i\gamma - 2)\eta \tag{A-9}$$

The following relationships have been used in deriving (A-9):

$$\frac{d}{d\gamma}[i\, exp(-i\gamma)\,\gamma\eta] = \gamma\eta\, exp(-i\gamma) + i\, exp(-i\gamma)\frac{4\eta + \gamma}{4 + \gamma^2}$$
$$\frac{d}{d\gamma}[exp(-i\gamma)\,\eta] = -i\, exp(-i\gamma)\,\eta + exp(-i\gamma)\frac{2(1 - \gamma\eta)}{4 + \gamma^2} \tag{A-10}$$

And therefore the solution for the stress components is given by

$$\tau_{11} = X_1 = \frac{\sqrt{2}}{2}[C_1 i\, exp(i\gamma) + C_2 i\, exp(-i\gamma)] + 2\mu\gamma\eta$$
$$\tau_{12} = X_2 = \frac{\sqrt{2}}{2}[C_2\, exp(-i\gamma) - C_1\, exp(i\gamma)] + 4\mu\eta \tag{A-11}$$

Assuming a stress-free state as the initial configuration yields $C_1=C_2=0$. Therefore the solution of the simple shear problem using the J rate of stress and the J rate of the Hencky strain can be found in closed form as follows:

$$\tau_{11} = 2\mu\gamma\eta = 2\mu\varepsilon_{11}$$
$$\tau_{12} = 4\mu\eta = 2\mu\varepsilon_{12} \tag{A-12}$$

which is identical to the Hookean response of the problem and was expected due to the unconditional integrability of the proposed Eulerian rate model.

A similar approach can be used to decouple and solve for the differential equations corresponding to the GMN spin given in equation (A-6). Using the

eigenvalues of matrix *A*, i.e. $\lambda_{1,2} = \pm i\cos^2\theta$, and its corresponding eigenvectors, the coupled differential equation (A-6) can be decoupled as follows:

$$\begin{Bmatrix}\dot{Y}_1\\ \dot{Y}_2\end{Bmatrix} = \begin{Bmatrix} iY_1 cos^2\,\theta \\ -iY_2 cos^2\,\theta\end{Bmatrix} - \sqrt{2}\mu \begin{Bmatrix} iB_1 + B_2\\ iB_1 - B_2\end{Bmatrix} \tag{A-13}$$

The general solution for *Y* is given by:

$$\begin{aligned} Y_1 &= C_1\, exp[g(\gamma)] - \sqrt{2}\mu\, exp[g(\gamma)] \int exp[-g(\gamma)]\,(iB_1 + B_2)d\gamma \\ Y_2 &= C_2\, exp[-g(\gamma)] - \sqrt{2}\mu\, exp[-g(\gamma)] \int exp[g(\gamma)]\,(iB_1 - B_2)d\gamma \end{aligned} \tag{A-14}$$

where $g(\gamma) = i\int \cos^2\theta\, d\gamma$. Substitution and simplifications give Y_1 and Y_2 to be:

$$\begin{aligned} Y_1 &= C_1\, exp[2i\theta] - \sqrt{2}\mu(i\gamma + 2)\eta \\ Y_2 &= C_2\, exp[-2i\theta] - \sqrt{2}\mu(i\gamma - 2)\eta \end{aligned} \tag{A-15}$$

Use of the following relations has been made in deriving the above solution (A-15):

$$\begin{aligned} \frac{d}{d\gamma}[i\gamma\eta\, exp(2i\theta)] &= -\gamma\eta\, exp(2i\theta)\, cos^2\,\theta + i\, exp(2i\theta)\frac{4\eta + \gamma}{4 + \gamma^2} \\ \frac{d}{d\gamma}[\eta\, exp(2i\theta)] &= i\eta\, exp(2i\theta)\, cos^2\,\theta + exp(2i\theta)\frac{2(1 - \gamma\eta)}{4 + \gamma^2} \end{aligned} \tag{A-16}$$

And therefore the solution for the stress components is given by:

$$\tau_{11} = X_1 = \frac{\sqrt{2}}{2} i[C_1\, exp(2i\theta) + C_2\, exp(-2i\theta)] + 2\mu\gamma\eta$$

$$\tau_{12} = X_2 = \frac{\sqrt{2}}{2} [C_2\, exp(-2i\theta) - C_1\, exp(2i\theta)] + 4\mu\eta \tag{A-17}$$

Assuming a stress-free state of the material for the initial configuration leads to $C_1=C_2=0$. Therefore the solution of the simple shear problem using the GMN rate of stress and the GMN rate of the Hencky strain returns the same closed form solution for the J rate given by (A-12) which was again expected due to unconditional integrability of the proposed Eulerian rate model.

Appendix B.

Closed form solution of the four-step loading using the proposed Eulerian rate form of elasticity

Step 1- Stretching $0 \leq t \leq 1$

The deformation gradient for this step can be given by

$$F = N_1 \otimes N_1 + A N_2 \otimes N_2 \tag{B-1}$$

The components of the logarithmic strain are:

$$\varepsilon = \frac{1}{2} ln\, F F^T = ln\, A\, (N_2 \otimes N_2) \tag{B-2}$$

For this pure extension, both the material spin Ω_J and the body spin Ω_{GMN} are zero, and therefore both the J and GMN rates of stress and strain are equivalent to their corresponding material time derivatives. Hence, the solution for this deformation step is as follows:

$$\tau = ln\, A\, [\lambda N_1 \otimes N_1 + (\lambda + 2\mu) N_2 \otimes N_2] \tag{B-3}$$

At time *t=1* the stress components are:

$$\tau = ln\, A_m\, [\lambda N_1 \otimes N_1 + (\lambda + 2\mu) N_2 \otimes N_2] \tag{B-4}$$

in which $A_m = 1 + \frac{u_m}{H}$. Equation (B-4) serves as the initial conditions for the next deformation step.

Step 2- Shearing at constant stretch $1 \leq t \leq 2$

The deformation gradient at this step is given by

$$F = N_1 \otimes N_1 + A_m N_2 \otimes N_2 + \gamma N_1 \otimes N_2 \tag{B-5}$$

And the Jaumann and GMN spin tensors can be found as follow:

$$\Omega_J = \frac{\dot{\gamma}}{2A_m}(N_1 \otimes N_2 - N_2 \otimes N_1)$$
$$\Omega_{GMN} = \frac{\dot{\gamma}\, cos^2\, \theta}{1 + A_m}(N_1 \otimes N_2 - N_2 \otimes N_1) \tag{B-6}$$

To calculate the components of the logarithmic strain, the method of spectral decomposition is used here. The eigenvalues of V^2 can be obtained as follow:

$$\Lambda_{1,2} = A_m\left(\xi \pm \sqrt{\xi^2 - 1}\right) \tag{B-7}$$

where $\xi = \frac{1+\gamma^2+A_m^2}{2A_m}$. Therefore, the components of the logarithmic strain can be written in the following form:

$$\begin{aligned}
\varepsilon_{11} &= \frac{1}{2} ln\, A_m + \frac{1}{2}(\xi - A_m)\eta \\
\varepsilon_{22} &= \frac{1}{2} ln\, A_m - \frac{1}{2}(\xi - A_m)\eta \\
\varepsilon_{12} &= \frac{1}{2}\gamma\eta
\end{aligned} \tag{B-8}$$

in which $\eta = \frac{\cosh^{-1}\xi}{\sqrt{\xi^2-1}}$. Taking the derivative of the logarithmic strain components with respect to γ gives:

$$\begin{aligned}
\frac{d\varepsilon_{11}}{d\gamma} = -\frac{d\varepsilon_{22}}{d\gamma} &= \frac{\gamma(\xi - A_m)}{2A_m(\xi^2 - 1)} + \frac{\gamma\eta}{2A_m} - \frac{\gamma\xi(\xi - A_m)\eta}{2A_m(\xi^2 - 1)} \\
\frac{d\varepsilon_{12}}{d\gamma} &= \frac{\eta}{2} + \frac{\gamma^2(1 - \xi\eta)}{2A_m(\xi^2 - 1)}
\end{aligned} \tag{B-9}$$

The following relationships have been used in deriving the eigenprojections of V^2 and time derivative of the logarithmic strain components:

$$\Lambda_1\Lambda_2 = A_m^2;\ \Lambda_1 + \Lambda_2 = 1 + \gamma^2 + A_m^2\ ;\ \Lambda_1 - \Lambda_2 = 2A_m\sqrt{\xi^2 - 1};\ \frac{d\xi}{d\gamma} = \frac{\gamma}{A_m} \tag{B-10}$$

Using the J spin given in (B-6) gives the following for the J rate of the Kirchhoff stress tensor:

$$\overset{J}{\dot{\tau}}_{11} = \dot{\tau}_{11} - \frac{\dot{\gamma}}{A_m}\tau_{12}$$

$$\overset{J}{\dot{\tau}}_{12} = \dot{\tau}_{12} + \frac{\dot{\gamma}}{2A_m}(\tau_{11} - \tau_{22}) \tag{B-11}$$

$$\overset{J}{\dot{\tau}}_{22} = \dot{\tau}_{22} + \frac{\dot{\gamma}}{A_m}\tau_{12}$$

From (B-9) it is concluded that $\dot{\varepsilon}_{11} + \dot{\varepsilon}_{22} = 0$ and therefore $\dot{\tau}_{11} + \dot{\tau}_{22} = 0$ leading to $\varepsilon_{11} + \varepsilon_{22} = C_1$ and $\tau_{11} + \tau_{22} = C_2$. Use of the grade-zero form of the Eulerian rate model given in (4-3) leads to:

$$\frac{d\tau_{11}}{d\gamma} - \frac{\tau_{12}}{A_m} = 2\mu\left(\frac{d\varepsilon_{11}}{d\gamma} - \frac{\varepsilon_{12}}{A_m}\right)$$

$$\frac{d\tau_{12}}{d\gamma} + \frac{\tau_{11}}{A_m} = 2\mu\left(\frac{d\varepsilon_{12}}{d\gamma} + \frac{\varepsilon_{11}}{A_m} + C_3\right) \tag{B-12}$$

in which $C_3 = \frac{C_2}{4\mu A_m} - \frac{C_1}{2A_m}$.

Similarly, for the case of the GMN rate, the following coupled first order differential is obtained:

$$\frac{d\tau_{11}}{d\gamma} - \frac{2\,cos^2\theta}{1 + A_m}\tau_{12} = 2\mu\left(\frac{d\varepsilon_{11}}{d\gamma} - \frac{2\,cos^2\theta}{1 + A_m}\varepsilon_{12}\right)$$

$$\frac{d\tau_{12}}{d\gamma} + \frac{2\,cos^2\theta}{1 + A_m}\tau_{11} = 2\mu\left(\frac{d\varepsilon_{12}}{d\gamma} + \frac{2\,cos^2\theta}{1 + A_m}\varepsilon_{11} + \frac{cos^2\theta}{1 + A_m}C_4\right) \tag{B-13}$$

in which $C_4 = \frac{C_2}{2\mu} - C_1$. Similar to the approach used to solve the simple shear problem in Appendix A, equations (B-12) and (B-13) are coupled first order

differential of the form $\dot{X} = AX + B$ in which, $A = \begin{bmatrix} 0 & A_m^{-1} \\ -A_m^{-1} & 0 \end{bmatrix}$ and $B = \{B_1, B_2\}^T = 2\mu \left\{ \frac{d\varepsilon_{11}}{d\gamma} - \frac{\varepsilon_{12}}{A_m}, \frac{d\varepsilon_{12}}{d\gamma} + \frac{\varepsilon_{11}}{A_m} + C_3 \right\}^T$ for (B-12), and $A = \begin{bmatrix} 0 & \frac{2\cos^2\theta}{1+A_m} \\ -\frac{2\cos^2\theta}{1+A_m} & 0 \end{bmatrix}$ and $\{B_1, B_2\}^T = 2\mu \left\{ \frac{d\varepsilon_{11}}{d\gamma} - \frac{2\cos^2\theta}{1+A_m}\varepsilon_{12}, \frac{d\varepsilon_{12}}{d\gamma} + \frac{2\cos^2\theta}{1+A_m}\varepsilon_{11} + \frac{\cos^2\theta}{1+A_m} C_4 \right\}^T$ in (B-13). Here the solution of (B-12) is considered first. To simplify the solution of (B-12) it is decoupled with the help of eigenvalues and eigenvectors of its coefficient matrix A. Doing so, the followings are obtained for the decoupled form of (B-12):

$$\dot{Y} = (S^{-1}AS)Y + S^{-1}B \tag{B-14}$$

in which $S = \frac{\sqrt{2}}{2}\begin{bmatrix} i & i \\ -1 & 1 \end{bmatrix}$ is the matrix of the eigenvectors of A. Solution of (B-14) is given as follows:

$$\begin{aligned} Y_1 &= K_1 g(\gamma) - \sqrt{2}\mu g(\gamma) \int g^{-1}(\gamma)\,(iB_1 + B_2)d\gamma \\ Y_2 &= K_2 g^{-1}(\gamma) - \sqrt{2}\mu g^{-1}(\gamma) \int g(\gamma)(iB_1 - B_2)d\gamma \end{aligned} \tag{B-15}$$

where $g(\gamma) = \exp\left(\frac{i\gamma}{A_m}\right)$. After simplifications the followings are obtained for the solution of (B-15):

$$Y_1 = K_1 g(\gamma) - \frac{\sqrt{2}}{2}\mu[i(\xi - A_m)\eta + \gamma\eta + iA_m K_3] \tag{B-16}$$

$$Y_2 = K_2 g^{-1}(\gamma) - \frac{\sqrt{2}}{2}\mu[i(\xi - A_m)\eta - \gamma\eta + iA_m K_3]$$

in which $K_3 = \frac{C_2}{4\mu A_m} - \frac{C_1}{2A_m} + \frac{\ln A_m}{2A_m}$. The following relationships were used to find the solution (B-16):

$$\frac{d}{d\gamma}\left[\frac{1}{2} i g^{-1}(\gamma)(\xi - A_m)\eta\right] = \frac{1}{2A_m} g^{-1}(\gamma)\left[(\xi - A_m)\eta + i\gamma\left\{\eta + \frac{(\xi - A_m)(1 - \xi\eta)}{\xi^2 - 1}\right\}\right] \tag{B-17}$$

$$\frac{d}{d\gamma}\left[\frac{1}{2} g^{-1}(\gamma)\gamma\eta\right] = \frac{1}{2A_m} g^{-1}(\gamma)\left[-i\gamma\eta + A_m\left\{\eta + \frac{\gamma^2(1 - \xi\eta)}{A_m(\xi^2 - 1)}\right\}\right]$$

Using the backward relationship $X = SY$, the solution for the stress components can be obtained as follows:

$$\begin{aligned} \tau_{11} = X_1 &= \frac{\sqrt{2}}{2} i[K_1 g(\gamma) + K_2 g^{-1}(\gamma)] + \mu(\xi - A_m)\eta + 2\mu A_m K_3 \\ \tau_{12} = X_2 &= \frac{\sqrt{2}}{2}[K_2 g^{-1}(\gamma) - K_1 g(\gamma)] + \mu\gamma\eta \end{aligned} \tag{B-18}$$

Applying the initial conditions (B-4) at time *t=1* to (B-18) leads to:

$$\begin{aligned} \varepsilon_{11}|_{t=1} + \varepsilon_{22}|_{t=1} &= C_1 = ln\, A_m \\ \tau_{11}|_{t=1} + \tau_{22}|_{t=1} &= C_2 = 2(\lambda + \mu)\, ln\, A_m \end{aligned} \tag{B-19}$$

which leads to:

$$K_3 = \frac{(\lambda+\mu)\, ln\, A_m}{2\mu A_m}\ ;\ K_1 = K_2 = 0 \tag{B-20}$$

Substituting (B-20) into (B-19) the final solution for the stress components will be as follows:

$$\tau_{11} = \lambda\, ln\, A_m + \frac{2\mu}{\Lambda_1 - \Lambda_2}\left[(A_m^2 - \Lambda_2)\, ln\, A_m + \frac{1}{2}(1+\gamma^2 - A_m^2)\, ln\, \Lambda_1\right]$$

$$\tau_{22} = \lambda\, ln\, A_m + \frac{2\mu}{\Lambda_1 - \Lambda_2}\left[(\Lambda_1 - A_m^2)\, ln\, A_m - \frac{1}{2}(1+\gamma^2 - A_m^2)\, ln\, \Lambda_1\right] \tag{B-21}$$

$$\tau_{12} = \mu\gamma\eta = 2\mu\frac{A_m\gamma(ln\,\Lambda_1 - ln\, A_m)}{\Lambda_1 - \Lambda_2}$$

In deriving (B-21) the following relationships were used:

$$\xi - A_m = \frac{1+\gamma^2 - A_m^2}{2A_m} = \frac{\Lambda_1 + \Lambda_2 - 2\Lambda_1\Lambda_2}{\Lambda_1 - \Lambda_2}$$

$$cosh^{-1}\,\xi = \frac{1}{2} ln \frac{\Lambda_1}{\Lambda_{2_1}} \tag{B-22}$$

A similar approach can be used for the solution of the differential equations (B-13) corresponding to the Green-McInnis-Naghdi rate. Using the eigenvalues and eigenvectors of the coefficient matrix A, the following decoupled form is obtained:

$$\begin{Bmatrix}\dot{Y}_1\\ \dot{Y}_2\end{Bmatrix} = \begin{bmatrix}\frac{2icos^2\theta}{1+A_m} & 0\\ 0 & -\frac{2icos^2\theta}{1+A_m}\end{bmatrix}\begin{Bmatrix}Y_1\\ Y_2\end{Bmatrix} + \sqrt{2}\mu\begin{bmatrix}-i & -1\\ -i & 1\end{bmatrix}\begin{Bmatrix}B_3\\ B_4\end{Bmatrix} \tag{B-23}$$

Similarly, the following solutions can be obtained for (B-23):

$$Y_1 = K_1\, exp(2i\theta) - \frac{\sqrt{2}}{2}\mu[i(\xi - A_m)\eta + \gamma\eta + iK_3]$$

$$Y_2 = K_2\, exp(-2i\theta) - \frac{\sqrt{2}}{2}\mu[i(\xi - A_m)\eta - \gamma\eta + iK_3] \tag{B-24}$$

in which $K_3 = \frac{C_2}{2\mu} - C_1 + \ln A_m$. The following relationships have been used in deriving (B-24):

$$\frac{d}{d\gamma}\left[\frac{1}{2} i\, exp(-2i\theta)\,(\xi - A_m)\eta\right] = exp(-2i\theta)\left[(\xi - A_m)\eta \frac{cos^2\theta}{1 + A_m} + \frac{i\gamma}{2A_m}\left\{\eta + \frac{(\xi - A_m)(1 - \xi\eta)}{\xi^2 - 1}\right\}\right] \tag{B-25}$$

$$\frac{d}{d\gamma}\left[\frac{1}{2} exp(-2i\theta)\,\gamma\eta\right] = exp(-2i\theta)\left[-i\gamma\eta \frac{cos^2\theta}{1 + A_m} + \frac{1}{2}\left\{\eta + \frac{\gamma^2(1 - \xi\eta)}{A_m(\xi^2 - 1)}\right\}\right]$$

Therefore a solution of the following form is obtained for the stress components:

$$\tau_{11} = X_1 = \frac{\sqrt{2}}{2} i[K_1\, exp(2i\theta) + K_2\, exp(-2i\theta)] + \mu(\xi - A_m)\eta + \mu K_3$$

$$\tau_{12} = X_2 = \frac{\sqrt{2}}{2}[K_2\, exp(-2i\theta) - K_1\, exp(2i\theta)] + \mu\gamma\eta \tag{B-26}$$

Using the same initial conditions at the start of the deformation step given by (B-18) leads to $K_1 = k_2 = 0$ and $K_3 = \frac{\lambda + \mu}{\mu} \ln A_m$. This leads to the same solution for the GMN rates given in (B-21).

Solution (B-21) is identical to the Hookean response for both the J and GMN rates as it was expected because of the unconditional integrability of the proposed Eulerian model.

Step 3- Removing the extension at constant shear $2 \leq t \leq 3$

The kinematical parameters of this deformation step is given by

$$F = N_1 \otimes N_1 + A N_2 \otimes N_2 + \gamma_m N_1 \otimes N_2$$

$$\Omega_J = \underset{\sim}{0}$$

$$\Omega_{GMN} = -\frac{\gamma_m \dot{A} \cos^2 \theta}{(1+A)^2}(N_1 \otimes N_2 - N_2 \otimes N_1) \tag{B-27}$$

The eigenvalues of V^2 can be written as follows:

$$\Lambda_{1,2} = A\left(\xi \pm \sqrt{\xi^2 - 1}\right) \tag{B-28}$$

where $\xi = \frac{1+A^2+\gamma_m^2}{2A}$. Using the spectral decomposition method, the components of the logarithmic strain are given by

$$\varepsilon_{11} = \frac{1}{2} ln\, A + \frac{1}{2}(\xi - A)\eta$$

$$\varepsilon_{22} = \frac{1}{2} ln\, A - \frac{1}{2}(\xi - A)\eta \tag{B-29}$$

$$\varepsilon_{12} = \frac{1}{2}\gamma_m \eta$$

in which $\eta = \frac{\cosh^{-1}\xi}{\sqrt{\xi^2-1}}$. Derivative of the logarithmic strain components with respect to the shearing parameter is given by

$$\frac{d\varepsilon_{11}}{d\gamma} = \frac{1}{2}\left(\frac{1}{A} - \eta\right) + \frac{A^2 - \gamma_m^2 - 1}{4A^2}\left[\frac{(\xi - A)(1 - \xi\eta)}{\xi^2 - 1} + \eta\right]$$

$$\frac{d\varepsilon_{22}}{d\gamma} = \frac{1}{2}\left(\frac{1}{A} + \eta\right) - \frac{A^2 - \gamma_m^2 - 1}{4A^2}\left[\frac{(\xi - A)(1 - \xi\eta)}{\xi^2 - 1} + \eta\right] \quad \text{(B-30)}$$

$$\frac{d\varepsilon_{12}}{d\gamma} = \frac{(A^2 - \gamma_m^2 - 1)(1 - \xi\eta)}{4A^2(\xi^2 - 1)}\gamma_m$$

The following relationships have been used in deriving the eigenprojections of V^2 and derivative of the logarithmic strain components:

$$\Lambda_1\Lambda_2 = A^2;\ \Lambda_1 + \Lambda_2 = 1 + A^2 + \gamma_m^2\ ;\ \Lambda_1 - \Lambda_2 = 2A\sqrt{\xi^2 - 1} \quad \text{(B-31)}$$

Since the Jaumann spin in this step is zero, the Jaumann rates of the Kirchhoff stress tensor and logarithmic strain are equivalent to their corresponding time derivative. Therefore, the stress solution for the case of J spin can be easily obtained as follows:

$$\tau_{11} = (\lambda + 2\mu)\varepsilon_{11} + \lambda\varepsilon_{22} + C_1$$

$$\tau_{22} = \lambda\varepsilon_{11} + (\lambda + 2\mu)\varepsilon_{22} + C_2 \quad \text{(B-32)}$$

$$\tau_{12} = 2\mu\varepsilon_{12} + C_3$$

Constants in (B-32) can be found using the initial condition for the stress response at time *t=2*, i.e.:

$$t = 2;\ \gamma = \gamma_m; A = A_m; \quad \text{(B-33)}$$

$$\tau_{11}|_{t=2} = (\lambda+\mu)\, ln\, A_m + \mu \frac{(\xi_m - A_m)\, cosh^{-1}\, \xi_m}{\sqrt{\xi_m^2 - 1}} \rightarrow C_1 = 0$$

$$\tau_{12}|_{t=2} = \mu \frac{\gamma_m\, cosh^{-1}\, \xi_m}{\sqrt{\xi_m^2 - 1}} \rightarrow C_3 = 0$$

$$\tau_{22}|_{t=2} = (\lambda+\mu)\, ln\, A_m - \mu \frac{(\xi_m - A_m)\, cosh^{-1}\, \xi_m}{\sqrt{\xi_m^2 - 1}} \rightarrow C_2 = 0$$

Therefore the solution for the stress components in this step for the J spin can be obtained as follows:

$$\begin{aligned} \tau_{11} &= \lambda\, ln\, A + \frac{2\mu}{\Lambda_1 - \Lambda_2}\left[(A^2 - \Lambda_2)\, ln\, A + \frac{1}{2}(1 + \gamma_m^2 - A^2)\, ln\, \Lambda_1\right] \\ \tau_{12} &= 2\mu \frac{A\gamma_m}{\Lambda_1 - \Lambda_2} ln \frac{\Lambda_1}{\Lambda_2} \end{aligned} \tag{B-34}$$

For the stress solution corresponding to the GMN rate, the following differential equation is obtained:

$$\begin{aligned} &\frac{d\tau_{11}}{dA} - 2\tau_{12}\frac{d\theta}{dA} = 2\mu\frac{d\varepsilon_{11}}{dA} + \frac{\lambda}{A} - 4\mu\frac{d\theta}{dA}\varepsilon_{12} \\ &\frac{d\tau_{12}}{d\gamma} + 2\tau_{11}\frac{d\theta}{dA} = [2(\lambda+\mu)\, ln\, A + C_1 + 2\mu(\xi - A)\eta]\frac{d\theta}{dA} + 2\mu\frac{d\varepsilon_{12}}{dA} \end{aligned} \tag{B-35}$$

A similar approach for decoupling the above equations and its solution, leads to the following stress solution:

$$\tau_{11} = X_1 = \frac{\sqrt{2}}{2} i[K_1\, exp(2i\theta) + K_2\, exp(-2i\theta)] + (\lambda + \mu)\, ln\, A + \mu(\xi - A)\eta + \frac{1}{2} C_1 \tag{B-36}$$

$$\tau_{12} = X_2 = \frac{\sqrt{2}}{2} [K_2\, exp(-2i\theta) - K_1\, exp(2i\theta)] + \mu\gamma_m \eta$$

Applying the initial conditions given by (B-33) to (B-36) leads to the same stress solution given by (B-34). Such a solution is in accordance with the finite Hookean response of the model and was expected because of the unconditional integrability of the Eulerian rate model.

Step 4- Removing the shear and back to the initial configuration $3 \leq t \leq 4$

The solution of this step is identical to the solution given in Appendix A for the simple shear motion. The only difference is the nonzero initial conditions for the stresses. The general stress solution for the simple shear problem with the J spin is given by (A-11). The stress solution at the end of the previous step using (B-34) serves as the following initial conditions for this step:

$t = 3;\ \gamma = \gamma_m; A = 1;$

$$\tau_{11}|_{t=3} = 2\mu \frac{\gamma_m\, sinh^{-1}\left(\frac{\gamma_m}{2}\right)}{\sqrt{4 + \gamma_m^2}} \tag{B-37}$$

$$\tau_{12}|_{t=3} = 4\mu \frac{sinh^{-1}\left(\frac{\gamma_m}{2}\right)}{\sqrt{4 + \gamma_m^2}}$$

in (B-37) use of the following relationships has been made:

$$\xi_m = \frac{2+\gamma_m^2}{2}\ ;\ \xi_m - A = \frac{\gamma_m^2}{2}\ ;\ \sqrt{\xi_m^2 - 1} = \frac{\gamma_m}{2}\sqrt{4+\gamma_m^2} \tag{B-38}$$

Applying the initial conditions (B-38) to (A-11) yields the stress response for the final step as follows:

$$\tau_{11} = 2\mu\frac{\gamma sinh^{-1}\left(\frac{\gamma}{2}\right)}{\sqrt{4+\gamma^2}}$$
$$\tau_{12} = 4\mu\frac{sinh^{-1}\left(\frac{\gamma}{2}\right)}{\sqrt{4+\gamma^2}} \tag{B-39}$$

which for $\gamma = 0$ yields the stress-free configuration of the material. This result was expected since the proposed Eulerian rate model is consistent with the Green elasticity and therefore for a closed path elastic loading the initial stress free configuration should be obtained from the model.

Appendix C.

Derivation of the proposed Lagrangian model coefficients

To derive a relation between the time rate of stress and plastic multiplier to be used for plastic integration and satisfying plastic consistency condition for the problem of simple shear, equations (5-66) and (5-67) yield:

$$\dot{\bar{\bar{U}}}_L^e = \frac{d}{dt}\left[exp\left(\frac{\bar{\bar{\tau}}_L}{2\mu}\right)\right] = \left[\dot{\mathfrak{B}}N_1 \otimes N_1 + \dot{\mathfrak{C}}N_2 \otimes N_2 + \dot{\mathfrak{J}}(N_1 \otimes N_2 + N_2 \otimes N_1)\right] \quad \text{(C-1)}$$

in which:

$$\dot{\mathfrak{B}} = \left(\mathscr{v}_1\bar{\bar{\tau}}_{L,11} - \mathscr{v}_0\right)\dot{\bar{\bar{\tau}}}_{L,11} + \mathscr{v}_1\bar{\bar{\tau}}_{L,12}\dot{\bar{\bar{\tau}}}_{L,12}$$

$$\dot{\mathfrak{J}} = \mathscr{v}_2\bar{\bar{\tau}}_{L,11}\dot{\bar{\bar{\tau}}}_{L,11} + \left(\mathscr{v}_2\bar{\bar{\tau}}_{L,12} - \mathscr{v}_0\right)\dot{\bar{\bar{\tau}}}_{L,12} \tag{C-2}$$

$$\dot{\mathfrak{C}} = \left(\mathscr{v}_3\bar{\bar{\tau}}_{L,11} + \mathscr{v}_0\right)\dot{\bar{\bar{\tau}}}_{L,11} + \mathscr{v}_3\bar{\bar{\tau}}_{L,12}\dot{\bar{\bar{\tau}}}_{L,12}$$

and the scalar $\mathscr{v}_i$'s are given as follows:

$$\mathscr{v}_0 = \frac{1-\mu^2}{2GT}$$

$$\mathscr{v}_1 = \frac{1}{2G\mu T^2}\left[\mu(1+\mu^2) + G^2\left(T + \bar{\bar{\tau}}_{L,11}\right) - \mathfrak{B}G(2\mu + T)\right]$$

$$\mathscr{v}_2 = \frac{1}{2\mu T^2}\left[G\bar{\bar{\tau}}_{L,12} - \mathfrak{J}(2\mu + T)\right] \tag{C-3}$$

$$\mathscr{v}_3 = \frac{1}{2G\mu T^2}\left[\mu(1+G^2) + G^2\left(T - \bar{\bar{\tau}}_{L,11}\right) - \mathfrak{C}G(2\mu + T)\right]$$

Use of equations (38), (39), and (43) yields:

$$\bar{\bar{U}}_L^e = R_E^{pT}UR_L^p\Lambda_d^{p-1} = \mathfrak{B}N_1\otimes N_1 + \mathfrak{C}N_2\otimes N_{2+}\mathfrak{J}(N_1\otimes N_2 + N_2\otimes N_1) \tag{C-4}$$

Taking the time derivative of (C-4) results into the followings for time rate of $\bar{\bar{U}}_L^e$:

$$\dot{\bar{\bar{U}}}_L^e = \left(-\Omega_E^p + R_E^{pT}\dot{U}U^{-1}R_E^p + R_E^{pT}U\Omega_L^pU^{-1}R_E^p\right)\bar{\bar{U}}_L^e + \bar{\bar{U}}_L^e\Lambda_d^p\dot{\Lambda}_d^{p-1} \tag{C-5}$$

Substituting for known kinematics quantities such as U, $\dot{U}$, and U^{-1} in (C-5) and knowing that $\frac{\mathrm{d}\Omega_E^p}{\mathrm{d}\gamma} = \frac{\mathrm{d}\theta_E^p}{\mathrm{d}\gamma}(N_1\otimes N_2 - N_2\otimes N_1)$, and $\frac{\mathrm{d}\Omega_L^p}{\mathrm{d}\gamma} = -\frac{\sqrt{6}\ell^{p\,2}\bar{\bar{N}}_{L,12}}{\ell^{p\,4}-1}\frac{\mathrm{d}\lambda}{\mathrm{d}\gamma}(N_1\otimes N_2 - N_2\otimes N_1)$, the followings are obtained for the components of the time derivative of the rotated elastic stretch tensor on the Lagrangian axis:

$$\frac{d\overline{\overline{U}}^e_{L,11}}{d\gamma} = -\mathfrak{I}\frac{d\theta^p_E}{d\gamma} - \left[\frac{\sqrt{6}\ell^{p\,2}\overline{\overline{N}}_{L,12}}{\ell^{p\,4}-1}(M_1L_1 + M_2L_3) + \sqrt{\frac{3}{2}}\mathfrak{B}\overline{\overline{N}}_{L,11}\right]\frac{d\lambda}{d\gamma} + (K_1L_1 + K_2L_3) \tag{C-6}$$

$$\frac{d\overline{\overline{U}}^e_{L,12}}{d\gamma} = -\mathfrak{C}\frac{d\theta^p_E}{d\gamma} + \left[-\frac{\sqrt{6}\ell^{p\,2}\overline{\overline{N}}_{L,12}}{\ell^{p\,4}-1}(M_1L_2 + M_2L_4) + \sqrt{\frac{3}{2}}\mathfrak{I}\overline{\overline{N}}_{L,11}\right]\frac{d\lambda}{d\gamma} + (K_1L_2 + K_2L_4) \tag{C-7}$$

$$\frac{d\overline{\overline{U}}^e_{L,22}}{d\gamma} = \mathfrak{B}\frac{d\theta^p_E}{d\gamma} - \left[\frac{\sqrt{6}\ell^{p\,2}\overline{\overline{N}}_{L,12}}{\ell^{p\,4}-1}(M_3L_1 + M_4L_3) + \sqrt{\frac{3}{2}}\mathfrak{I}\overline{\overline{N}}_{L,11}\right]\frac{d\lambda}{d\gamma} + (K_3L_1 + K_4L_3) \tag{C-8}$$

in which:

$$K_1\left(\theta^p_E;\gamma\right) = -g_1(\gamma)\cos\theta^p_E - g_3(\gamma)\sin\theta^p_E$$

$$K_2\left(\theta^p_E;\gamma\right) = g_2(\gamma)\cos\theta^p_E - g_1(\gamma)\sin\theta^p_E$$

$$K_3\left(\theta^p_E;\gamma\right) = -g_1(\gamma)\sin\theta^p_E + g_3(\gamma)\cos\theta^p_E$$

$$K_4\left(\theta^p_E;\gamma\right) = g_2(\gamma)\sin\theta^p_E + g_1(\gamma)\cos\theta^p_E$$

$$g_1(\gamma) = \frac{2\gamma}{4+\gamma^2}\ ;\ g_2(\gamma) = \frac{2}{4+\gamma^2}\ ;\ g_3(\gamma) = \frac{8-\gamma^2(2+\gamma^2)}{(4+\gamma^2)^2} \tag{C-9}$$

$$M_1\left(\theta^p_E;\gamma\right) = -\gamma\cos\theta^p_E + (1+\gamma^2)\sin\theta^p_E$$

$$M_2\left(\theta^p_E;\gamma\right) = \cos\theta^p_E - \gamma\sin\theta^p_E$$

$$M_3\left(\theta^p_E;\gamma\right) = -\gamma\sin\theta^p_E - (1+\gamma^2)\cos\theta^p_E$$

$$M_4\left(\theta_E^p;\gamma\right) = sin\,\theta_E^p + \gamma\, cos\,\theta_E^p$$

and:

$$\begin{aligned} L_1\left(\mathfrak{B},\mathfrak{J},\mathfrak{C},\theta_E^p\right) &= \mathfrak{B}\, cos\,\theta_E^p + \mathfrak{J}\, sin\,\theta_E^p \\ L_2\left(\mathfrak{B},\mathfrak{J},\mathfrak{C},\theta_E^p\right) &= \mathfrak{J}\, cos\,\theta_E^p + \mathfrak{C}\, sin\,\theta_E^p \\ L_3\left(\mathfrak{B},\mathfrak{J},\mathfrak{C},\theta_E^p\right) &= -\mathfrak{B}\, sin\,\theta_E^p + \mathfrak{J}\, cos\,\theta_E^p \\ L_4\left(\mathfrak{B},\mathfrak{J},\mathfrak{C},\theta_E^p\right) &= -\mathfrak{J}\, sin\,\theta_E^p + \mathfrak{C}\, cos\,\theta_E^p \end{aligned} \tag{C-10}$$

Equations (C-7) and (C-8) can be used to find a relation for the evolution of the θ_E^p during plastic loading. Symmetry of $\bar{\bar{U}}_L^e$ requires that $\dot{\bar{\bar{U}}}_L^e$ be also symmetric; as a result, $\frac{\mathrm{d}\bar{\bar{U}}_{L,21}^e}{\mathrm{d}\gamma} = \frac{\mathrm{d}\bar{\bar{U}}_{L,12}^e}{\mathrm{d}\gamma}$ which leads to:

$$\begin{aligned} \frac{d\theta_E^p}{d\gamma} = \frac{1}{\mathfrak{B}+\mathfrak{C}}&\left(K_1L_2 + K_2L_4 - K_3L_1 - K_4L_3\right) \\ &+ \frac{\sqrt{6}}{\mathfrak{B}+\mathfrak{C}}\left\{\mathfrak{J}\bar{\bar{N}}_{L,11} + \frac{\bar{\bar{N}}_{L,12}\ell^{p\,2}}{\ell^{p\,4}-1}\left(M_3L_1 + M_4L_3 - M_1L_2 - M_2L_4\right)\right\}\frac{d\lambda}{d\gamma} \end{aligned} \tag{C-11}$$

Or equivalently:

$$\frac{d\theta_E^p}{d\gamma} = \mathfrak{T}_1\frac{d\lambda}{d\gamma} + \mathfrak{T}_2 \tag{C-12}$$

Substituting (C-12) into (C-6) and (C-7) yields:

$$\frac{d\overline{\overline{U}}^{e}_{L,11}}{d\gamma} = -\left[\mathfrak{J}\mathfrak{T}_1 + \frac{\sqrt{6}{\ell^p}^2\overline{\overline{N}}_{L,12}}{{\ell^p}^4 - 1}(M_1L_1 + M_2L_3) + \sqrt{\frac{3}{2}}\mathfrak{B}\overline{\overline{N}}_{L,11}\right]\frac{d\lambda}{d\gamma} + (K_1L_1 + K_2L_3 - \mathfrak{J}\mathfrak{T}_2) \tag{C-13}$$

$$\frac{d\overline{\overline{U}}^{e}_{L,12}}{d\gamma} = \left[-\mathfrak{C}\mathfrak{T}_1 - \frac{\sqrt{6}{\ell^p}^2\overline{\overline{N}}_{L,12}}{{\ell^p}^4 - 1}(M_1L_2 + M_2L_4) + \sqrt{\frac{3}{2}}\mathfrak{J}\overline{\overline{N}}_{L,11}\right]\frac{d\lambda}{d\gamma} + (K_1L_2 + K_2L_4 - \mathfrak{C}\mathfrak{T}_2) \tag{C-14}$$

Or equivalently:

$$\frac{d\overline{\overline{U}}^{e}_{L,11}}{d\gamma} = \mathcal{F}_1\left(\ell^p, \theta^p_E, \mathfrak{B}, \mathfrak{J}, \mathfrak{C}, \overline{\overline{N}}_{L,11}, \overline{\overline{N}}_{L,12}; \gamma\right)\frac{d\lambda}{d\gamma} + \mathcal{G}_1\left(\ell^p, \theta^p_E, \mathfrak{B}, \mathfrak{J}, \mathfrak{C}, \overline{\overline{N}}_{L,11}, \overline{\overline{N}}_{L,12}; \gamma\right) \tag{C-15}$$

$$\frac{d\overline{\overline{U}}^{e}_{L,12}}{d\gamma} = \mathcal{F}_2\left(\ell^p, \theta^p_E, \mathfrak{B}, \mathfrak{J}, \mathfrak{C}, \overline{\overline{N}}_{L,11}, \overline{\overline{N}}_{L,12}; \gamma\right)\frac{d\lambda}{d\gamma} + \mathcal{G}_2\left(\ell^p, \theta^p_E, \mathfrak{B}, \mathfrak{J}, \mathfrak{C}, \overline{\overline{N}}_{L,11}, \overline{\overline{N}}_{L,12}; \gamma\right) \tag{C-16}$$

It is worth mentioning that use of a definition for the plastic spin is bypassed due to the symmetry property of the elastic stretch tensor. In other words, in isotropic plasticity the plastic spin is function of the known kinematics variables and does not require a separate evolution equation.

Using equations (C-2), (C-15), and (C-16) gives the followings for the time rate of stress tensors:

$$\dot{\mathfrak{B}} = \left(\mathcal{v}_1 \bar{\bar{\tau}}_{L,11} - \mathcal{v}_0\right)\dot{\bar{\bar{\tau}}}_{L,11} + \mathcal{v}_1 \bar{\bar{\tau}}_{L,12}\dot{\bar{\bar{\tau}}}_{L,12} = \mathcal{F}_1 \frac{d\lambda}{d\gamma} + \mathcal{G}_1$$

$$\dot{\mathfrak{J}} = \mathcal{v}_2 \bar{\bar{\tau}}_{L,11}\dot{\bar{\bar{\tau}}}_{L,11} + \left(\mathcal{v}_2 \bar{\bar{\tau}}_{L,12} - \mathcal{v}_0\right)\dot{\bar{\bar{\tau}}}_{L,12} = \mathcal{F}_2 \frac{d\lambda}{d\gamma} + \mathcal{G}_2 \tag{C-17}$$

Therefore, equation (C-17) yields the following expression for the time rate of stress components:

$$\frac{d\bar{\bar{\tau}}_{L,11}}{d\gamma} = \mathcal{A}_1\left(\ell^p, \theta_E^p, \theta_L^p, \mathfrak{B}, \mathfrak{J}, \mathfrak{C}; \gamma\right)\frac{d\lambda}{d\gamma} + \mathcal{B}_1\left(\ell^p, \theta_E^p, \theta_L^p, \mathfrak{B}, \mathfrak{J}, \mathfrak{C}; \gamma\right)$$

$$\frac{d\bar{\bar{\tau}}_{L,12}}{d\gamma} = \mathcal{A}_2\left(\ell^p, \theta_E^p, \theta_L^p, \mathfrak{B}, \mathfrak{J}, \mathfrak{C}; \gamma\right)\frac{d\lambda}{d\gamma} + \mathcal{B}_2\left(\ell^p, \theta_E^p, \theta_L^p, \mathfrak{B}, \mathfrak{J}, \mathfrak{C}; \gamma\right) \tag{C-18}$$

in which:

$$\begin{bmatrix} \mathcal{A}_1 & \mathcal{B}_1 \\ \mathcal{A}_2 & \mathcal{B}_2 \end{bmatrix} = \begin{bmatrix} \mathcal{v}_1 \bar{\bar{\tau}}_{L,11} - \mathcal{v}_0 & \mathcal{v}_1 \bar{\bar{\tau}}_{L,12} \\ \mathcal{v}_2 \bar{\bar{\tau}}_{L,11} & \mathcal{v}_2 \bar{\bar{\tau}}_{L,12} - \mathcal{v}_0 \end{bmatrix}^{-1} \begin{bmatrix} \mathcal{F}_1 & \mathcal{G}_1 \\ \mathcal{F}_2 & \mathcal{G}_2 \end{bmatrix} \tag{C-19}$$

Equations (C-12) and (C-19) are used during the time integration for the plastic consistency and update of the Eulerian triad angle for the problem of simple shear.

References

[1] Khan, A. S., Chen, X., Abdel-Karim, M., "Cyclic multiaxial and shear finite deformation response of OFHC: Part I, experimental results", International Journal of Plasticity, Vol. 23, 2007, pp. 1285-1306.

[2] Eshraghi, A., Jahed, H., Lambert, S., "A finite deformation constitutive model for the prediction of cyclic behavior of shape memory alloys", 12th International Conference of Fracture (ICF12), Ottawa, Canada, July 2009.

[3] Nagtegaal, J. C., de Jong, J. E., "Some aspects of non-isotropic work-hardening in finite strain plasticity", In Proceeding of the Workshop on Plasticity of Metals at Finite Strain: Theory, Experimental and Computation, Stanford University 1981, pp. 65–102.

[4] Koji, M., Bathe, K. J., "Studies of finite element procedures-stress solution of a closed elastic strain path with stretching and shearing using the updated Lagrangian Jaumann formulation", Computers and Structures, Vol. 26, 1987, pp. 175–179.

[5] Xiao, H., Bruhns, O. T., Meyers, A., "Elastoplasticity beyond small deformations", Acta Mechanica, Vol. 182, 2006, pp. 31-111.

[6] Truesdell, C., Noll, W., "The non-linear field theories of mechanics", third edition. Springer: Berlin, 2003.

[7] Lemaitre, J., Chaboche, J. L., "Mechanics of Solid Materials", Cambridge University Press: UK, 1994.

[8] Malvern, L. E., "Introduction to the Mechanics of a Continuum Medium", Prentice-Hall, Englewood Cliffs: NJ, 1969.

[9] Noll, W., "On the continuity of the solids and fluid states", Journal of Rational Mechanics and Analysis, Vol. 4, 1955, pp. 3-81.

[10] Truesdell, C., "Corrections and additions to the mechanical foundations of elasticity and fluid dynamics", Journal of Rational Mechanics and Analysis, Vol. 2, 1953, pp. 593-616.

[11] Cotter, B. A., Rivlin, R. S., "Tensors associated with time-dependent stress", Quarterly of Applied Mathematics, Vol. 13, 1955, pp. 177-182.

[12] Green, A. E., Naghdi, P. M., "A general theory of an elastic-plastic continuum", Archive for Rational Mechanics and Analysis, Vol. 18, 1965, pp. 251-281.

[13] Dienes, J. K., "On the analysis of rotation and stress rate in deforming bodies", Acta Mechanica, Vol. 32, 1979, pp. 217-232.

[14] Dafalias, Y. F., “Corotational rates for kinematic hardening at large plastic deformations”, ASME Journal of Applied Mechanics, Vol. 50, 1983, pp. 561–565.

[15] Lee, E. H., Mallett, R. L., Wertheimer, T. B., “Stress analysis for anisotropic hardening in finite deformation plasticity”, Transaction of the ASME, Vol. 50, 1983, pp. 554-560.

[16] Bernstein, B., “Hypoelasticity and elasticity”, Archive for Rational Mechanics and Analysis, Vol. 6, 1960, pp. 89-103.

[17] Bernstein, B., “Relations between hypoelasticity and elasticity”, Transactions of the Society of Rheology, Vol. IV, 1960, pp. 23-28.

[18] Ericksen, J. L. “Hypoelastic potentials”, Quarterly Journal of Mechanics and Applied Mathematics, Vol. XI, 1958, Pt. 1.

[19] Swift, W., “Length changes in metals under torsional overstrain”, Engineering, Vol. 163, 1947, pp. 253-257.

[20] Atluri, S. N., Reed, K. W., “Constitutive modeling and computational implementation for finite strain plasticity”, International Journal of Plasticity, Vol. 1, 1985, pp. 61-87.

[21] Reinhardt, W. D., Dubey, R. N., “Application of objective rates in mechanical modeling of solids”, Journal of Applied Mechanics (ASME), Vol. 118, 1996, pp. 692-698.

[22] Xiao, H., Bruhns, O. T., Meyers, A., “Logarithmic strain, logarithmic spin and logarithmic rate”, Acta Mechanica, Vol. 124, 1997, pp. 89-105.

[23] Anand, L., “Moderate deformations in extension-torsion of incompressible isotropic elastic materials”, Journal of the Mechanics and Physics of Solids, Vol. 34, 1986, pp. 293–304.

[24] Anand, L., “On H. Hencky’s approximate strain-energy function for moderate deformations”, Journal of Applied Mechanics (ASME), Vol. 46, 1979, pp. 78–82.

[25] Lehmann, T., Guo, Z. H., Liang, H. Y., “The conjugacy between Cauchy stress and logarithm of the left stretch tensor”, European Journal of Mechanics - A/Solids, Vol. 10, 1991, pp. 395–404.

[26] Xiao, H., Bruhns, O. T., Meyers, A., "Hypoelasticity model based upon the logarithmic stress rate", Journal of Elasticity, Vol. 47, 1997, pp. 51-68.

[27] Bruhns O.T., Xiao H., Meyers A., “Self-consistent Eulerian rate type elastoplasticity models based upon the logarithmic stress rate”, International Journal of Plasticity, Vol. 15, 1999, pp. 479-520.

[28] Xiao, H., Bruhns, O. T., Meyers, A., "Large strain responses of elastic-perfect plasticity and kinematic hardening plasticity with the logarithmic rate: Swift effect in torsion", International Journal of Plasticity, Vol. 17, 2001, pp. 211-235.

[29] Asaro, R. J., "Micromechanics of crystals and polycrystals", Advances in Applied Mechanics, Vol. 23, 1983, pp. 1–115.

[30] Simo, J. C., Hughes, T. J. R., “Computational Inelasticity”, Springer: Berlin, 1998.

[31] Khan, A. S., Huang, S., “Continuum Theory of Plasticity”, Wiley: NY, 1995.

[32] Gabriel, G., Bathe, K. J., “Some computational issues in large strain elastoplastic analysis”, Computers and Structures, Vol. 56, 1995, pp. 249-267.

[33] Hoger, A., “The stress conjugate to logarithmic strain”, International Journal of Solids and Structures, Vol. 23, 1987, pp. 1645-1656.

[34] Belytschko, T., Liu, W. K., Moran, B., "Nonlinear finite elements for continua and structures", Wiley: NY, 2000.

[35] Simo, J. C., “A framework for finite strain elastoplasticity based on maximum plastic dissipation and the multiplicative decomposition: Part I. Continuum Formulation”, Computer Methods in Applied Mechanics and Engineering, Vol. 66, 1988, pp. 199-219.

[36] Simo, J. C., “A framework for finite strain elastoplasticity based on maximum plastic dissipation and the multiplicative decomposition: Part II. Computational aspects”, Computer Methods in Applied Mechanics and Engineering, Vol. 68, 1988, pp. 1-31.

[37] Wilkins, M. L., "Calculation of elastic-plastic flow", in: B. Alder et al., eds., Methods of Computational Physics, Vol. 3, Academic Press: NY, 1964.

[38] Pinsky, P. M., Ortiz, M., and Pister, K. S., "Numerical integration of rate constitutive equations in finite deformation analysis", Computer Methods in Applied Mechanics and Engineering, Vol. 40, 1983, pp. 137-150.

[39] Hill, R., "Aspects of invariance in solid mechanics", Advances in Applied Mechanics, Vol. 18, 1978, pp. 1-75.

[40] Reinhardt, W. D., “A rate dependent constitutive description for metals subjected to large deformations”, Ph.D. Thesis, University of Waterloo, 1996, Canada.

[41] Dubey, R. N., “Corotational rates on the principal axes”, Solid Mechanics archives, Vol. 10, 1985, pp. 233-244.

[42] Dubey, R. N., “Choice of tensor rates – a methodology”, Solid Mechanics archives, Vol. 12, 1987, pp. 233-244.

[43] Metzger, D. R., Dubey, R. N., “Corotational rates in constitutive modeling of elastic-plastic deformation”, International Journal of Plasticity, Vol. 4, 1987, pp. 341-368.

[44] Marsden, J. E., Hughes, T. J. R., “Mathematical Foundations of Elasticity”, New York: Dover, 1994.

[45] Hill, R., "On constitutive inequalities for simple materials", Journal of the Mechanics and Physics of Solids, Vol. 16, 1968, pp. 229-242.

[46] Hill, R., "Constitutive inequalities for isotropic elastic solids under finite strain", Proceedings of the Royal Society, London, A326, 1970, pp. 131-147.

[47] Ogden, R. W., "Non-linear elastic deformations", Ellis Horwood: Chichester, 1984.

[48] Simo, J. C., Marsden, J. E., "On the rotated stress tensor and the material version of the Doyle-Ericksen formula", Archive for Rational Mechanics and Analysis, Vol. 86, 1984, pp. 213-231.

[49] Lehmann, T., Liang, H. Y., "The stress conjugate to the logarithmic strain ln V", Journal of Applied Mathematics and Mechanics, Vol. 73, 1993, pp. 357-363.

[50] Xiao, H., "Unified explicit basis-free expressions for time rate and conjugate stress of an arbitrary Hill's strain", International Journal of Solids and Structures, Vol. 32, 1995, pp. 3327-3341.

[51] Nicholson, D. W., "On stress conjugate to Eulerian strains", Acta Mechanica, Vol. 165, 2003, pp. 87–98.

[52] Nicholson, D. W. "On stress conjugate to Eulerian strains", Acta Mechanica, Vol. 169, 2004, pp. 225–226.

[53] Nicholson, D. W., Lin, B., "Extension of Kronecker-product algebra with applications in continuum and computational mechanics", Acta Mechanica, Vol. 136, 1999, pp. 223–241.

[54] Asghari, M., Naghdabadi, R., Sohrabpour, S., "Stresses conjugate to the Jaumann rate of Eulerian strain measures", Acta Mechanica, Vol. 190, 2007, pp. 45-56.

[55] Doyle, T. C., Ericksen, J. L., "Nonlinear elasticity", Advances in Applied Mechanics, Vol. 4, 1956, pp. 53-115.

[56] Xiao, H., Bruhns, O. T., Meyers, A., "Objective corotational rates and unified work-conjugacy relation between Eulerian and Lagrangian strain and stress measures", Archives of Mechanics, Vol. 50, 1998, pp. 1015-1045.

[57] Nemat-Nasser, S., "On finite deformation elastoplasticity", International Journal of Solids and Structures, Vol. 18, 1982, pp. 857-872.

[58] Rivlin, R. S., "Further remarks on the stress deformation relations for isotropic materials", Journal of Rational Mechanics and Analysis, Vol. 4, 1955, pp. 681-702.

[59] Truesdell, C., "The simplest rate theory of pure elasticity", Communications on Pure and Applied Mathematics, Vol. 8, 1955, pp. 123-132.

[60] Lin, R. C., Schomburg, U., Kletschkowski, T., "Analytical stress solutions of a closed deformation path with stretching and shearing using the hypoelastic formulations", European Journal of Mechanics–A/Solids, Vol. 22, 2003, pp. 443–461.

[61] Xiao, H., Bruhns, O. T., Meyers, A., "On objective corotational rates and their defining spin tensors", International Journal of Solids and Structures, Vol. 35, 1998, pp. 4001-4014.

[62] Xiao, H., Bruhns, O. T., Meyers, A., "The integrability criterion in finite elastoplasticity and its constitutive implications", Acta Mechanica, Vol. 188, 2007, pp. 227-244.

[63] Truesdell, C., "The mechanical foundations of elasticity and fluid dynamics", Journal of Rational Mechanics and Analysis, Vol. 1, 1952, pp. 125–300.

[64] Bathe, K. J., “Finite Elements Procedures”, Prentice Hall: New Jersey, 1996.

[65] Wilkins, M. L., ”Calculation of elastic-plastic flow”, in Methods of Computational Physics 3, eds., B. Alder et al., Academic Press: New York, 1964.

[66] Needleman, A., “Finite elements for finite strain plasticity problems”, Plasticity of Metals at Finite Strains: Theory, Computation, and Experiment, eds., E.H. Lee and R.L. Mallet, Division of Applied Mechanics, Stanford University, Stanford, California, 1982, pp. 387–436.

[67] Rolph, W. D., Bathe, K. J., “On a large strain finite element formulation for elastoplastic analysis”, in Constitutive Equations, Macro and Computational Aspects, ed., K.J. Willam, Winter Annual Meeting, ASME, New York, 1984.

[68] Prager, W., "An elementary discussion of definitions of stress rate", Quarterly of Applied Mathematics, Vol. 18, 1960, pp. 403-407.

[69] Xiao, H., Bruhns, O. T., Meyers, A., "The choice of objective rates in finite elastoplasticity: general results on the uniqueness of the logarithmic rate", The Royal Society, Vol. 456, 2000, pp. 1865-1882.

[70] Hughes, T. J. R., Winget, J., “Finite rotation effects in numerical integration of rate constitutive equations arising in large deformation analysis”, International Journal for Numerical Methods in Engineering, Vol. 15, 1980, pp. 1862–1867.

[71] Moler, C., Loan, C.V., "Nineteen dubious ways to compute the exponential of a matrix, twenty-five years later", Society for industrial and applied mathematics, SIAM Review, Vol. 45, 2003.

[72] Fish, J., Shek, K., "Computational aspects of incrementally objective algorithms for large deformation plasticity", International Journal for Numerical Methods in Engineering, Vol. 44, 1999, pp. 839-851.

[73] Voyiadjis, G. Z., Abed, F. H., "Implicit algorithm for finite deformation hypoelastic-viscoplasticity in fcc metals", International Journal for Numerical Methods in Engineering, Vol. 67, 2006, pp. 933-959.

[74] ABAQUS Theory Manual, Ver. 6-5-1, Hibbit, Karlsson, Sorensen, 2004.

[75] Colak, O. U., "Modeling of large simple shear using a viscoplastic overstress model and classical plasticity model with different objective stress rates", Acta Mechanica, Vol. 167, 2004, pp. 171-187.

[76] Meyers, A., Bruhns, O. T., Xiao, H., “Objective stress rates in repeated elastic deformation cycles”, Proceedings in Applied Mathematics and Mechanics, Vol. 5, 2005, pp. 249-250.

[77] Jahed, H., Eshraghi, A., Lambert, S., “Generalized hypo-elastoplasticity for arbitrary stress rates”, The International Conference of Plasticity 2008, Kona, Hawaii, 2008.

[78] Eshraghi, A., Jahed, H., Lambert, S., “Rate type constitutive models and their applications in finite deformation elastoplasticity”, Proceeding of the third

Canadian Conference on Nonlinear Solid Mechanics (CanCNSM), Toronto, 2008, pp. 303-310.

[79] Eshraghi, A., Jahed, H., Lambert, S., "Elastoplastic modeling of hardening materials at finite deformation using an Eulerian rate formulation", Submitted to the Journal of Pressure Vessels and Technology, October 2008.

[80] Scheidler, M., "Time rates of generalized strain tensors. Part I: Component formulas", Mechanics of Materials, Vol. 11, 1991, pp. 199-210.

[81] Armstrong, P. J., Frederick, O. C., "A mathematical representation of the multiaxial Bauschinger effect", CEGB report No. RD/B/N731, 1966.

[82] Voce, E., "Metallurgica", 1955, Col. 51, pp. 219.

[83] Ishikawa, H., "Constitutive model of plasticity in finite deformation", International Journal of Plasticity, Vol. 15, 1999, pp. 299-317.

[84] Taylor, G. I., Elam, C. F., "Bakerian Lecture: The distortion of an aluminum crystal during a tensile test", Proceedings of the Royal Society of London, A102, 1923, pp. 643–667.

[85] Taylor, G. I., Elam, C. F., "The plastic extension and fracture of aluminum crystals", Proceedings of the Royal Society of London, A108, 1925, pp. 28–51.

[86] Taylor, G. I., "Analysis of plastic strain in a cubic crystal," in Stephen Timoshenko 60th Anniversary Volume, ed., J. M. Lessels, Macmillan, New York, 1938.

[87] Asaro, R. J., Rice, J. R., “Strain localization in ductile single crystals”, Journal of Mechanics and Physics of Solids, Vol. 25, 1977, pp. 309–338.

[88] Asaro, R. J., “Geometrical effects in the inhomogeneous deformation of ductile single crystals”, Acta Metallurgica Vol. 27, 1979, pp. 445–453.

[89] Naghdi, P. M., "A critical review of the state of finite plasticity", Journal of Applied Mathematics and Physics (ZAMP), Vol. 41, 1990, pp. 315-394.

[90] Simo, J. C., Ortiz, M., "A unified approach to finite deformation elastoplastic analysis based on the use of hyperelastic constitutive equations", Computer Methods in Applied Mechanics and Engineering, Vol. 49, 1985, pp. 221-245.

[91] Moran, B., Ortiz, M., Shih, C. F., “Formulation of implicit finite element methods for multiplicative finite deformation plasticity”, International Journal for Numerical Methods in Engineering, Vol. 29, 1990, pp. 483–514.

[92] Anand, L., “Constitutive equations for hot-working of metals”, International Journal of Plasticity, Vol. 1, 1985, pp. 213–231.

[93] Simo, J. C., “On the computational significance of the intermediate configuration and hyperelastic relations infinite deformation elastoplasticity”, Mechanics of Materials, Vol. 4, 1986, pp.439–451.

[94] Eterovic, A. L., Bathe, K. J., "A hyperelastic-based large strain elastoplastic constitutive formulation with combined isotropic-kinematic hardening using the logarithmic stress and strain measures", International Journal for Numerical Methods in Engineering, Vol. 30, 1990, pp. 1099 –1114.

[95] Montans, F. J., Bathe, K. J., "Computational issues in large strain elastoplasticity: an algorithm for mixed hardening and plastic spin", International Journal for Numerical Methods in Engineering, Vol. 63, 2005, pp. 159-196.

[96] Mandel, J., "Thermodynamics and plasticity. In Foundations of Continuum Thermodynamics", Delgado JJ, Nina NR, Whitelaw JH (eds). Macmillan: London, 1974, pp. 283–304.

[97] Weber, G., Anand, L., "Finite deformation constitutive equations and a time integration procedure for isotropic hyperelastic-viscoplastic solids", Computer Methods in Applied Mechanics and Engineering, Vol. 79, 1990, pp. 173-202.

[98] Reinhardt, W. D., Dubey, R. N., "An Eulerian-based approach to elastic-plastic decomposition", Acta Mechanica, Vol. 131, 1998, pp. 111-119.

[99] Ghavam, K., Naghdabadi, R., "Hardening materials modeling in finite elastic-plastic deformations based on the stretch tensor decomposition", Materials and Design, Vol. 29, 2008, pp. 161-172.

[100] Eshraghi, A., Jahed, H., Lambert, S., "A Lagrangian model for hardening behavior of materials at finite deformation based on the right plastic stretch tensor", Submitted to the Journal of Materials and Design, January 2009.

[101] Eterovic, A. L., Bathe, K. J., "A note on the use of the additive decomposition of the strain tensor in finite deformation inelasticity", Computer Methods in Applied Mechanics and Engineering, Vol. 93, 1991, pp. 31-38.